The Large Magellanic Cloud and dark matter searches

Nassim Bozorgnia

UNIVERSITY OF ALBERTA

2026 CAP Congress, Ottawa
23 June 2026

Canada Research Chairs
Chaires de recherche du Canada

NSERC
CRSNG

Dark matter in the galaxy

- **Galactic dark matter (DM) distribution** is the key input parameter in DM searches. → Its determination is crucial for characterizing the *DM particle properties*.

Dark matter in the galaxy

- **Galactic dark matter (DM) distribution** is the key input parameter in DM searches. → Its determination is crucial for characterizing the *DM particle properties*.

- *How does a close passage of a massive satellite affect the DM distribution in the Solar neighborhood?*

Dark matter direct detection

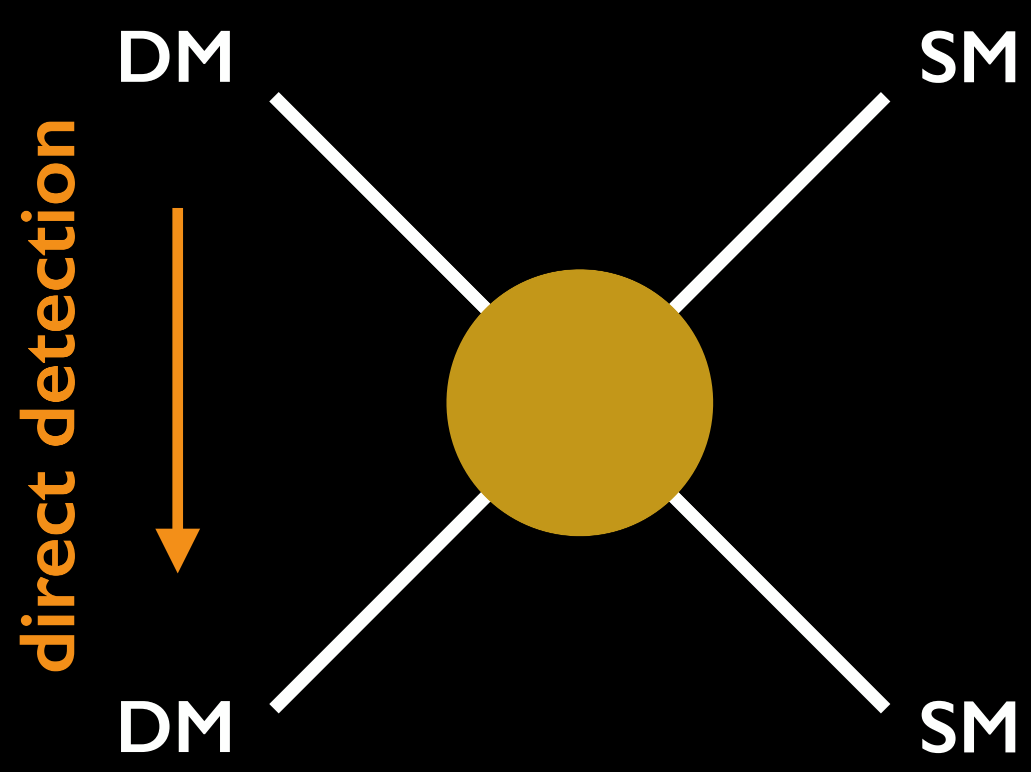

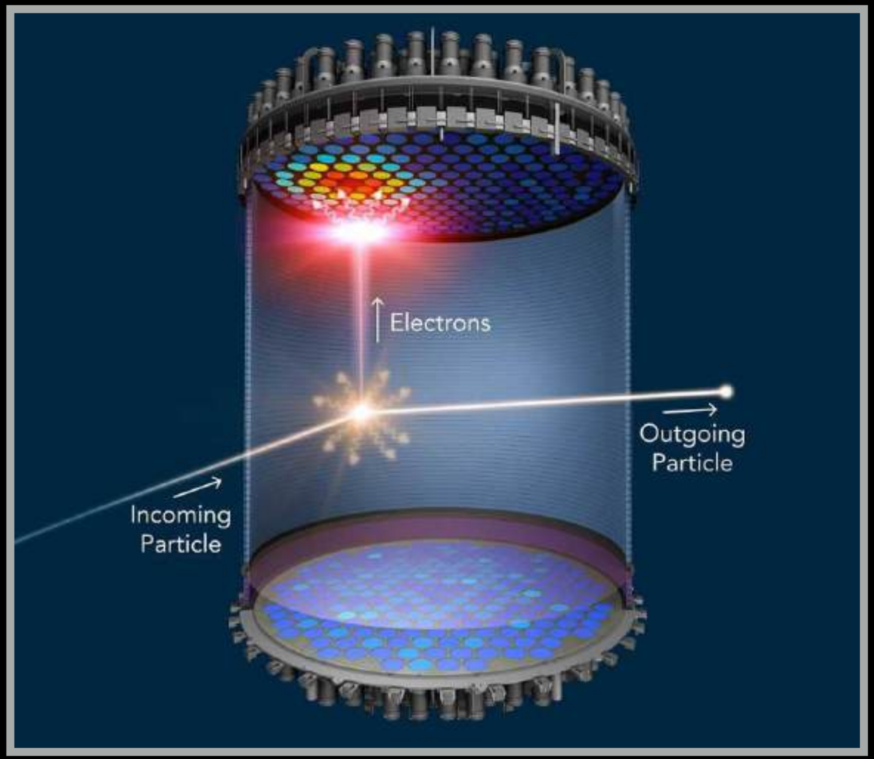

Dark matter direct detection

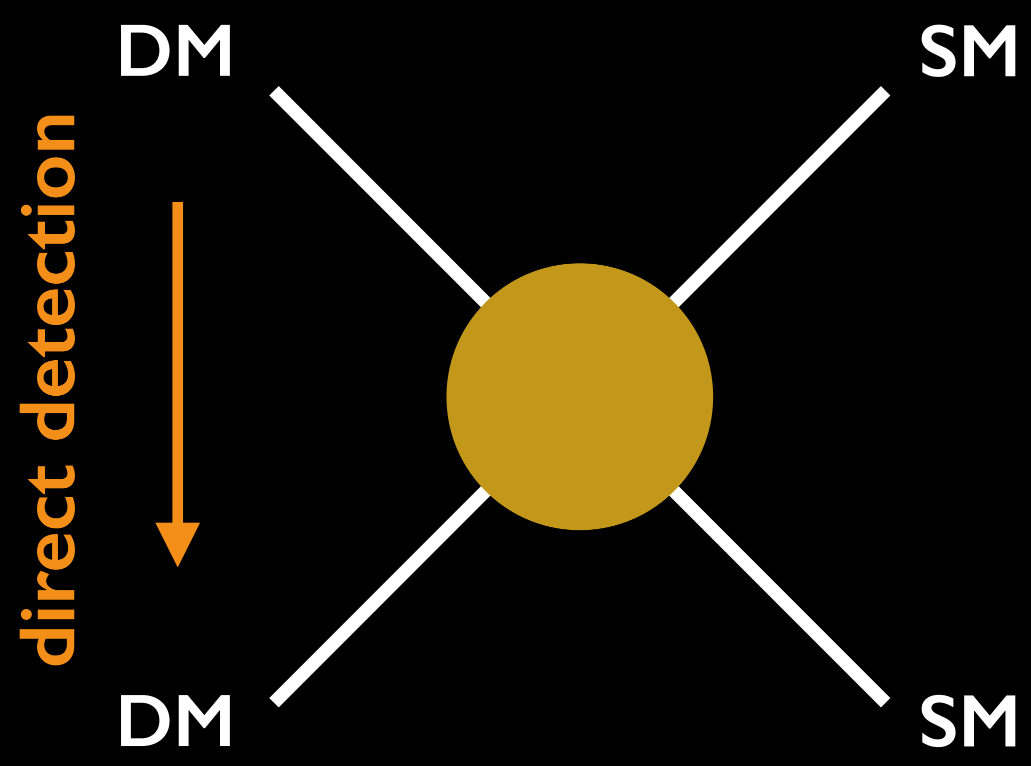

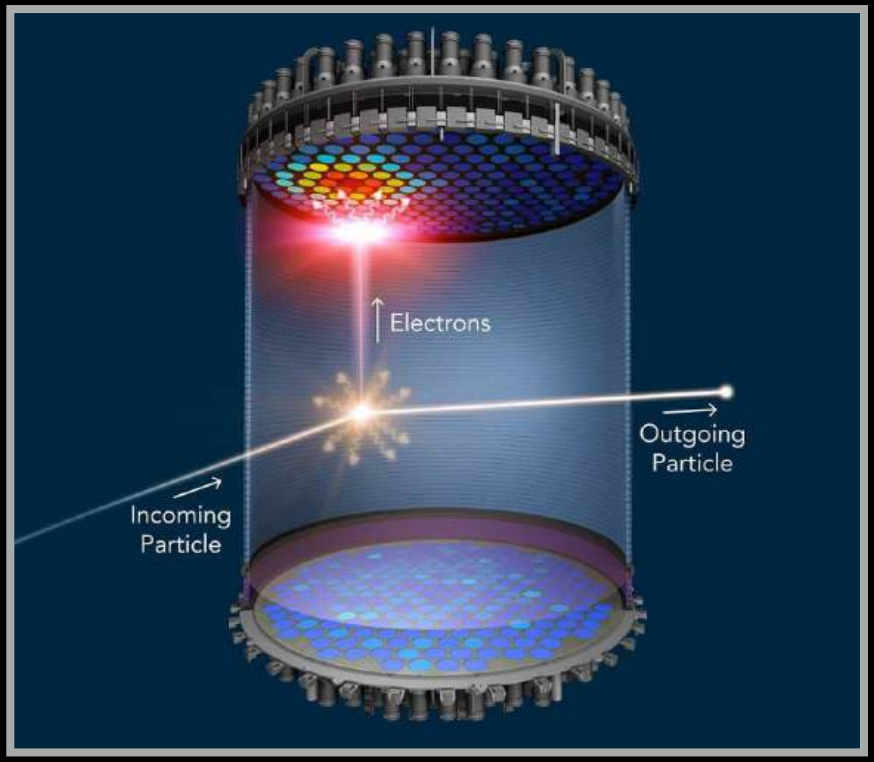

Signals in direct DM searches strongly depend on the DM distribution in the **Solar neighborhood**.

Dark matter direct detection

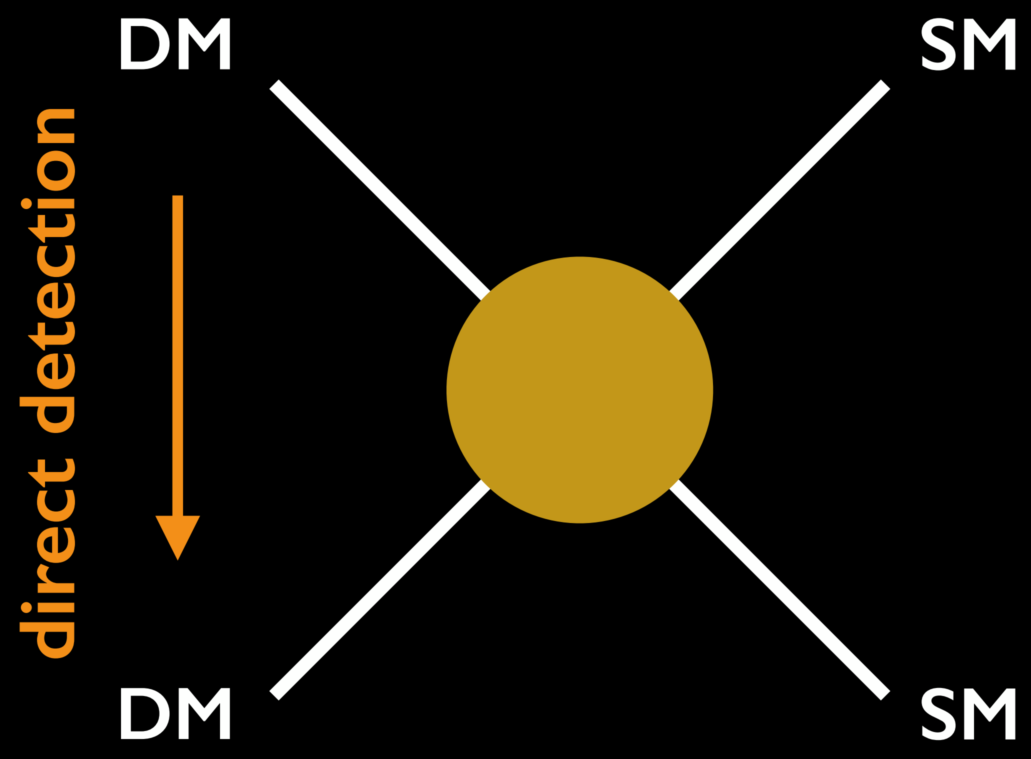

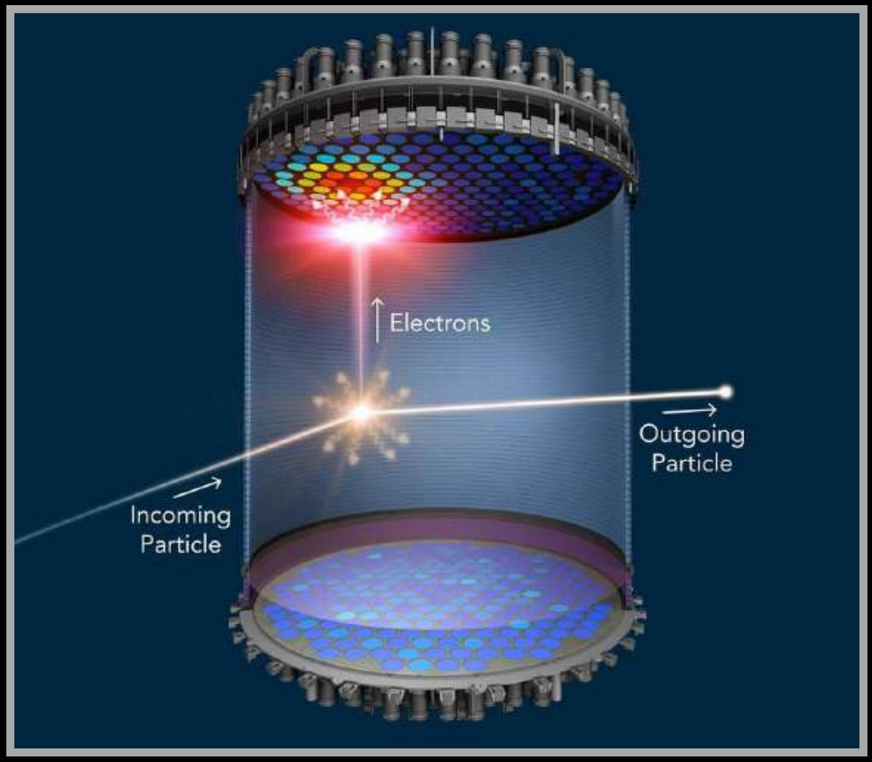

Signals in direct DM searches strongly depend on the DM distribution in the **Solar neighborhood**.

Uncertainties in the local DM distribution ➡ *large uncertainties in the interpretation of direct detection data.*

Direct detection event rate

- The differential event rate (per unit detector mass):

$$\frac{dR}{dE_R} = \frac{\rho_\chi}{m_\chi m_N} \int_{v>v_{\rm min}} d^3v \, \frac{d\sigma_{\chi N}}{dE_R} \, v \, f_{\rm det}(\mathbf{v}, t)$$

$v_{\rm min} = \sqrt{m_N E_R/(2\mu_{\chi N}^2)}$: minimum DM speed required to produce a recoil energy E_R.

Direct detection event rate

- The differential event rate (per unit detector mass):

astrophysics

$$\frac{dR}{dE_R} = \frac{\rho_\chi}{m_\chi m_N} \int_{v>v_{\min}} d^3v \, \frac{d\sigma_{\chi N}}{dE_R} \, v \, f_{\rm det}(\mathbf{v}, t)$$

$v_{\min} = \sqrt{m_N E_R/(2\mu_{\chi N}^2)}$: minimum DM speed required to produce a recoil energy E_R.

- Astrophysical inputs:
  - **local DM density:** *normalization in event rate.*
  - **local DM velocity distribution:** *enters the event rate through an integration.*

Direct detection status

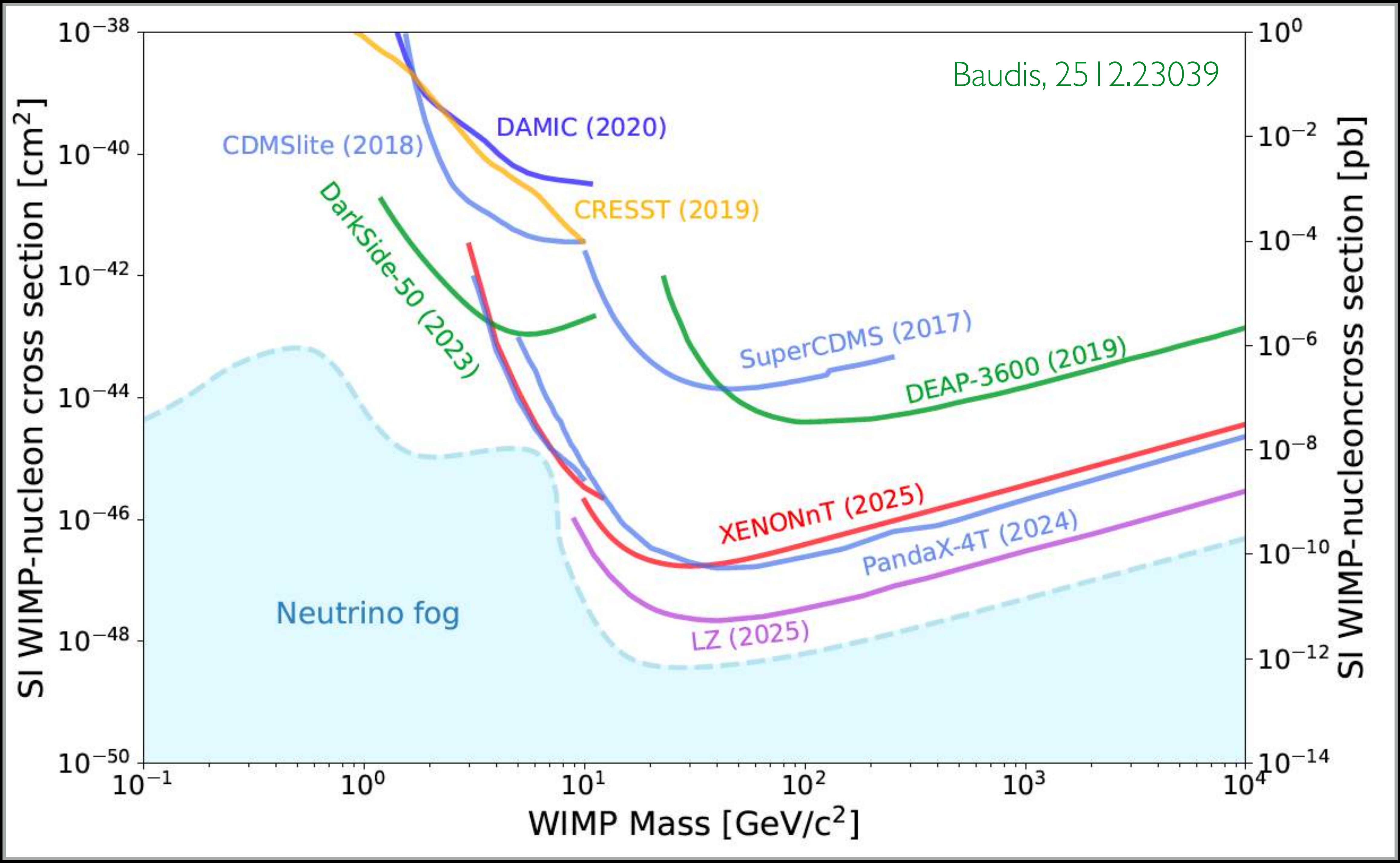

Assumption for the DM distribution: **Standard Halo Model**

Standard Halo Model

- The simplest model for the DM distribution in our Galaxy is the **Standard Halo Model (SHM)**: isothermal sphere with an isotropic Maxwell-Boltzmann velocity distribution.

Drukier, Freese, Spergel, 1986

Standard Halo Model

- Local DM density:

$$\rho_\chi = 0.3\ \mathrm{GeV/cm^3}$$

DM density profile:

$$\rho(r) \propto r^{-2}$$

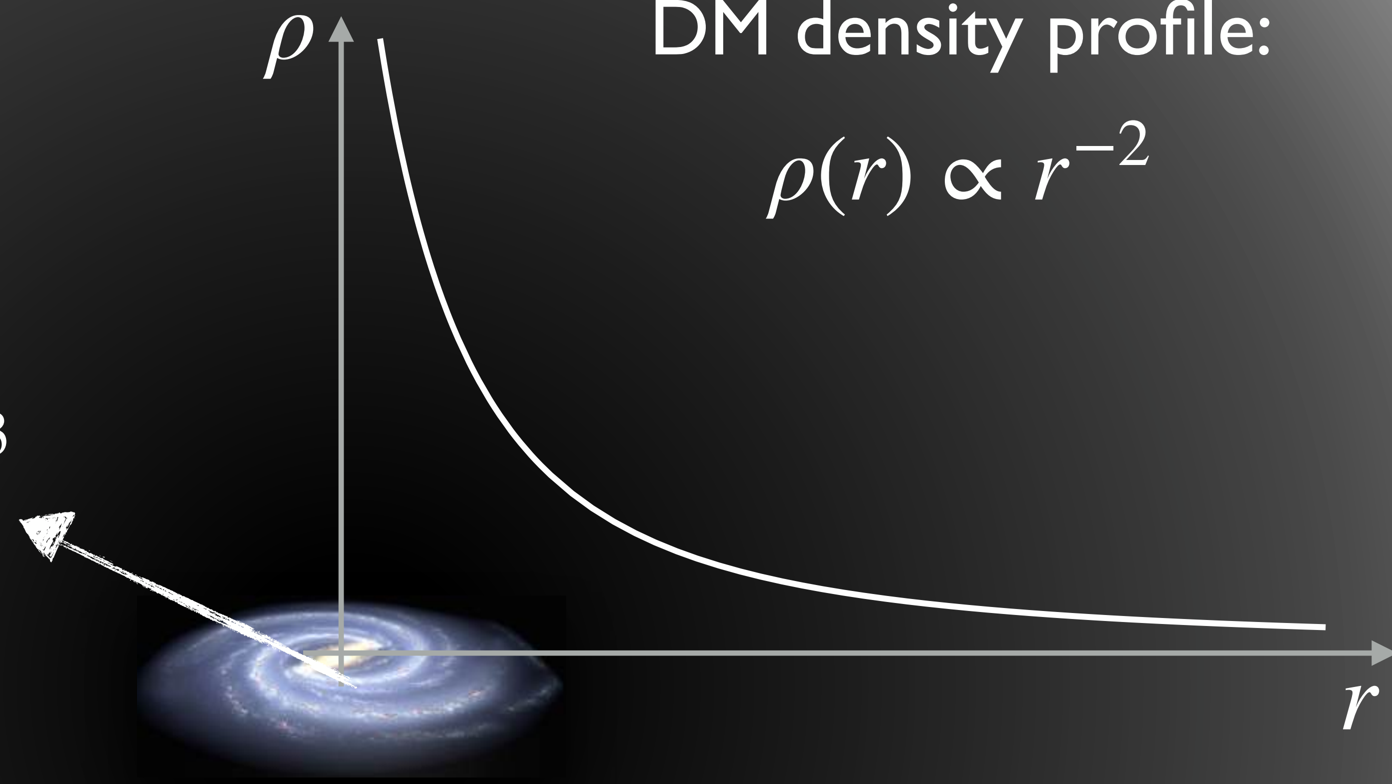

Standard Halo Model

DM density profile:

$$\rho(r) \propto r^{-2}$$

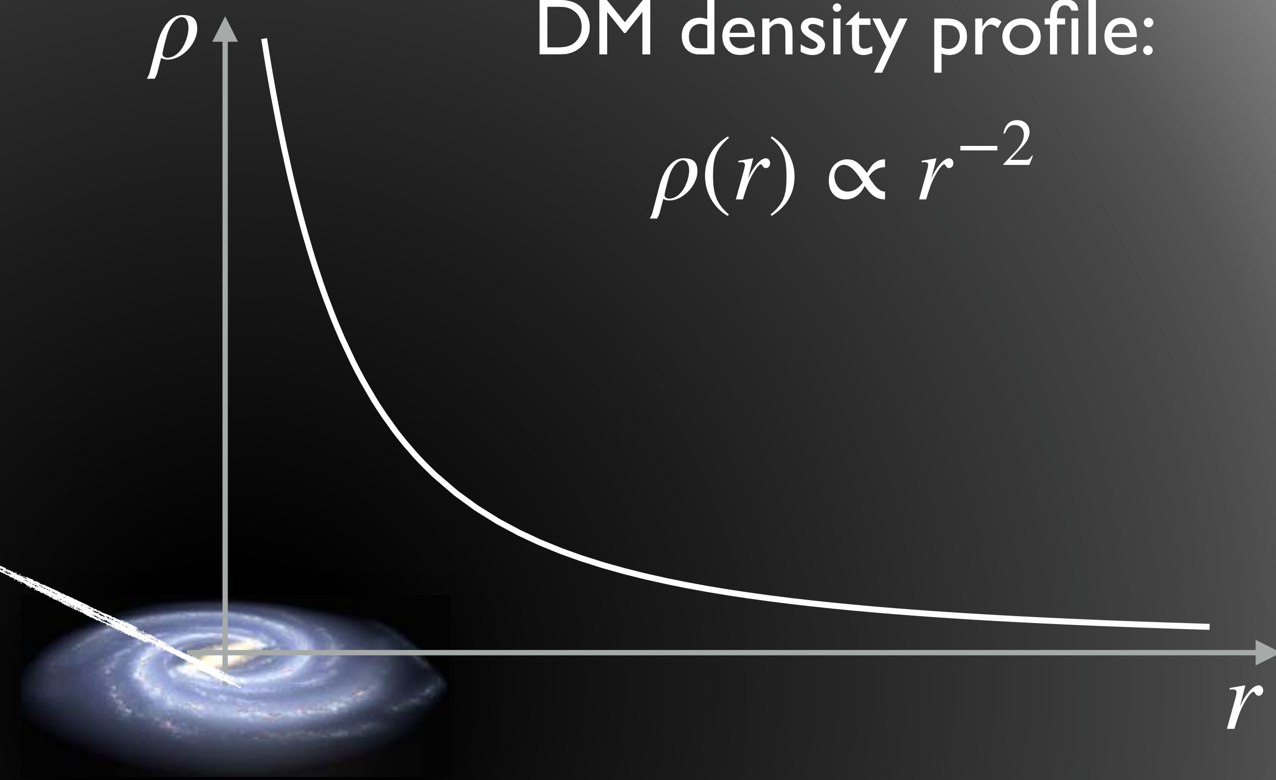

- Local DM density:

$$\rho_\chi = 0.3\ \mathrm{GeV/cm^3}$$

- Most probable DM speed: $v_c = 220\ \mathrm{km/s}$
- Local DM velocity distribution:

$$f_{\mathrm{gal}}(\mathbf{v}) = \begin{cases} N \exp\left(-\mathbf{v}^2/v_c^2\right) & v < v_{\mathrm{esc}} \\ 0 & v \geq v_{\mathrm{esc}} \end{cases}$$

Standard Halo Model

DM density profile:

$$\rho(r) \propto r^{-2}$$

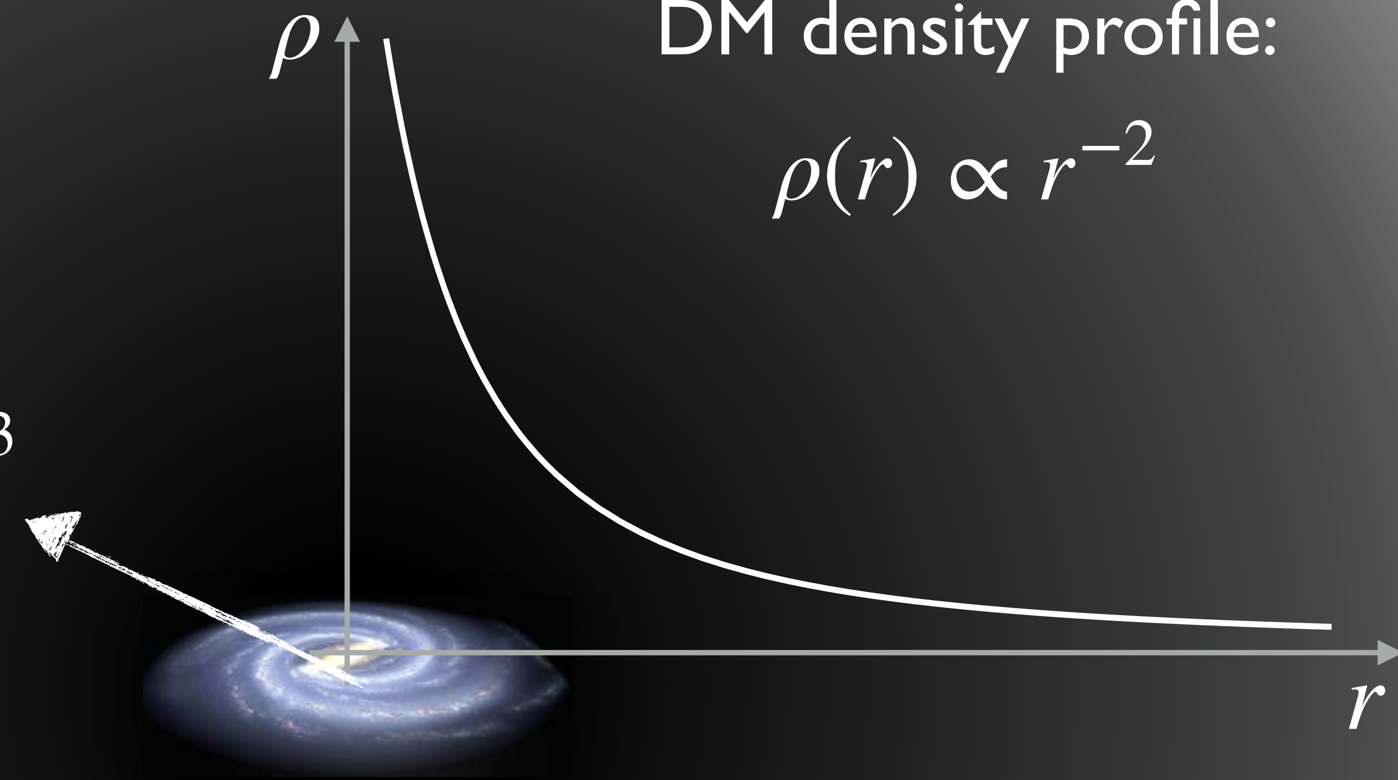

- Local DM density:

$$\rho_\chi = 0.3\ \mathrm{GeV/cm^3}$$

- Most probable DM speed: $v_c = 220\ \mathrm{km/s}$
- Local DM velocity distribution:

$$f_{\mathrm{gal}}(\mathbf{v}) = \begin{cases} N \exp\left(-\mathbf{v}^2/v_c^2\right) & v < v_{\mathrm{esc}} \\ 0 & v \geq v_{\mathrm{esc}} \end{cases}$$

How accurate is this picture?

Astrophysical uncertainties

- **Local DM density:** *Estimates from observations are model dependent and vary in the literature:*

$$\rho_\chi = (0.2 - 0.8)\ \mathrm{GeV/cm^3}$$

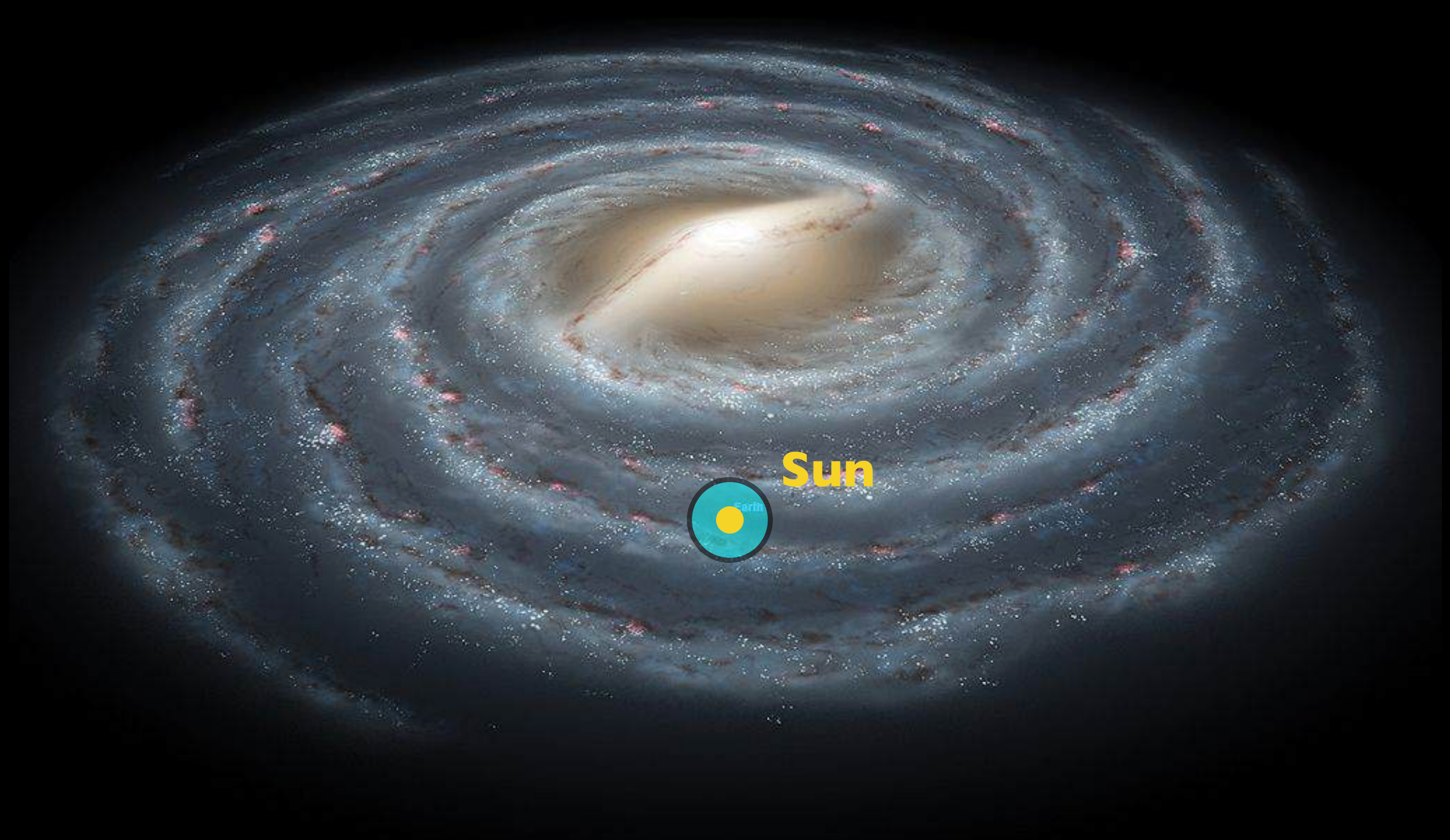

Astrophysical uncertainties

- **Local DM density:** *Estimates from observations are model dependent and vary in the literature:*

$$\rho_\chi = (0.2 - 0.8)\ \mathrm{GeV/cm^3}$$

- **Local DM velocity distribution:** *cannot be directly measured, but we can infer it from cosmological simulations and observations.*

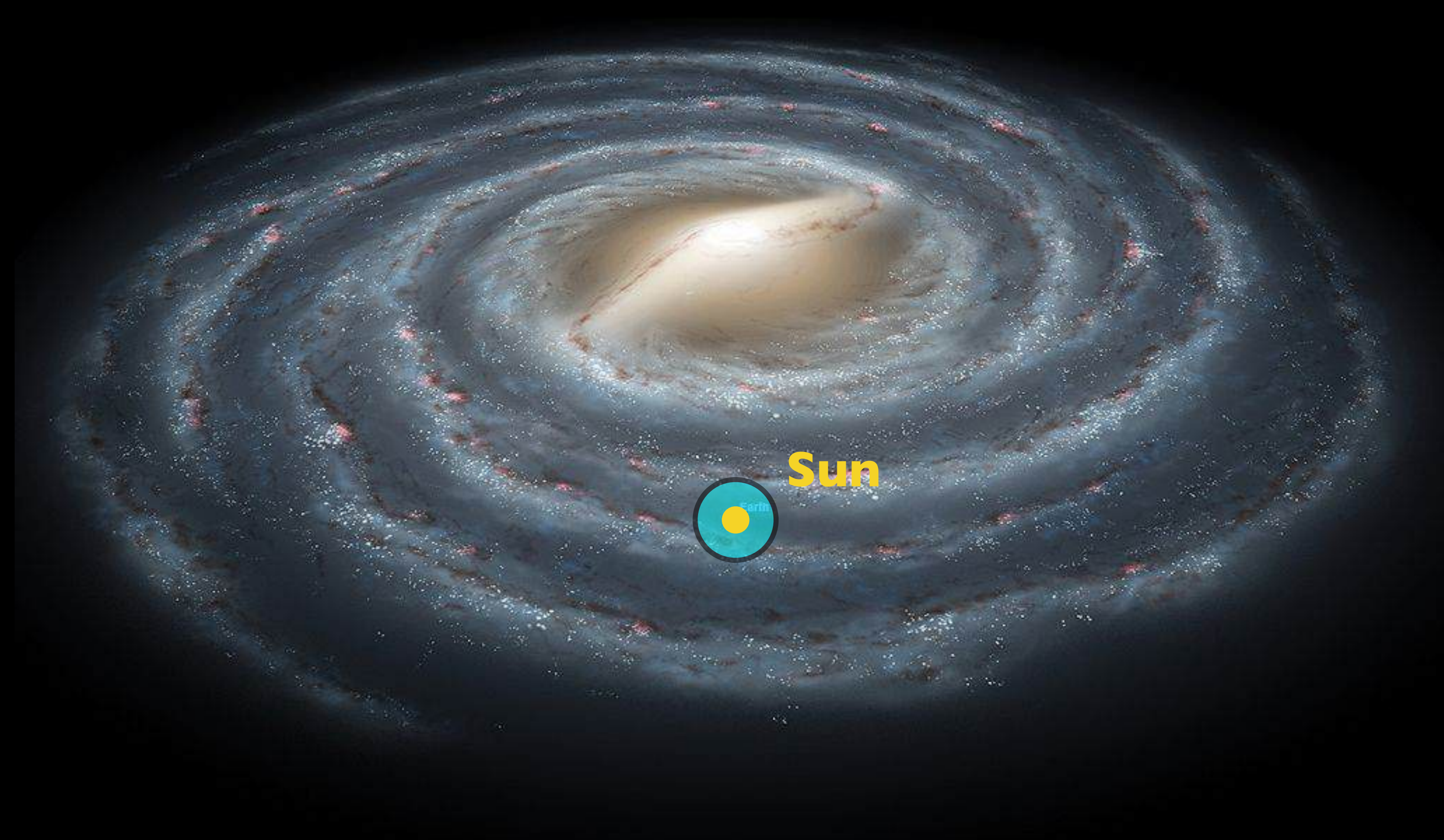

The dark matter halo

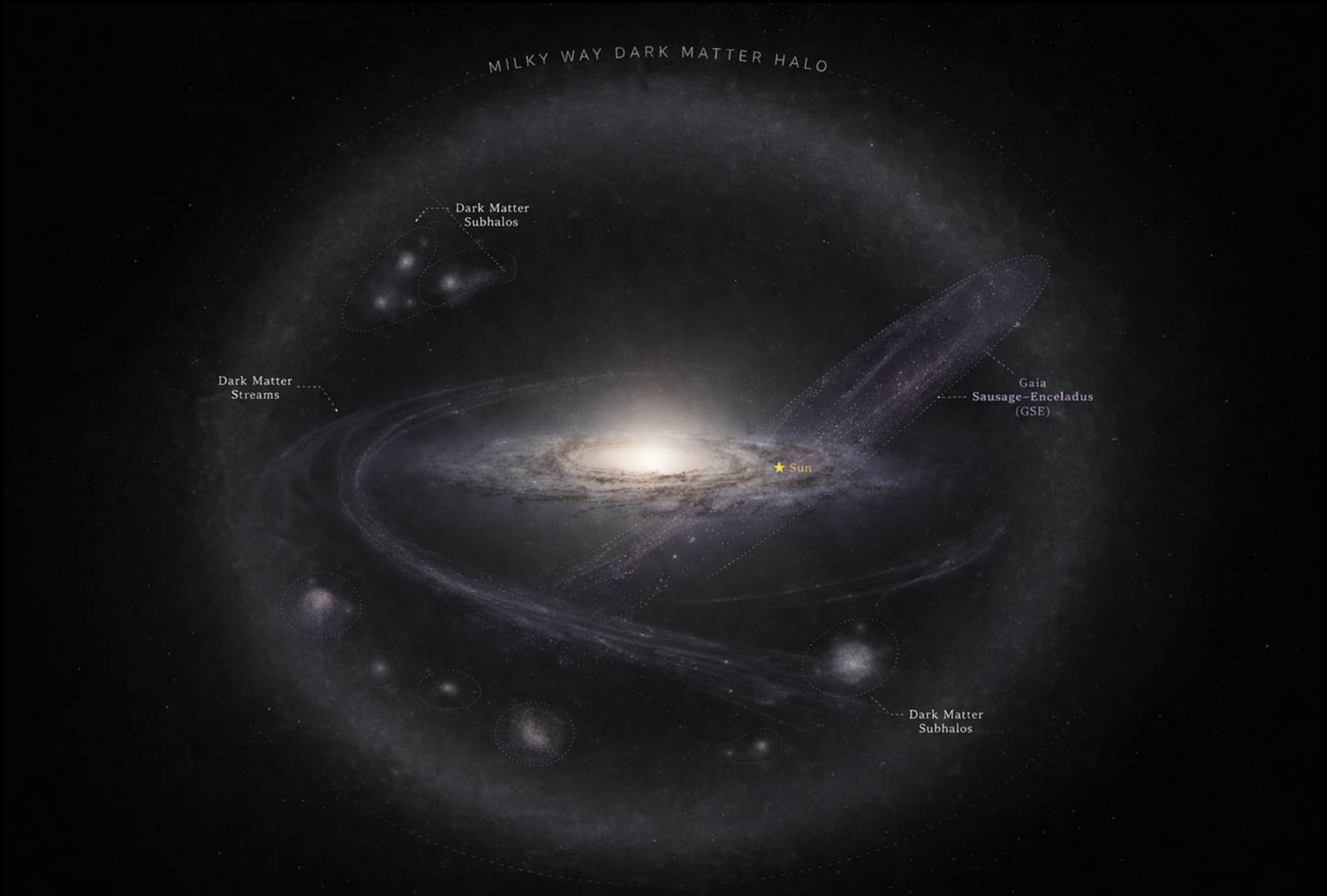

The dark matter halo

The DM halo has both smooth and un-virialized components:

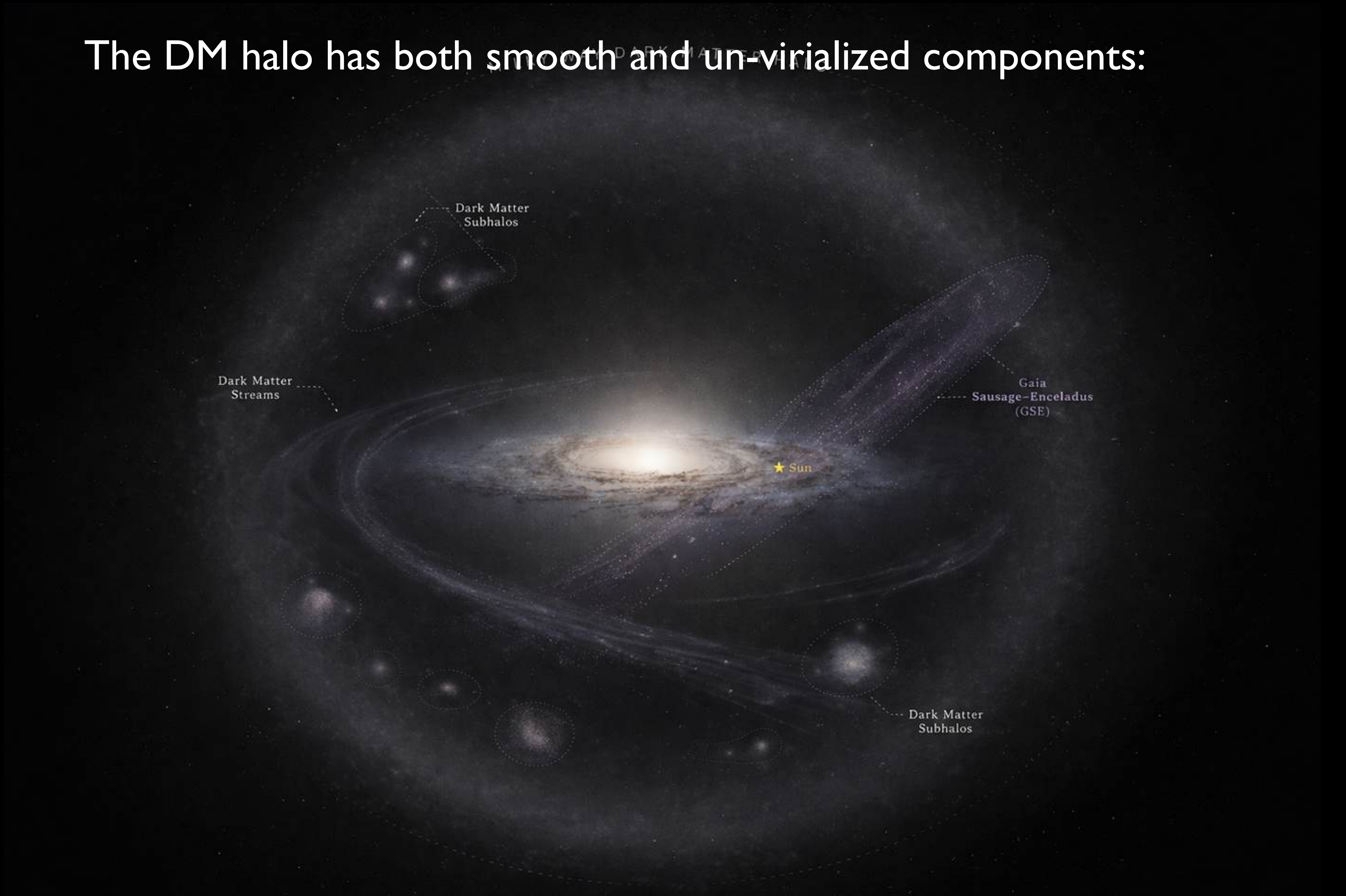

The dark matter halo

The DM halo has both smooth and un-virialized components:

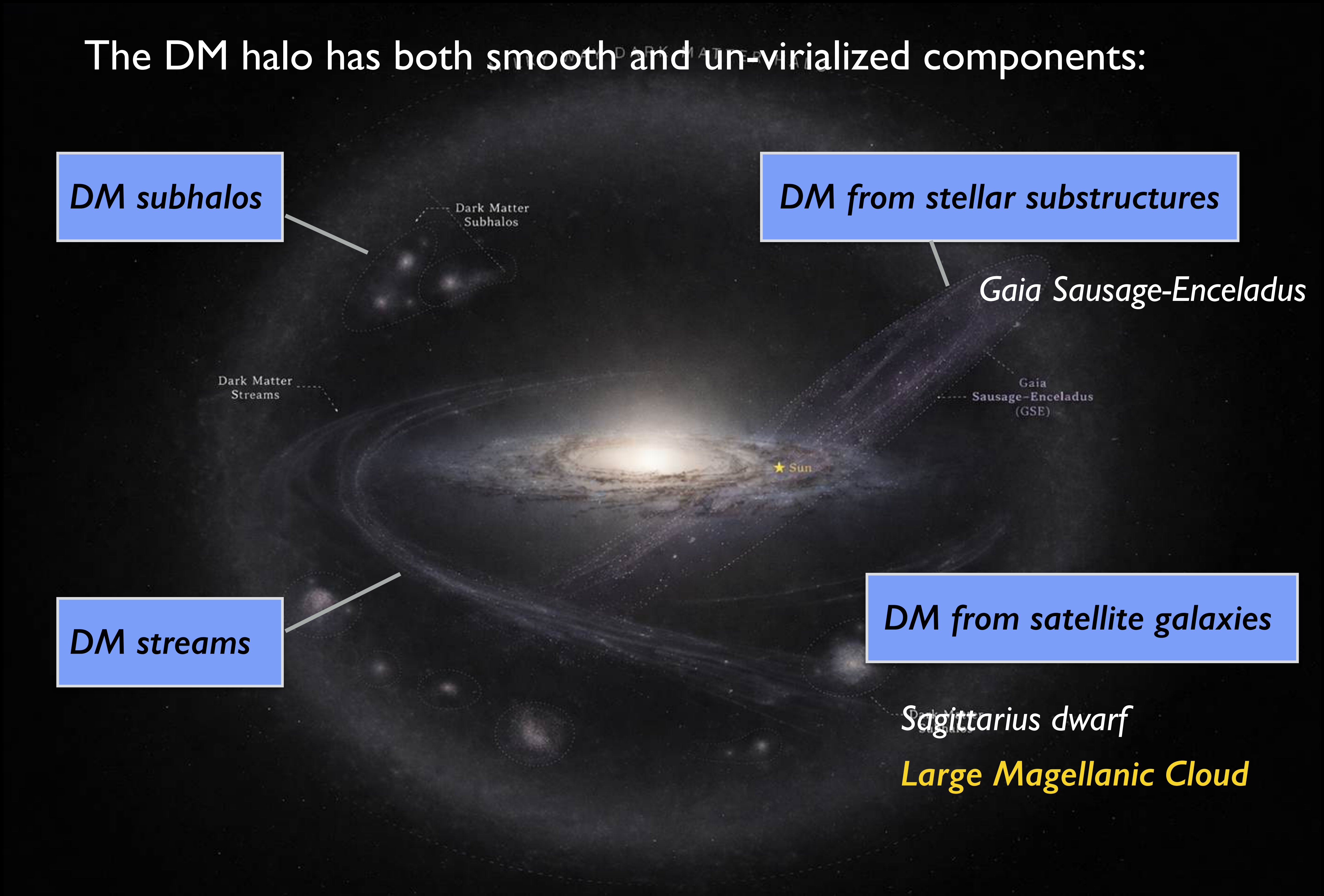

The Large Magellanic Cloud

The **LMC** is the most massive satellite of the Milky Way and on its first passage around the Galaxy.

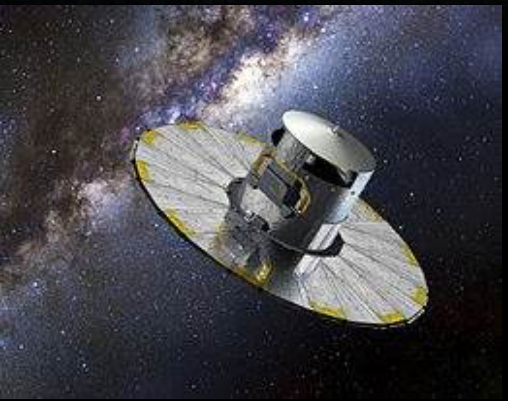

Gaia's EDR3 sky map. Credit: ESA/Gaia/DPAC

The impact of the LMC

The **LMC** introduces perturbations in the DM and stellar halo.

DM halo

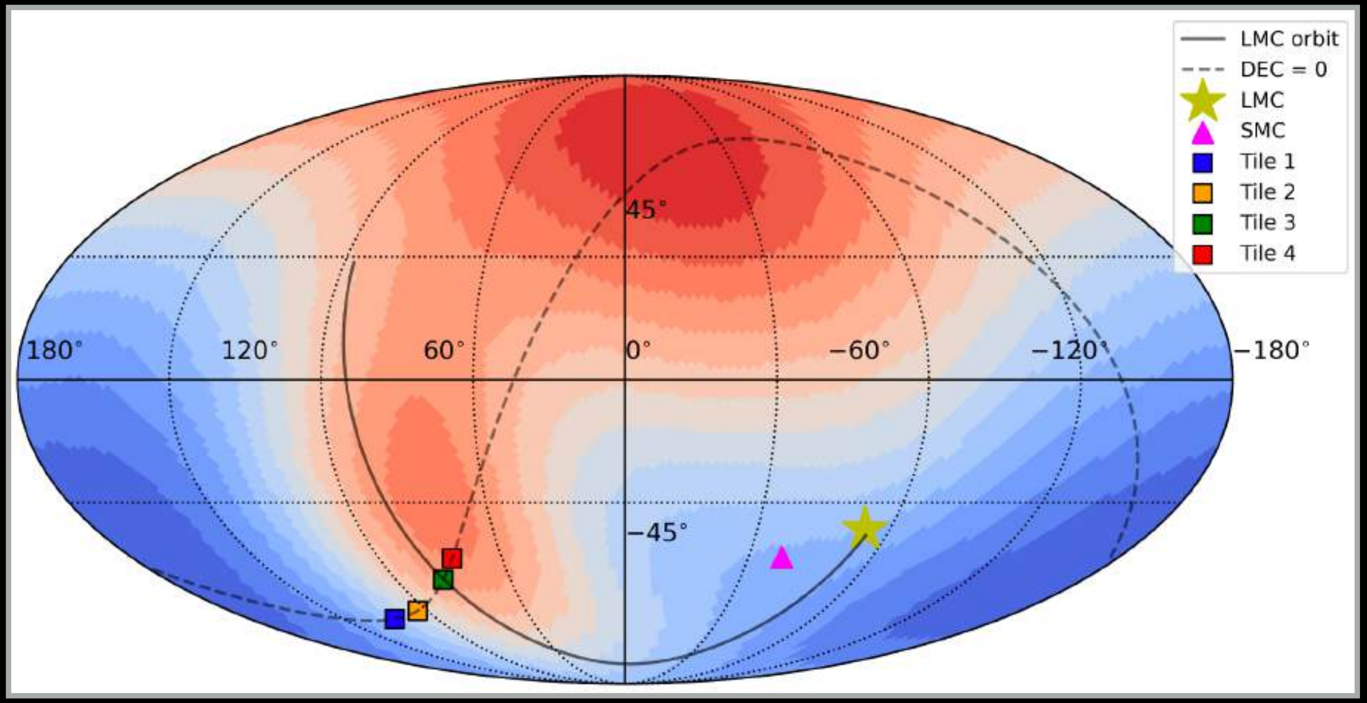

Cavieres et al., ApJ 983, 83 (2025)
Garavito-Camargo et al., ApJ 919, 2, 109 (2021)
Garavito-Camargo et al., ApJ 884, 51 (2019)

Stellar halo

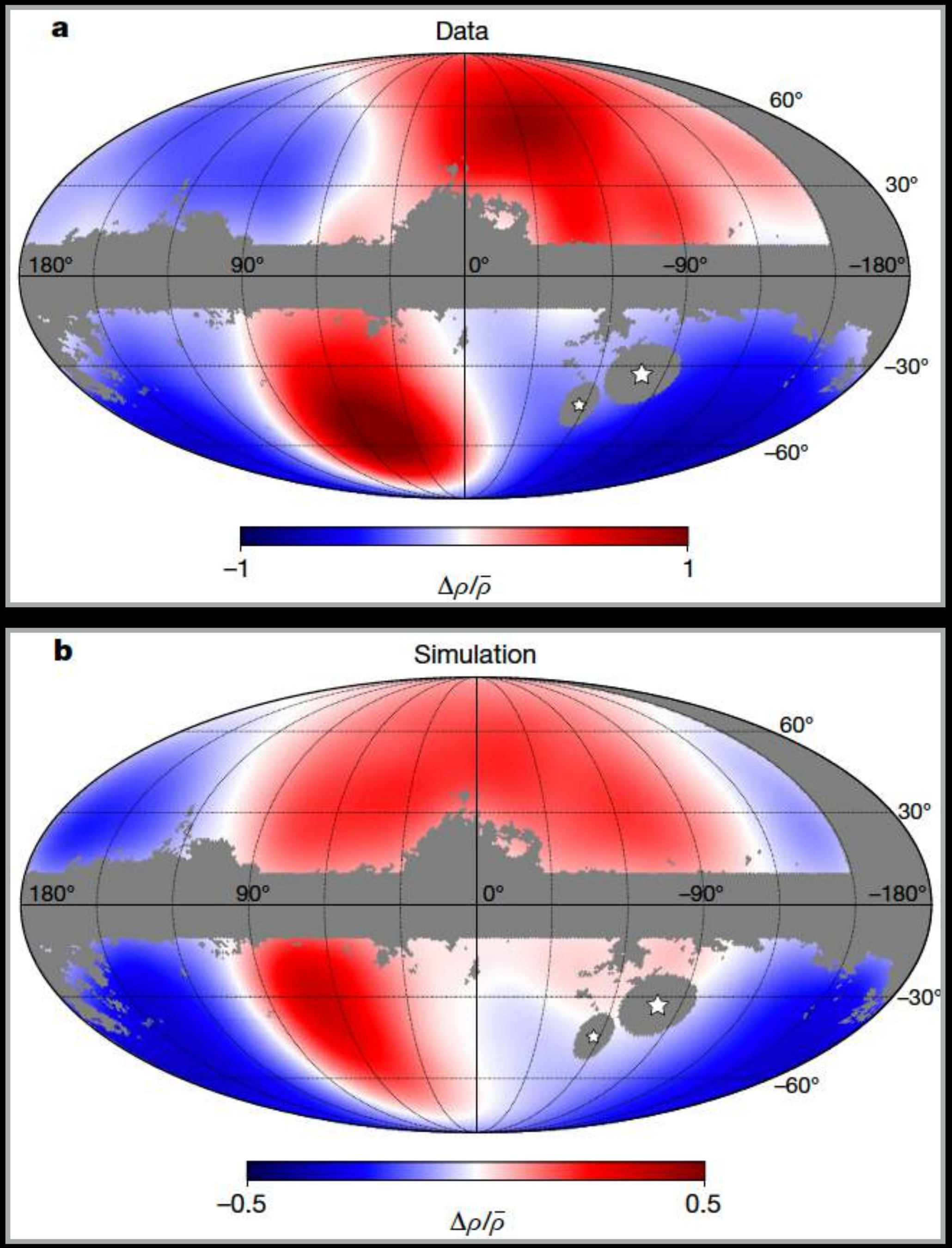

Conroy et al., Nature 592, 534–536 (2021)

The impact of the LMC

The **LMC** introduces perturbations in the DM and stellar halo.

Stellar halo

DM halo

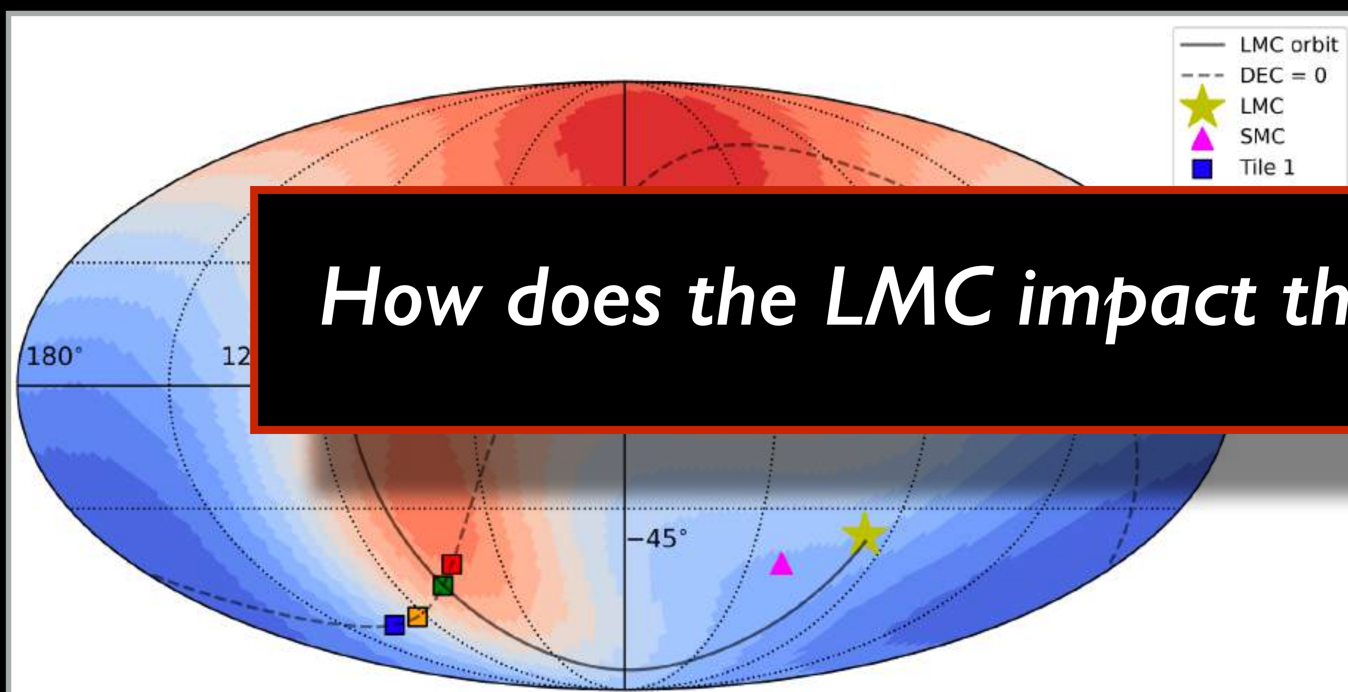

How does the LMC impact the local DM distribution?

Cavieres et al., ApJ 983, 83 (2025)
Garavito-Camargo et al., ApJ 919, 2, 109 (2021)
Garavito-Camargo et al., ApJ 884, 51 (2019)

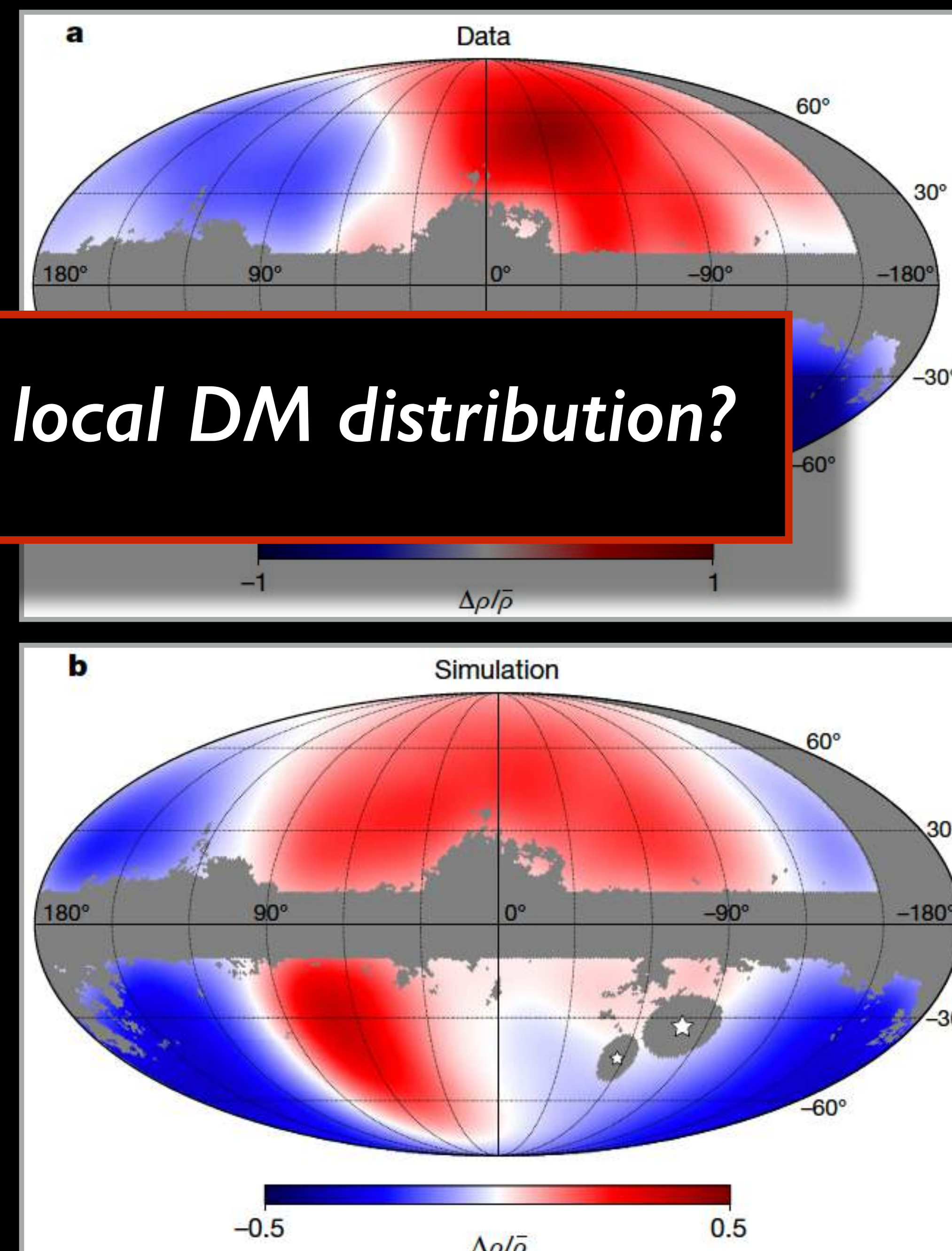

Conroy et al., Nature 592, 534–536 (2021)

Local dark matter velocity distribution

- The **LMC** is moving in the opposite direction of the Solar motion.
  → Large relative speeds of LMC DM particles with respect to Sun.

Local dark matter velocity distribution

- The **LMC** is moving in the opposite direction of the Solar motion.
  → Large relative speeds of LMC DM particles with respect to Sun.
  → *Impacts the high speed tail of the local DM distribution*

Local dark matter velocity distribution

- The **LMC** is moving in the opposite direction of the Solar motion.
  → Large relative speeds of LMC DM particles with respect to Sun.
  → *Impacts the high speed tail of the local DM distribution*

- Studied in specially designed idealized simulations.

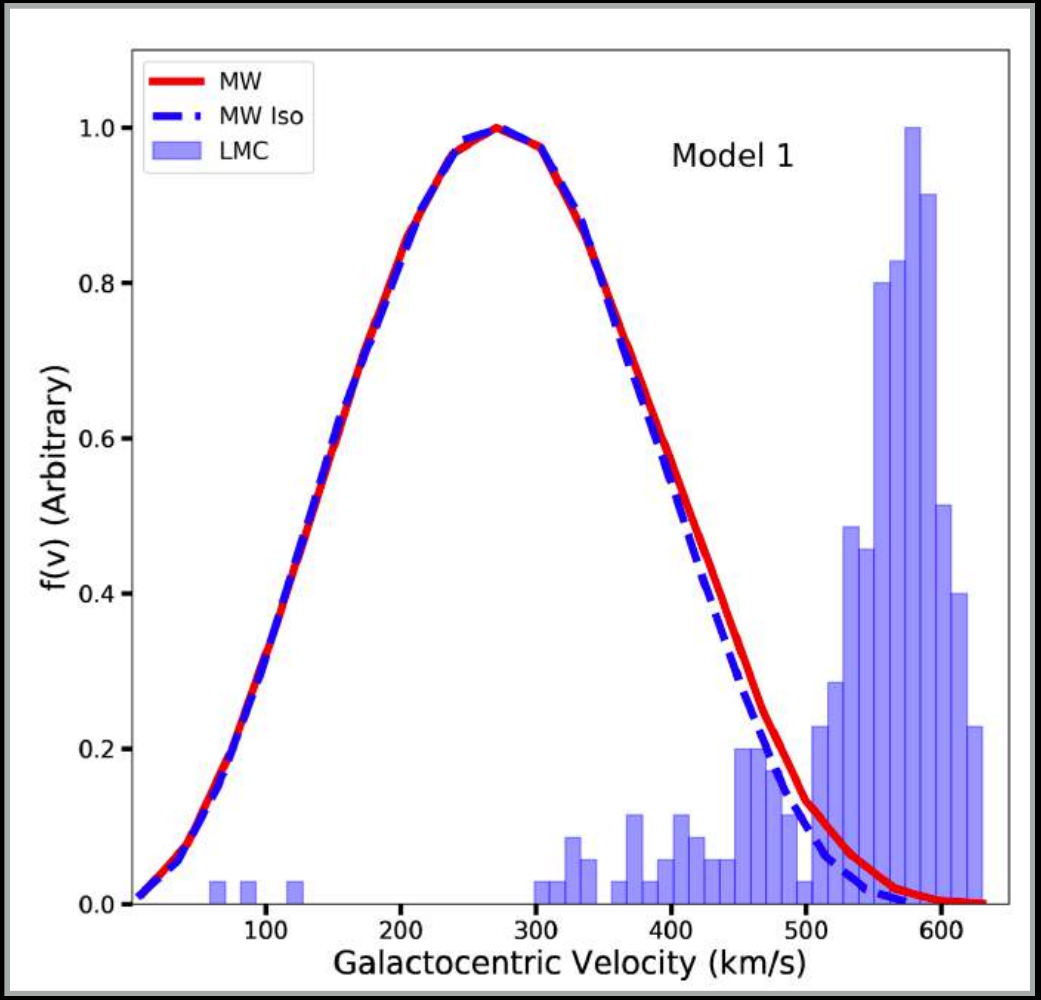

Besla et al., JCAP 11, 013 (2019)
See also: Donaldson et al., MNRAS 513, 1, 46 (2022)

Local dark matter velocity distribution

- The **LMC** is moving in the opposite direction of the Solar motion.
  → Large relative speeds of LMC DM particles with respect to Sun.
  → *Impacts the high speed tail of the local DM distribution*
- Studied in specially designed idealized simulations.

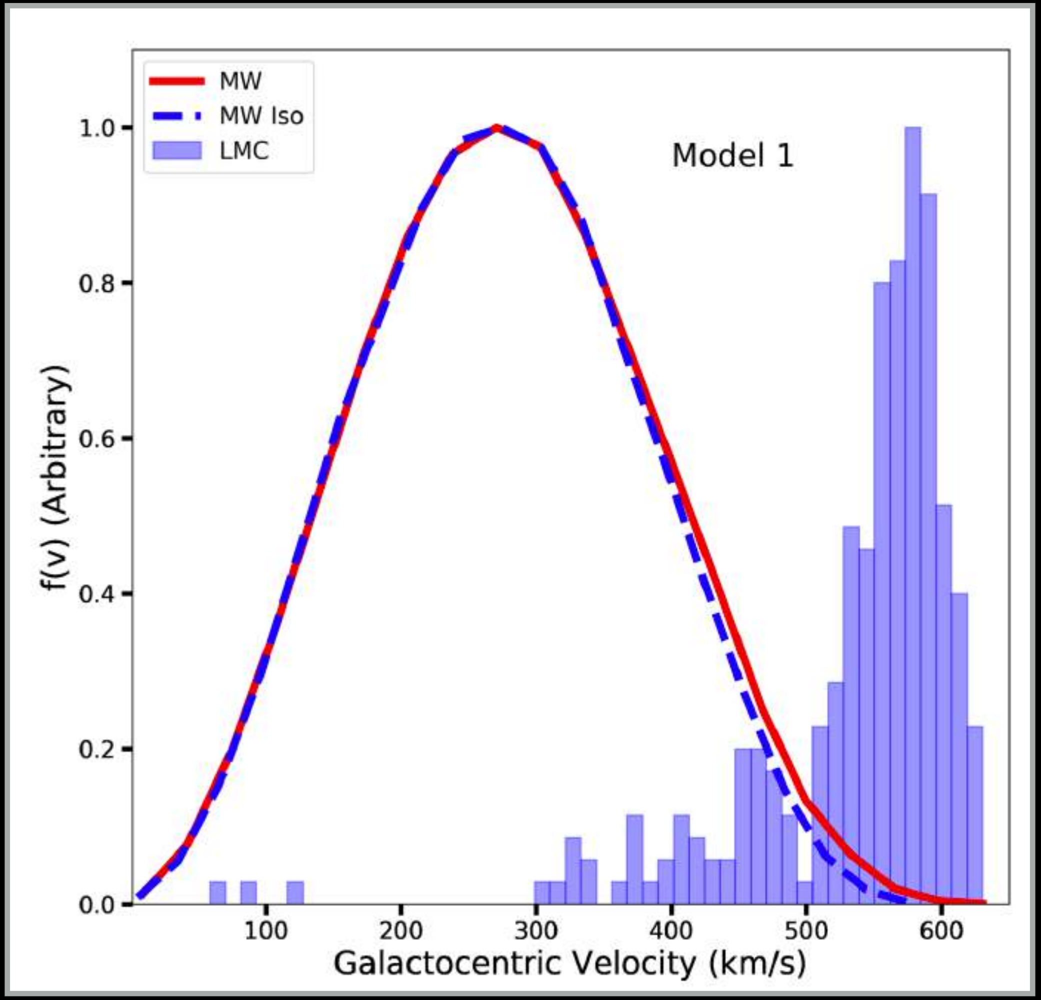

Are these results valid for fully cosmological halos with complex accretion histories?

Besla et al., JCAP 11, 013 (2019)
See also: Donaldson et al., MNRAS 513, 1, 46 (2022)

Auriga cosmological simulations

- State-of-the-art cosmological magneto-hydrodynamical zoom-in simulations of Milky Way size halos.

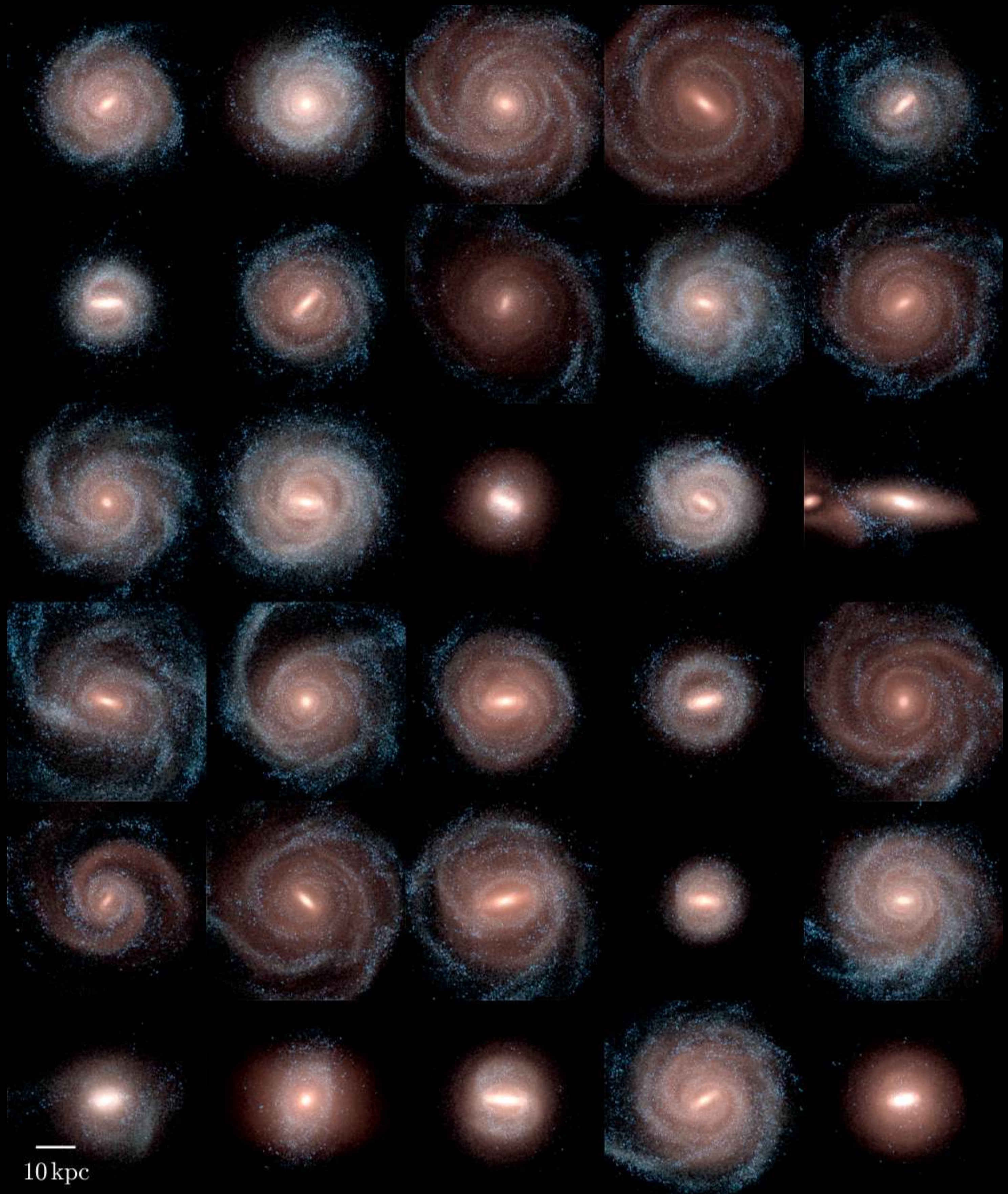

Auriga cosmological simulations

- State-of-the-art cosmological magneto-hydrodynamical zoom-in simulations of Milky Way size halos.
- Identify **Milky Way-LMC analogues** based on **LMC's stellar mass** and **distance from host** at first pericenter approach.

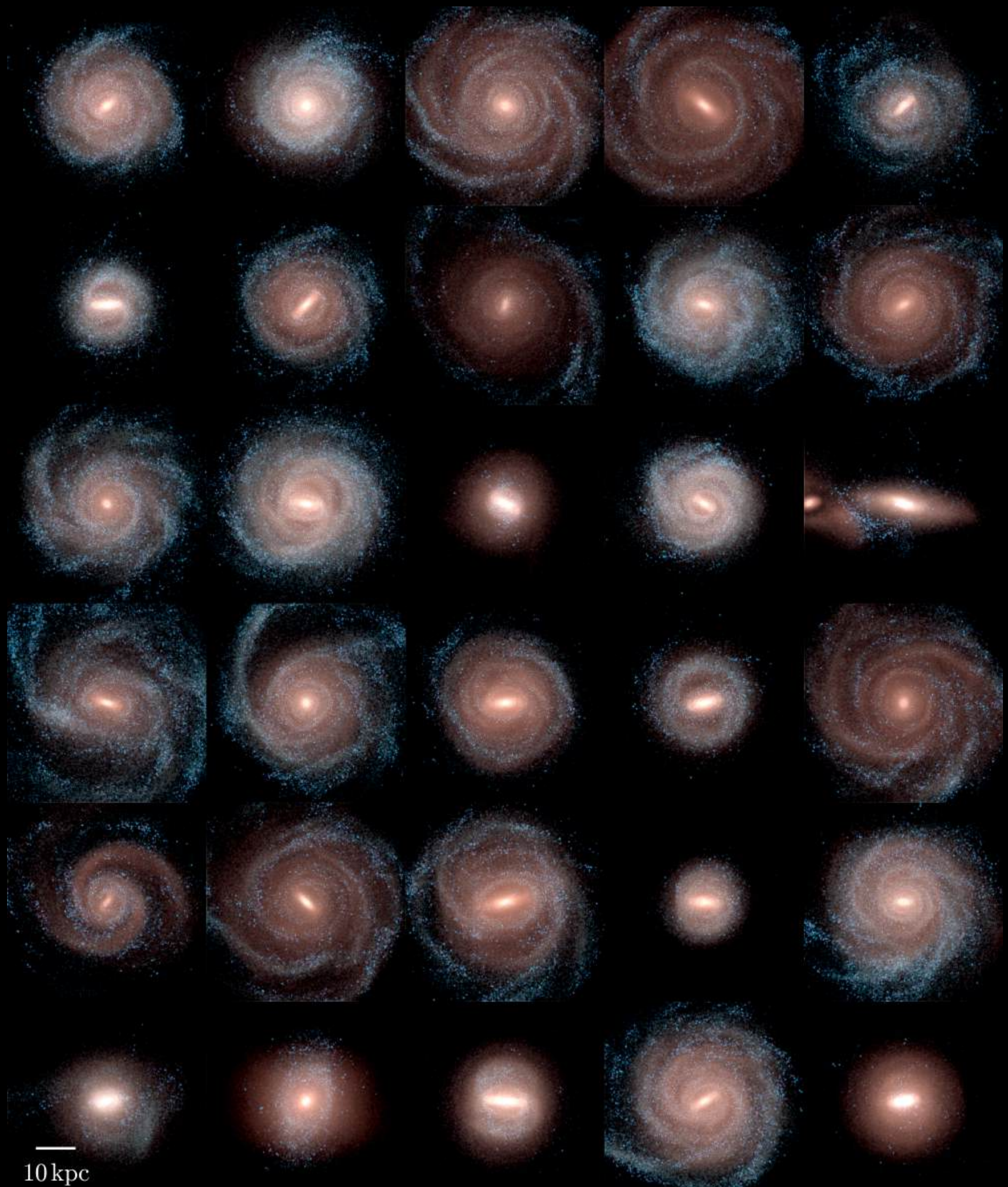

Auriga cosmological simulations

- Consider one **Milky Way-LMC analogue** and study the impact of the LMC on the local DM distribution at different times (snapshots) in its orbit.

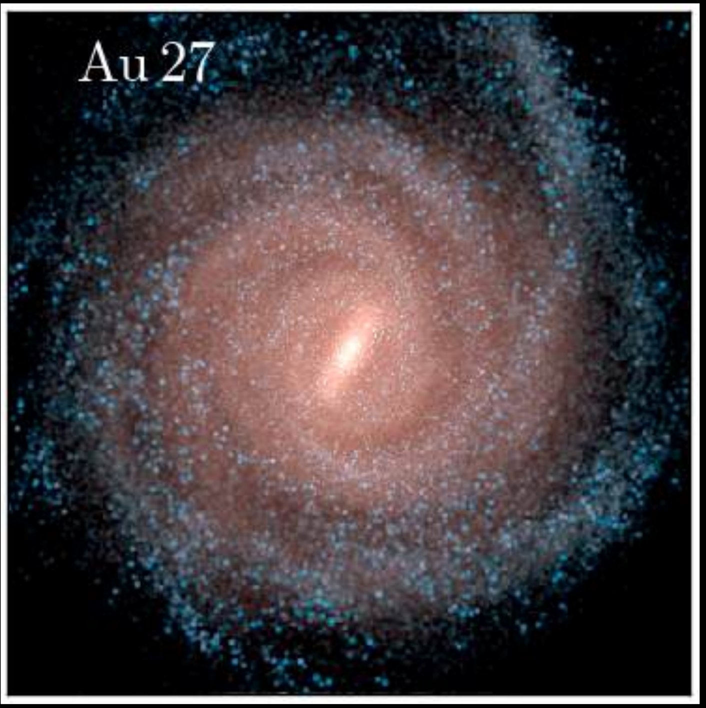

Auriga cosmological simulations

- Consider one **Milky Way-LMC analogue** and study the impact of the LMC on the local DM distribution at different times (snapshots) in its orbit.

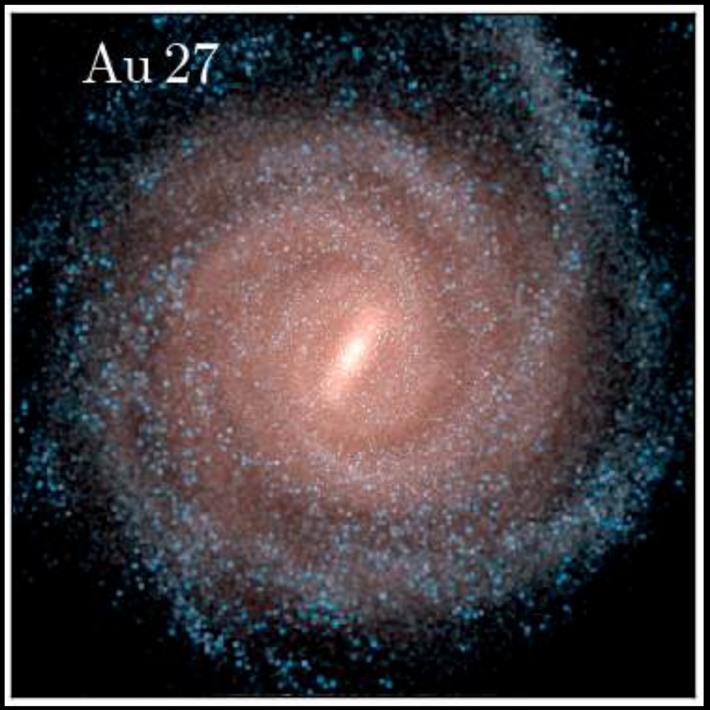

- Four representative snapshots:

Snapshot	Description	$t - t_{\mathrm{Pres.}}$ [Gyr]	r_{LMC} [kpc]
Iso.	Isolated MW analogue	-2.83	384
Peri.	LMC's 1st pericenter approach	-0.133	32.9
Pres.	Present day MW-LMC analogue	0	50.6
Fut.	Future MW-LMC analogue	0.175	80.3

Auriga cosmological simulations

- Consider one **Milky Way-LMC analogue** and study the impact of the LMC on the local DM distribution at different times (snapshots) in its orbit.

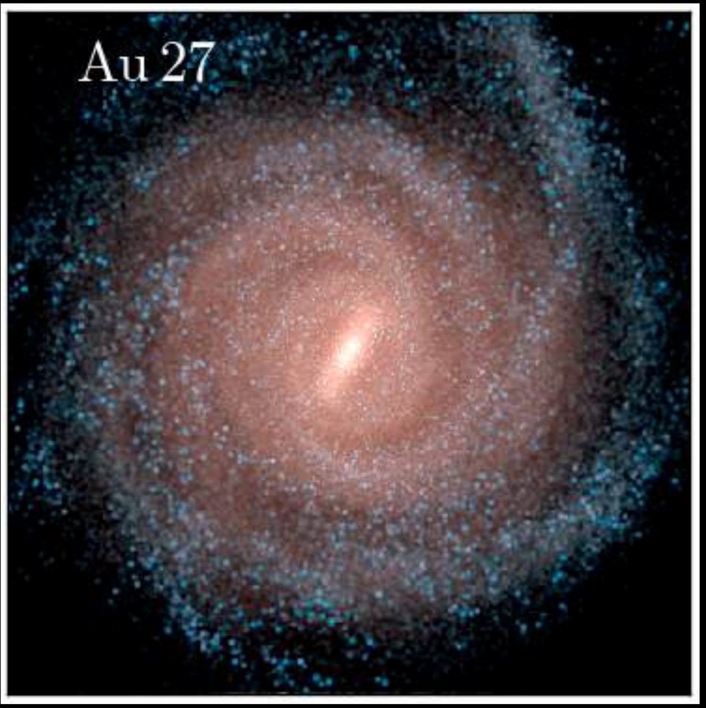

- Four representative snapshots:

Snapshot	Description	$t - t_{\rm Pres.}$ [Gyr]	$r_{\rm LMC}$ [kpc]
Iso.	Isolated MW analogue	-2.83	384
Peri.	LMC's 1st pericenter approach	-0.133	32.9
Pres.	Present day MW-LMC analogue	0	50.6
Fut.	Future MW-LMC analogue	0.175	80.3

Local dark matter velocity distribution

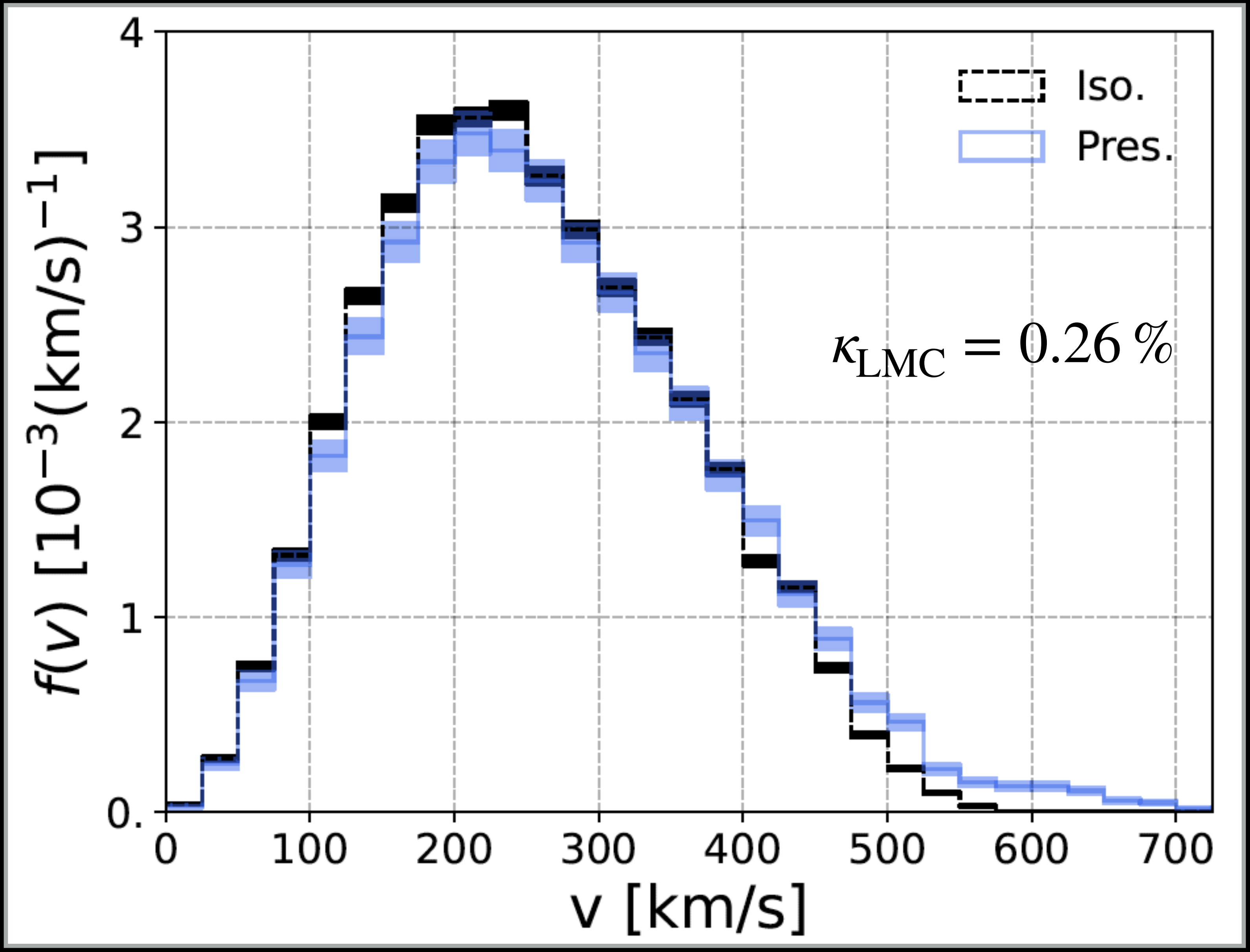

Smith-Orlik, Ronaghi, **NB** et al., JCAP 10, 070 (2023)
Reynoso, **NB**, Piro, JCAP 12, 037 (2024)

Local dark matter velocity distribution

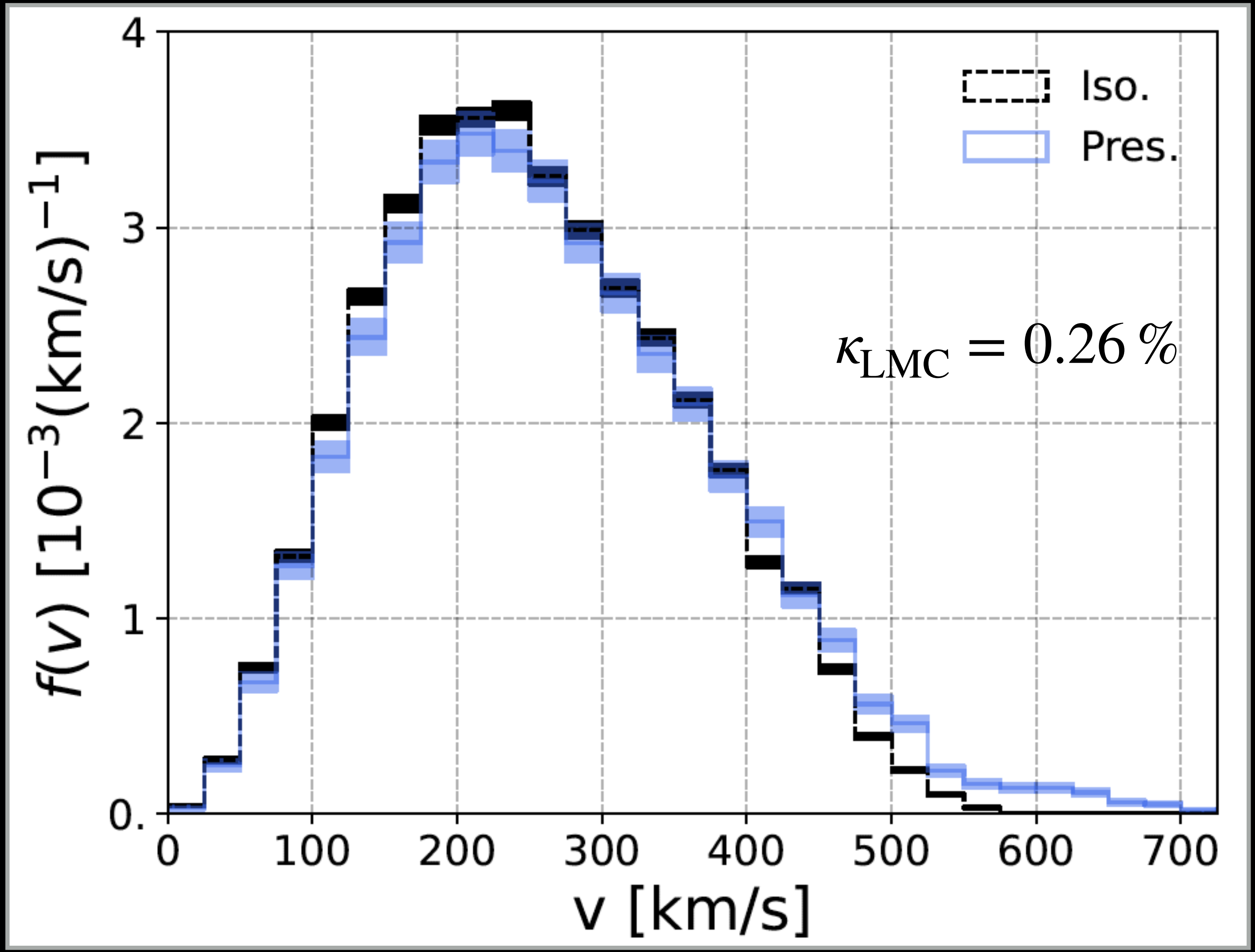

Smith-Orlik, Ronaghi, **NB** et al., JCAP 10, 070 (2023)
Reynoso, **NB**, Piro, JCAP 12, 037 (2024)

- **Two effects:** High speed LMC particles in the Solar region + boosted Milky Way particles in response to the LMC

Implications for direct detection

Simulate the signal in an idealized near-future **Xe-based detector:**

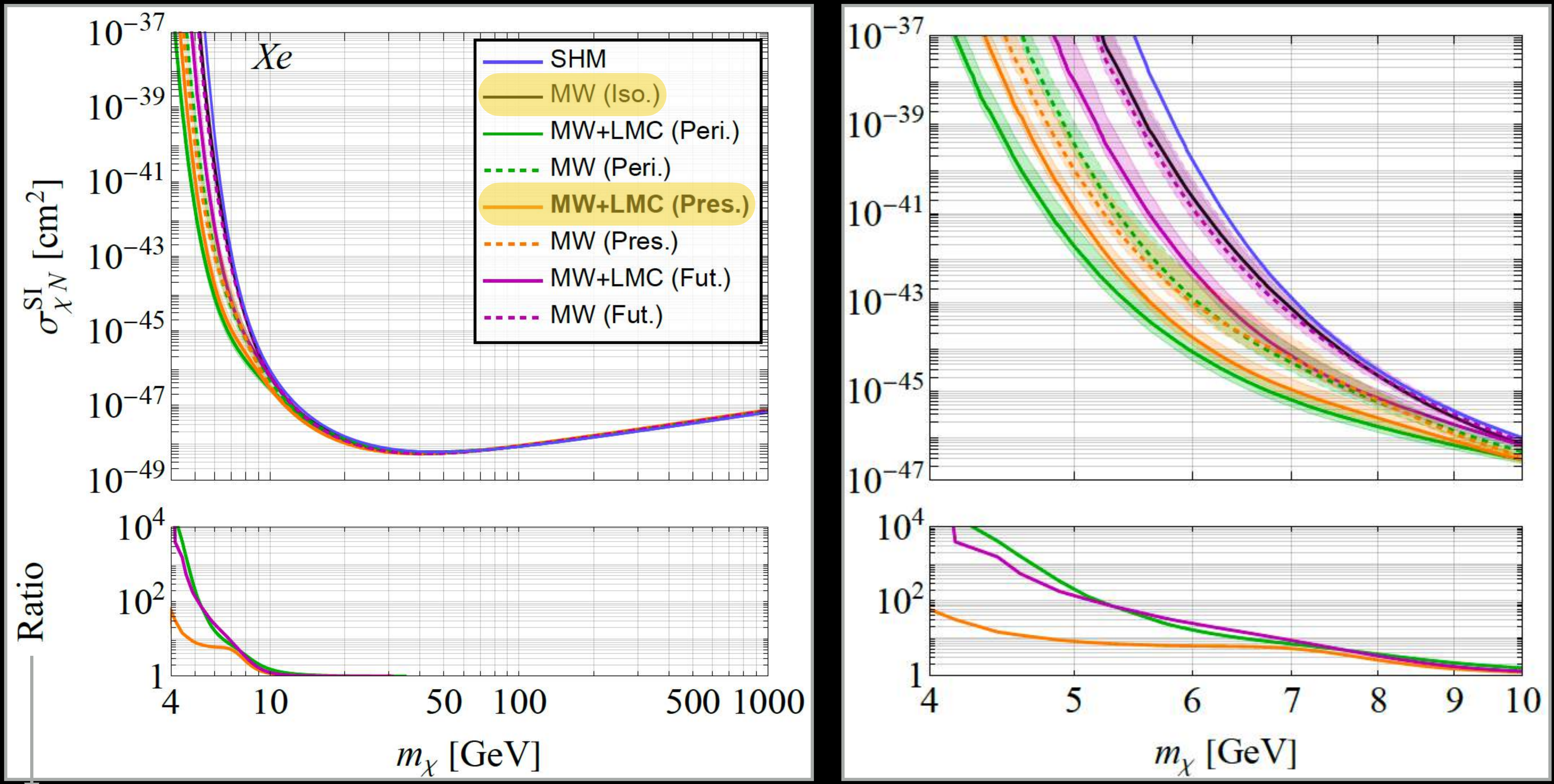

$$\text{Ratio} = \frac{\sigma^{SI}_{\chi,\text{MW}}}{\sigma^{SI}_{\chi,\text{MW+LMC}}}$$

Smith-Orlik, Ronaghi, **NB** et al., JCAP 10, 070 (2023)

Fix $\rho_\chi = 0.3\ \text{GeV/cm}^3$

Implications for direct detection

Simulate the signal in an idealized near-future **Xe-based detector:**

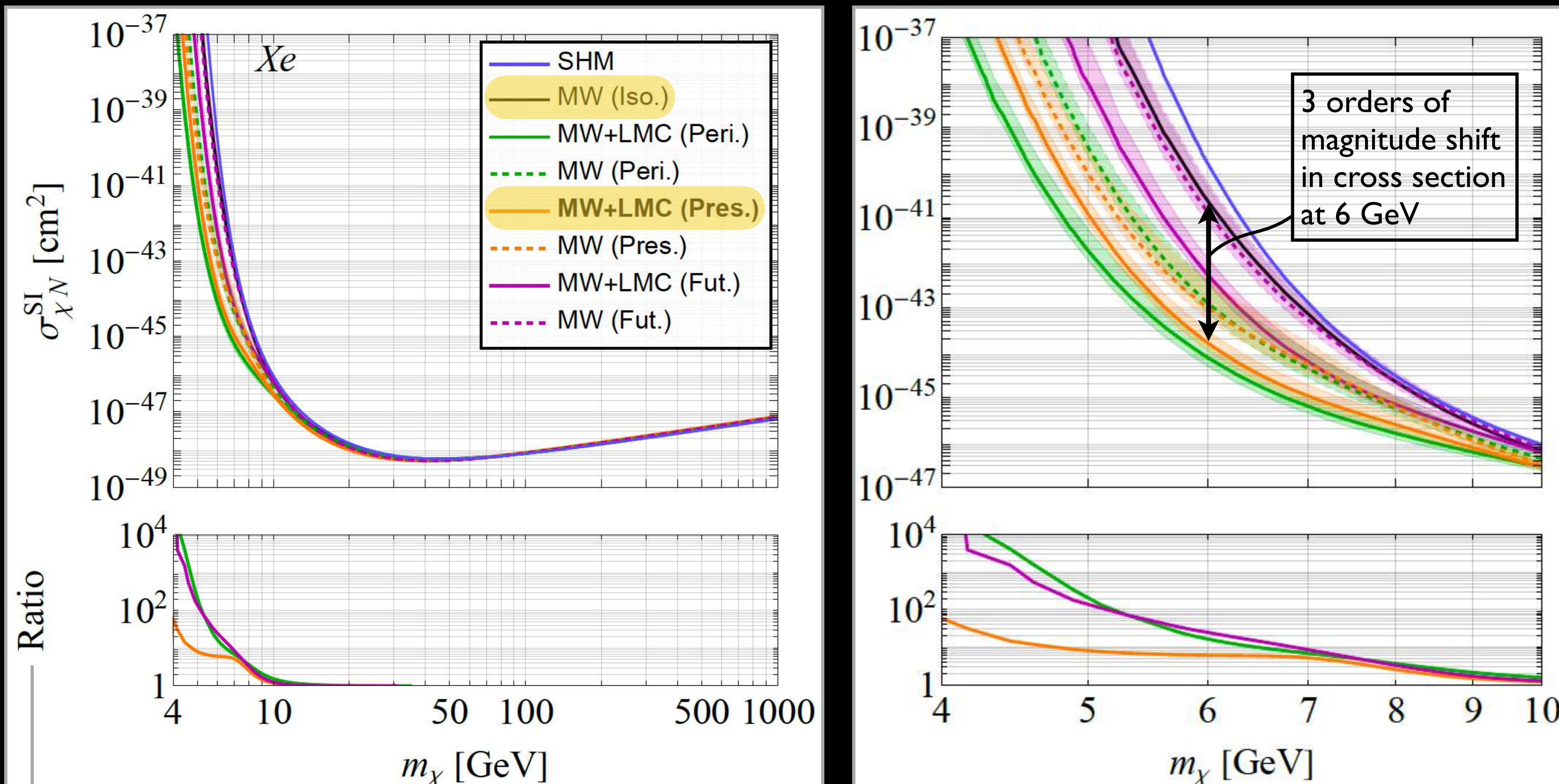

$$\text{Ratio} = \frac{\sigma^{\rm SI}_{\chi,\rm MW}}{\sigma^{\rm SI}_{\chi,\rm MW+LMC}}$$

Smith-Orlik, Ronaghi, **NB** et al., JCAP 10, 070 (2023)

Fix $\rho_\chi = 0.3\ \text{GeV/cm}^3$

Implications for direct detection

Simulate the signal in an idealized near-future **Xe-based detector:**

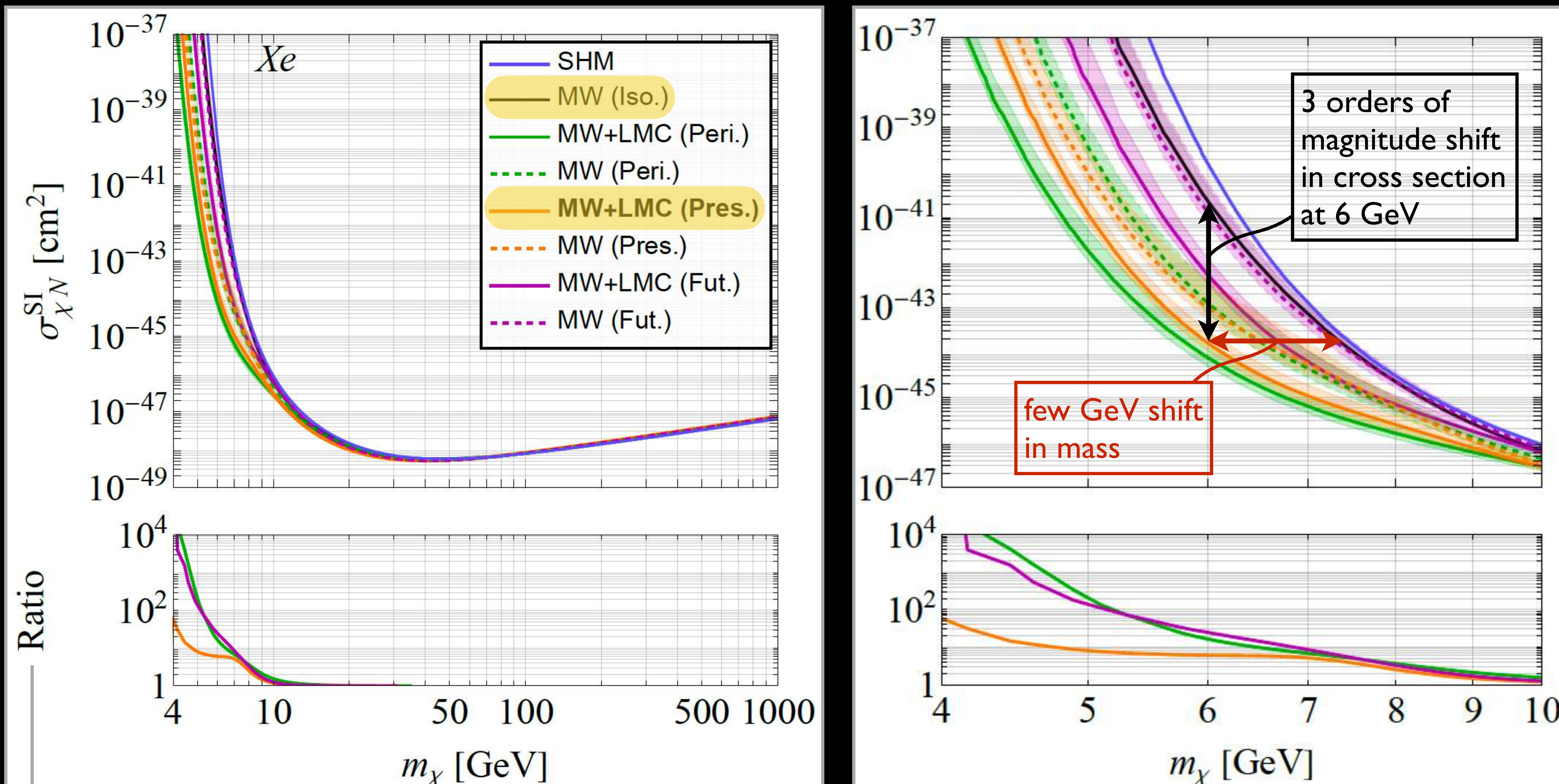

$$\text{Ratio} = \frac{\sigma^{\rm SI}_{\chi,\rm MW}}{\sigma^{\rm SI}_{\chi,\rm MW+LMC}}$$

Smith-Orlik, Ronaghi, **NB** et al., JCAP 10, 070 (2023)

Fix $\rho_\chi = 0.3\ \text{GeV/cm}^3$

Implications for direct detection

Simulate the signal in an idealized near-future **Xe-based detector:**

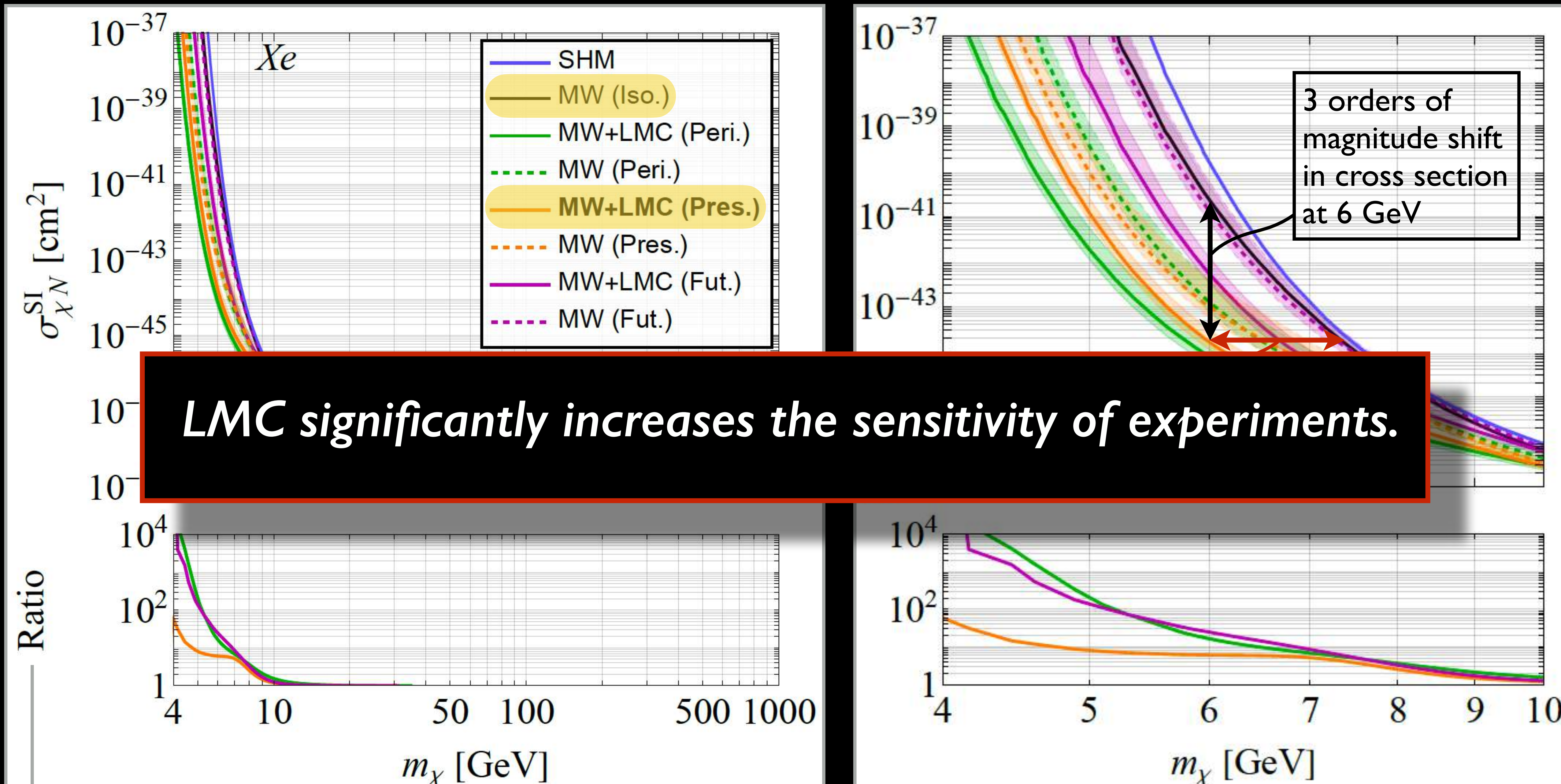

LMC significantly increases the sensitivity of experiments.

$$\text{Ratio} = \frac{\sigma^{SI}_{\chi,\text{MW}}}{\sigma^{SI}_{\chi,\text{MW+LMC}}}$$

Smith-Orlik, Ronaghi, **NB** et al., JCAP 10, 070 (2023)

Fix $\rho_\chi = 0.3\ \text{GeV/cm}^3$

Beyond standard interactions

- Parametrize possible DM-nucleon contact interactions using nonrelativistic effective field theory.

Operator	Scaling factor
$\mathcal{O}_1 = 1_\chi 1_N$	1
$\mathcal{O}_3 = i\vec{S}_N \cdot (\vec{q}/m_N \times \vec{v}_\perp)$	$q^2 v_\perp^2,\ q^4$
$\mathcal{O}_4 = \vec{S}_\chi \cdot \vec{S}_N$	1
$\mathcal{O}_5 = i\vec{S}_\chi \cdot (\vec{q}/m_N \times \vec{v}_\perp)$	$q^2 v_\perp^2,\ q^4$
$\mathcal{O}_6 = \left(\vec{S}_\chi \cdot \vec{q}/m_N\right)\left(\vec{S}_N \cdot \vec{q}/m_N\right)$	q^4
$\mathcal{O}_7 = \vec{S}_N \cdot \vec{v}_\perp$	$v_\perp^2$
$\mathcal{O}_8 = \vec{S}_\chi \cdot \vec{v}_\perp$	$v_\perp^2,\ q^2$
$\mathcal{O}_9 = i\vec{S}_\chi \cdot \left(\vec{S}_N \times \vec{q}/m_N\right)$	q^2
$\mathcal{O}_{10} = i\vec{S}_N \cdot \vec{q}/m_N$	q^2
$\mathcal{O}_{11} = i\vec{S}_\chi \cdot \vec{q}/m_N$	q^2
$\mathcal{O}_{12} = \vec{S}_\chi \cdot \left(\vec{S}_N \times \vec{v}_\perp\right)$	$v_\perp^2,\ q^2$
$\mathcal{O}_{13} = i\left(\vec{S}_\chi \cdot \vec{v}_\perp\right)\left(\vec{S}_N \cdot \vec{q}/m_N\right)$	$q^2 v_\perp^2,\ q^4$
$\mathcal{O}_{14} = i\left(\vec{S}_\chi \cdot \vec{q}/m_N\right)\left(\vec{S}_N \cdot \vec{v}_\perp\right)$	$q^2 v_\perp^2$
$\mathcal{O}_{15} = -\left(\vec{S}_\chi \cdot \vec{q}/m_N\right)\left(\left(\vec{S}_N \times \vec{v}_\perp\right) \cdot \vec{q}/m_N\right)$	$q^4 v_\perp^2,\ q^6$

Beyond standard interactions

- Parametrize possible DM-nucleon contact interactions using nonrelativistic effective field theory.
- Study the impact of the LMC on expected results from different near-future experiments.

Operator	Scaling factor
$\mathcal{O}_1 = 1_\chi 1_N$	1
$\mathcal{O}_3 = i\vec{S}_N \cdot (\vec{q}/m_N \times \vec{v}_\perp)$	$q^2 v_\perp^2,\ q^4$
$\mathcal{O}_4 = \vec{S}_\chi \cdot \vec{S}_N$	1
$\mathcal{O}_5 = i\vec{S}_\chi \cdot (\vec{q}/m_N \times \vec{v}_\perp)$	$q^2 v_\perp^2,\ q^4$
$\mathcal{O}_6 = \left(\vec{S}_\chi \cdot \vec{q}/m_N\right)\left(\vec{S}_N \cdot \vec{q}/m_N\right)$	q^4
$\mathcal{O}_7 = \vec{S}_N \cdot \vec{v}_\perp$	$v_\perp^2$
$\mathcal{O}_8 = \vec{S}_\chi \cdot \vec{v}_\perp$	$v_\perp^2,\ q^2$
$\mathcal{O}_9 = i\vec{S}_\chi \cdot \left(\vec{S}_N \times \vec{q}/m_N\right)$	q^2
$\mathcal{O}_{10} = i\vec{S}_N \cdot \vec{q}/m_N$	q^2
$\mathcal{O}_{11} = i\vec{S}_\chi \cdot \vec{q}/m_N$	q^2
$\mathcal{O}_{12} = \vec{S}_\chi \cdot \left(\vec{S}_N \times \vec{v}_\perp\right)$	$v_\perp^2,\ q^2$
$\mathcal{O}_{13} = i\left(\vec{S}_\chi \cdot \vec{v}_\perp\right)\left(\vec{S}_N \cdot \vec{q}/m_N\right)$	$q^2 v_\perp^2,\ q^4$
$\mathcal{O}_{14} = i\left(\vec{S}_\chi \cdot \vec{q}/m_N\right)\left(\vec{S}_N \cdot \vec{v}_\perp\right)$	$q^2 v_\perp^2$
$\mathcal{O}_{15} = -\left(\vec{S}_\chi \cdot \vec{q}/m_N\right)\left(\left(\vec{S}_N \times \vec{v}_\perp\right) \cdot \vec{q}/m_N\right)$	$q^4 v_\perp^2,\ q^6$

DARWIN/XLZD

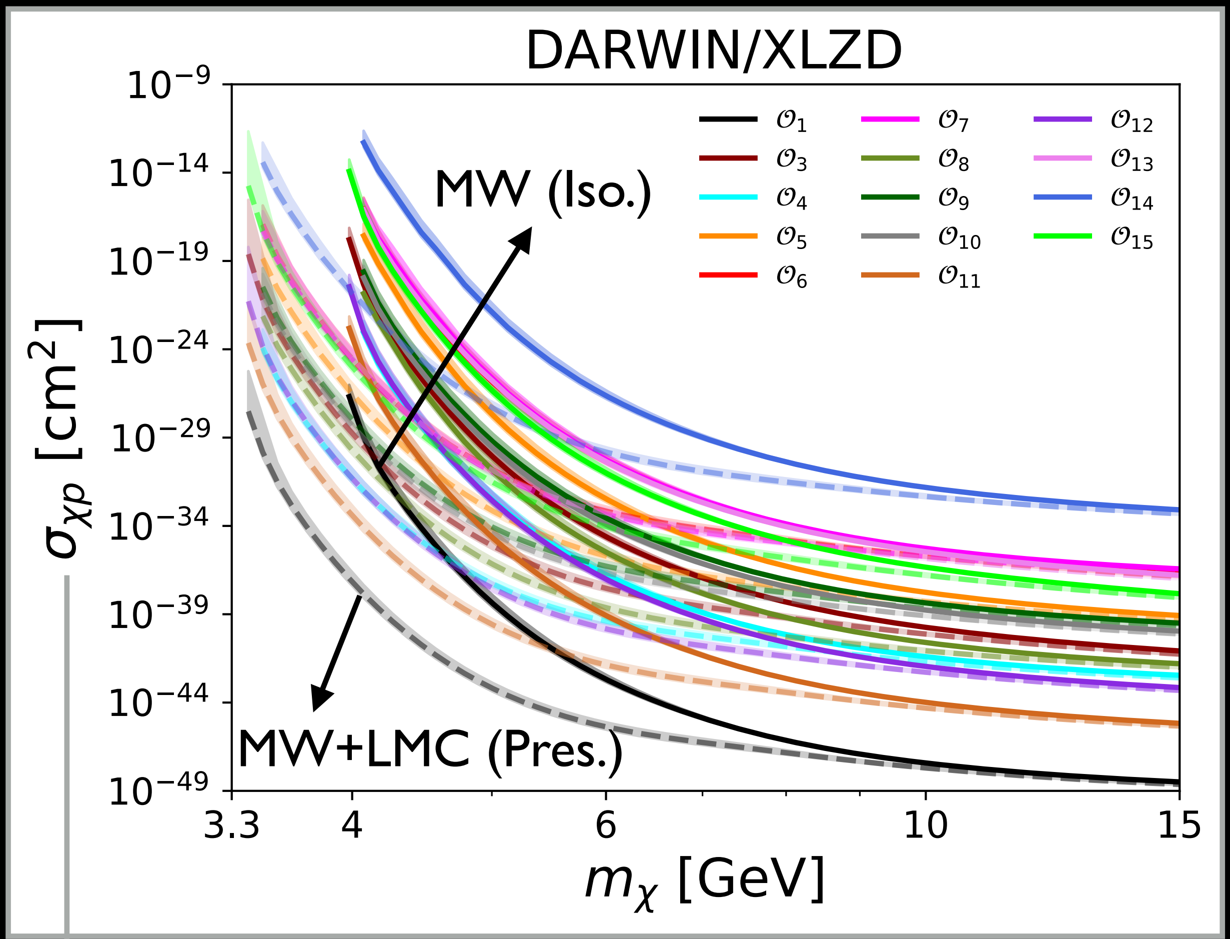

$$\sigma_{\chi p} \equiv \frac{(c_i^p \mu_p)^2}{\pi}$$

Reynoso, **NB**, Piro, JCAP 12, 037 (2024)

DARWIN/XLZD

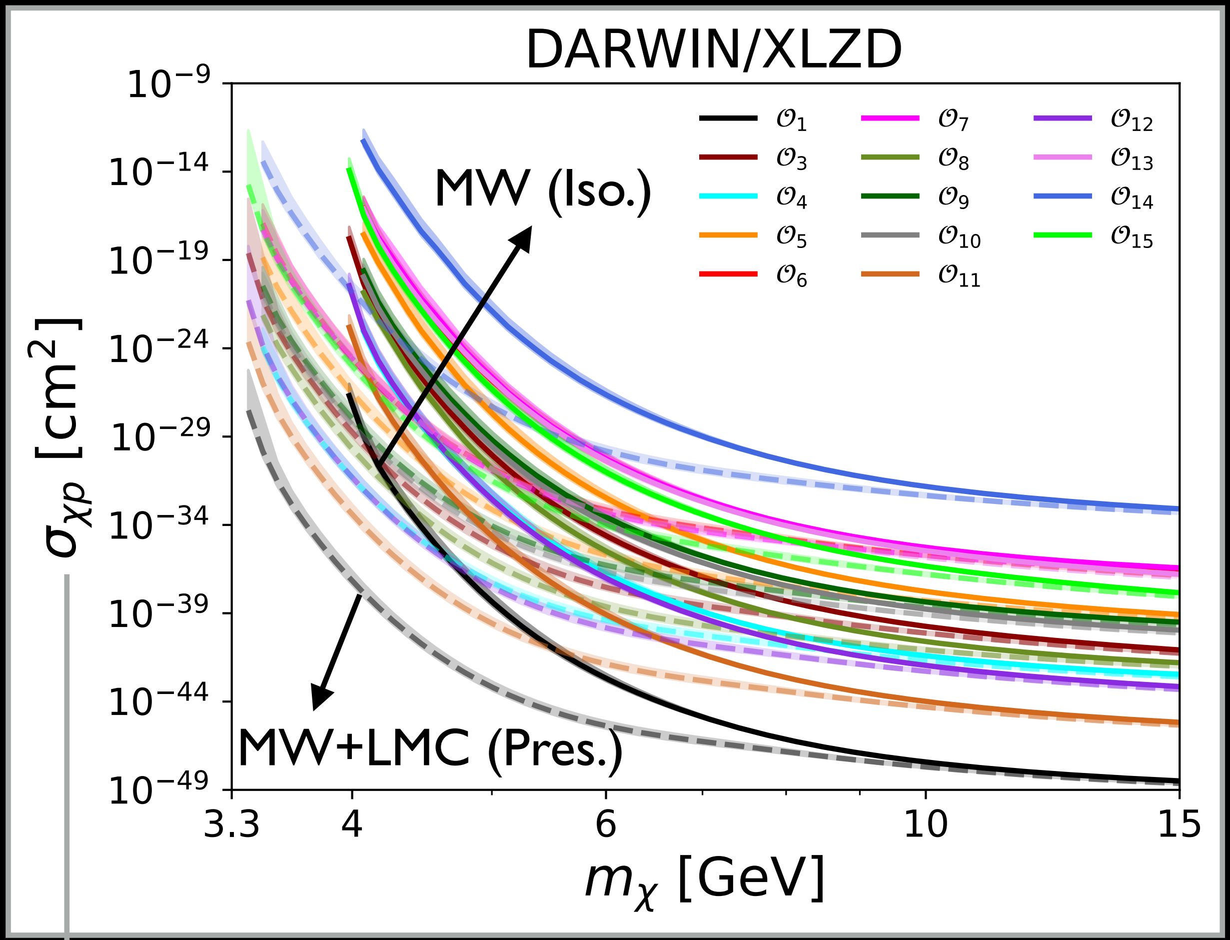

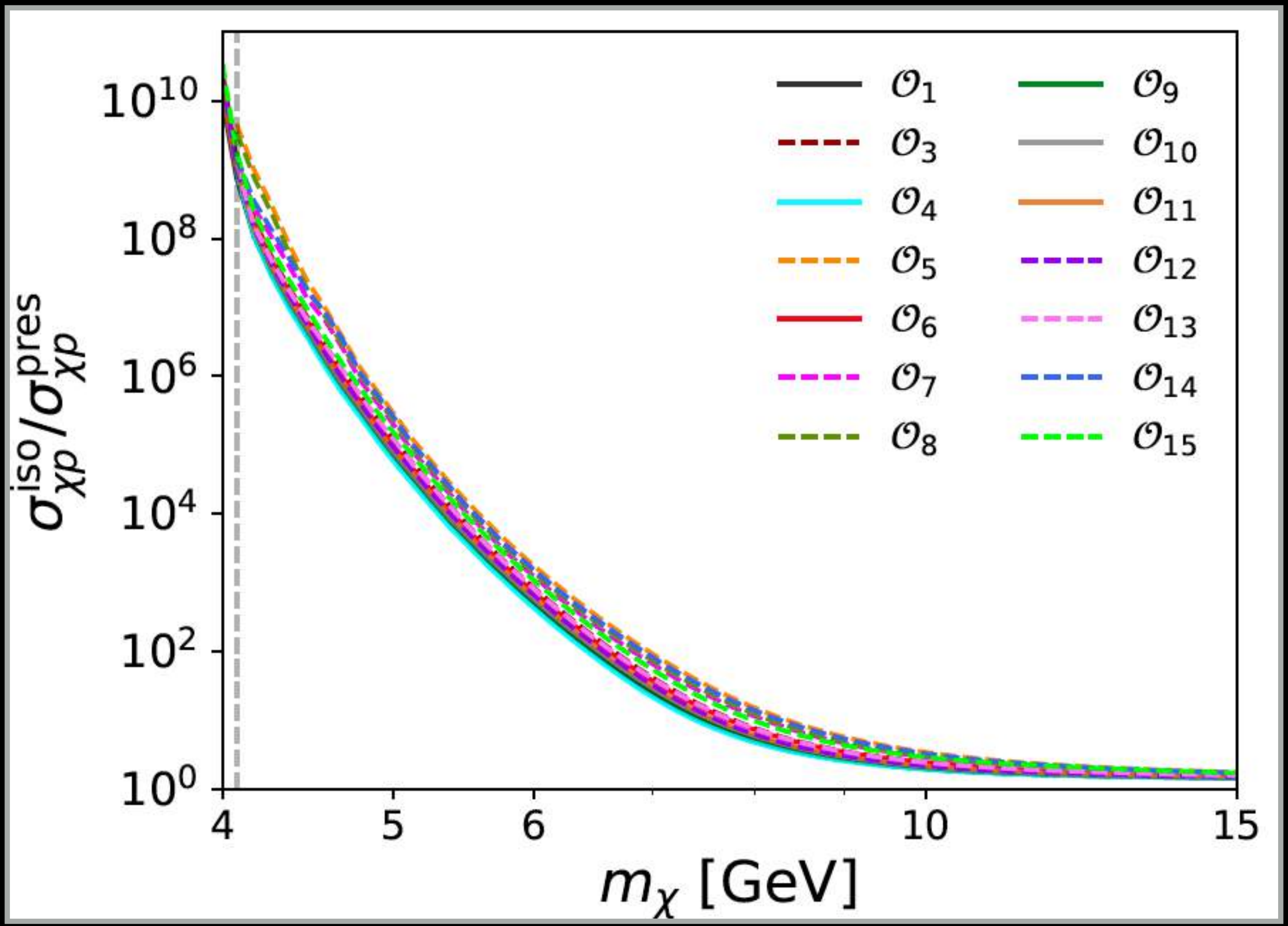

$$\sigma_{\chi p} \equiv \frac{(c_i^p \mu_p)^2}{\pi}$$

Reynoso, **NB**, Piro, JCAP 12, 037 (2024)

DARWIN/XLZD

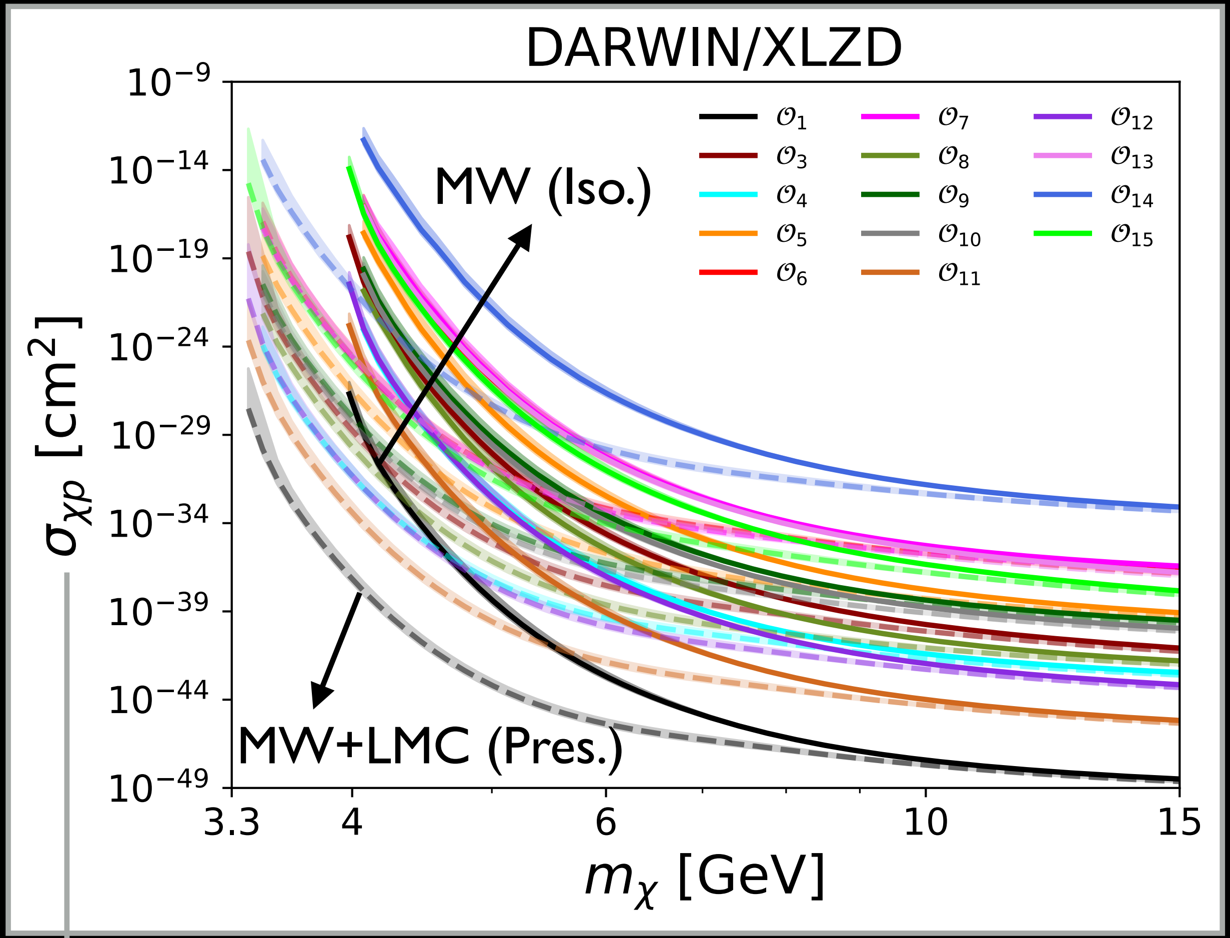

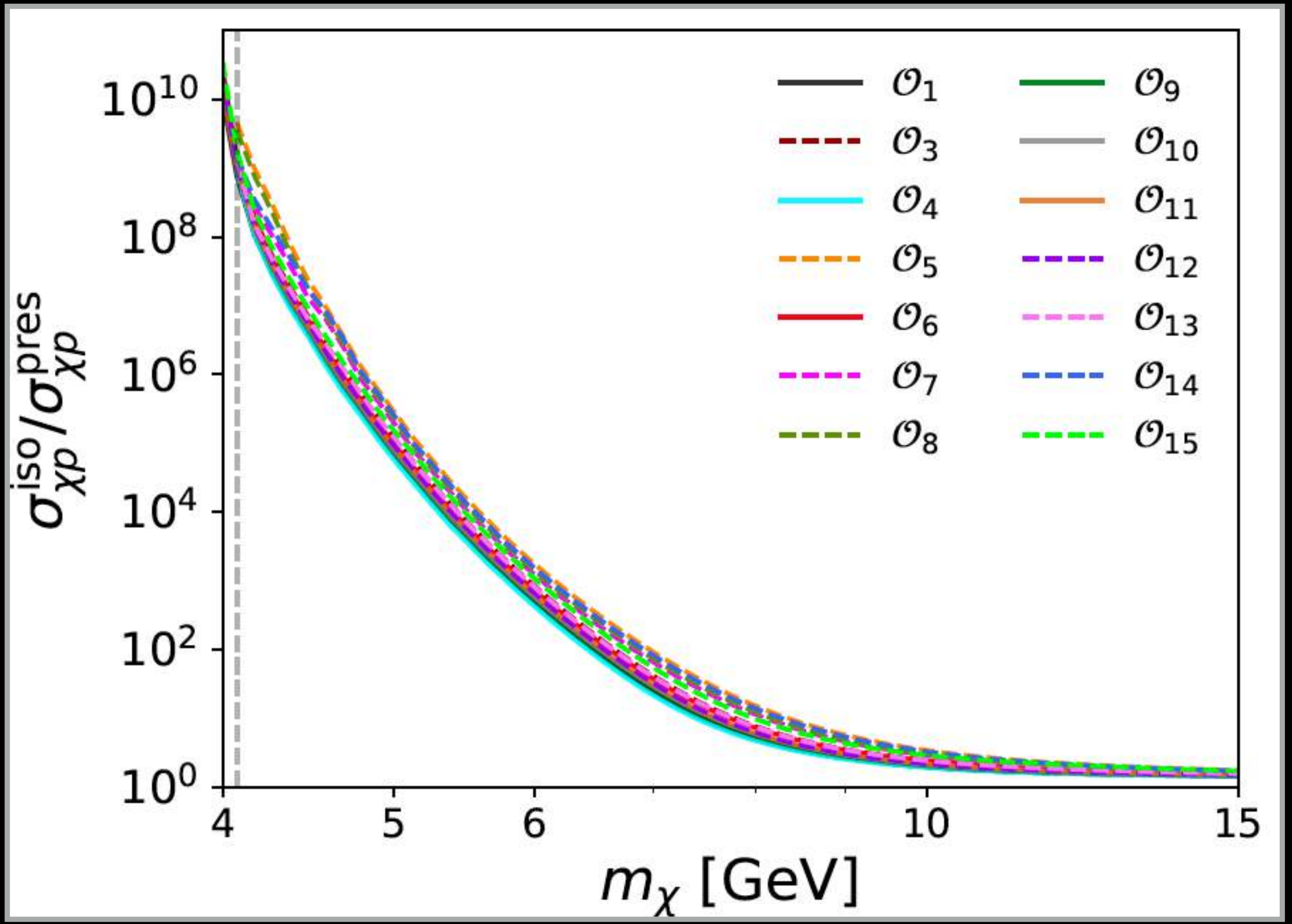

$$\sigma_{\chi p} \equiv \frac{(c_i^p \mu_p)^2}{\pi}$$

Reynoso, **NB**, Piro, JCAP 12, 037 (2024)

- The impact of the LMC is larger for operators that lead to a velocity-dependent scaling in the DM-nucleus cross section.

Inelastic dark matter

- DM particle χ scatters to an excited state χ^* with $\delta = m_{\chi^*} - m_\chi$.

Inelastic dark matter

- DM particle χ scatters to an excited state χ^* with $\delta = m_{\chi^*} - m_\chi$.
- Minimum DM speed required to produce a recoil energy E_R:

$$v_{\min} = \sqrt{\frac{1}{2m_N E_R}} \left(\frac{m_N E_R}{\mu_{\chi N}} + \delta \right)$$

Inelastic dark matter

- DM particle χ scatters to an excited state χ^* with $\delta = m_{\chi^*} - m_\chi$.

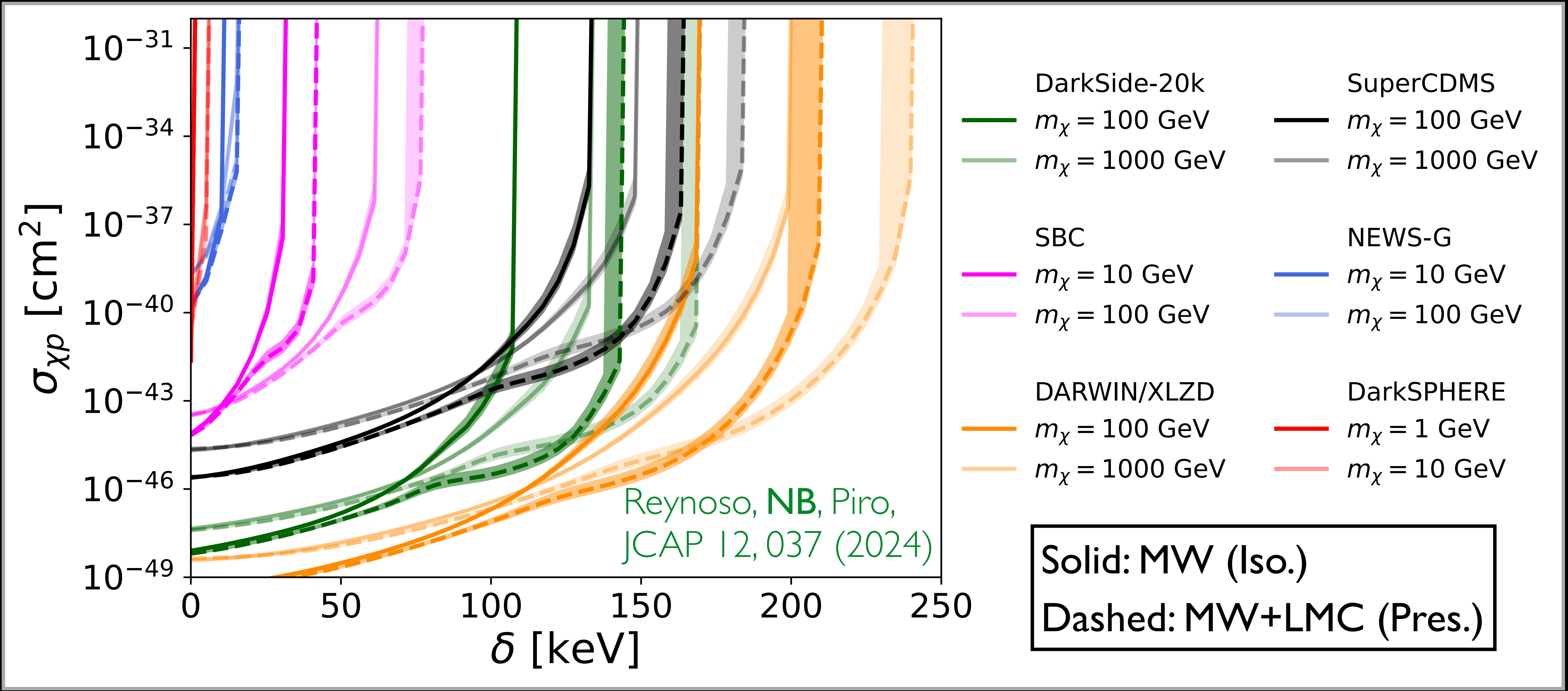

Inelastic dark matter

- DM particle χ scatters to an excited state χ^* with $\delta = m_{\chi^*} - m_\chi$.

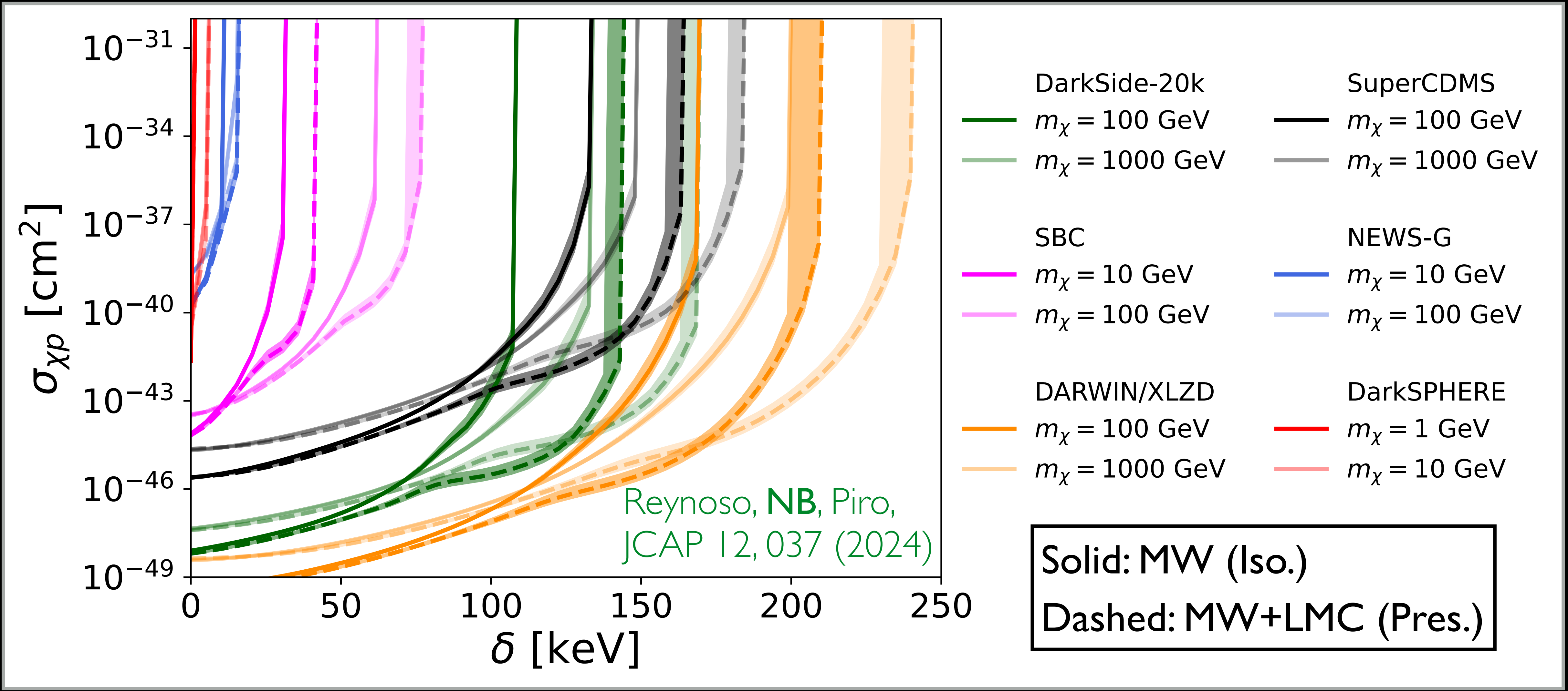

The LMC shifts the exclusion limits towards larger δ and smaller $\sigma_{\chi p}$. ➡ ***The LMC increases the sensitivity of the experiments for probing larger values of δ.***

Heavy dark matter

- DM mass: $m_\chi \gg 10\ \text{TeV}$

Heavy dark matter

- DM mass: $m_\chi \gg 10\ \mathrm{TeV}$
- Low number density → allows large scattering cross sections without violating existing bounds

Heavy dark matter

- DM mass: $m_\chi \gg 10\ \mathrm{TeV}$
- Low number density → allows large scattering cross sections without violating existing bounds
- Multiple scatters with little deflection

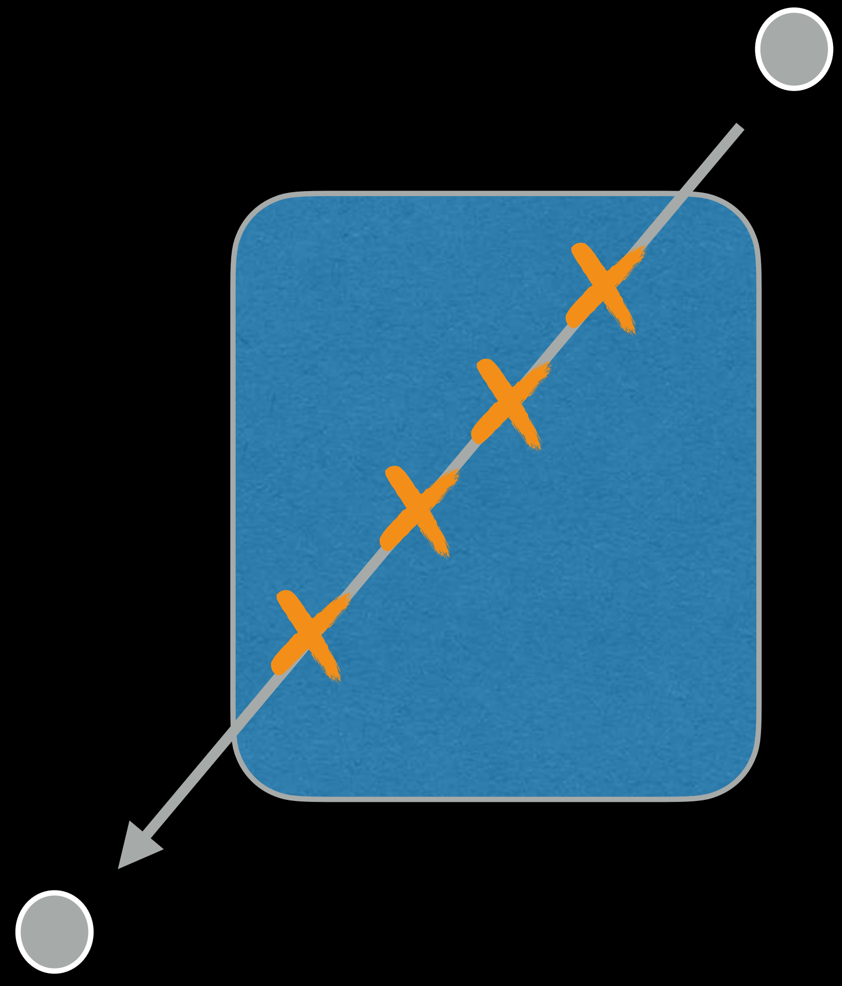

Heavy dark matter

- DM mass: $m_\chi \gg 10\ \mathrm{TeV}$
- Low number density → allows large scattering cross sections without violating existing bounds
- Multiple scatters with little deflection
- Energy loss in overburden → motivates near-surface and space-based searches

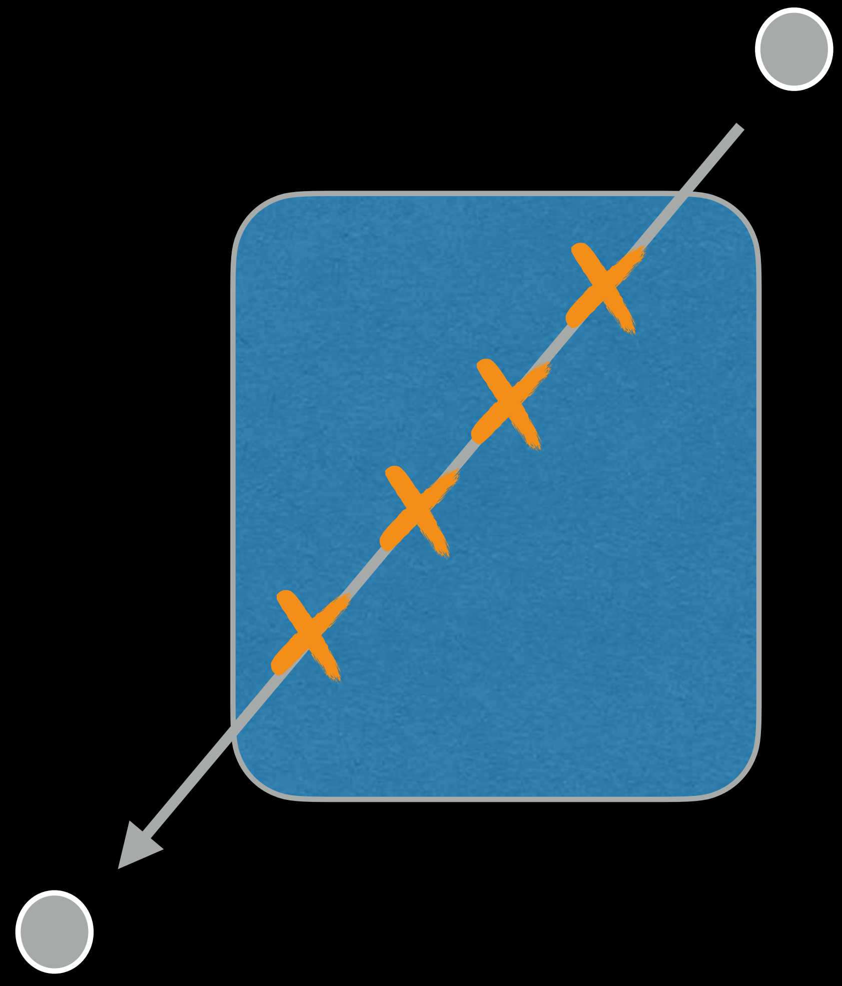

Heavy dark matter

- DM mass: $m_\chi \gg 10\ \mathrm{TeV}$
- Low number density → allows large scattering cross sections without violating existing bounds
- Multiple scatters with little deflection
- Energy loss in overburden → motivates near-surface and space-based searches
- *Sensitivity strongly depends on the DM velocity distribution.*

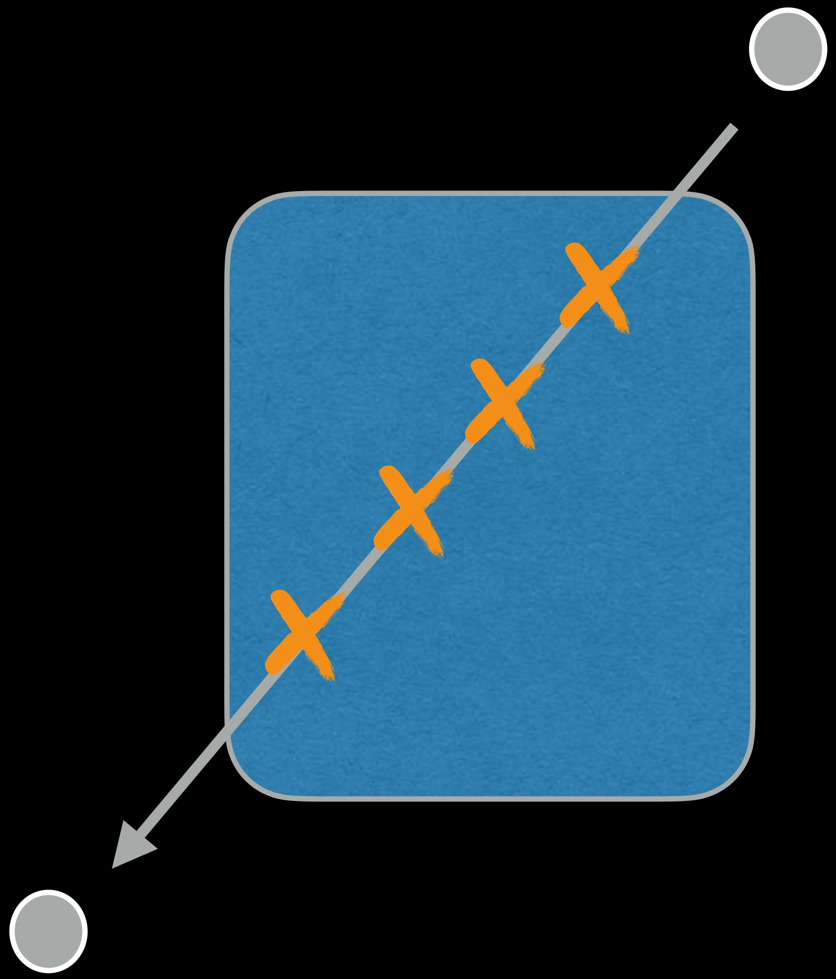

Heavy dark matter

- DM mass: $m_\chi \gg 10\ \mathrm{TeV}$
- Low number density → allows large scattering cross sections without violating existing bounds
- Multiple scatters with little deflection
- Energy loss in overburden → motivates near-surface and space-based searches
- *Sensitivity strongly depends on the DM velocity distribution.*
- *How does the LMC impact the sensitivity of multiscatter searches?*

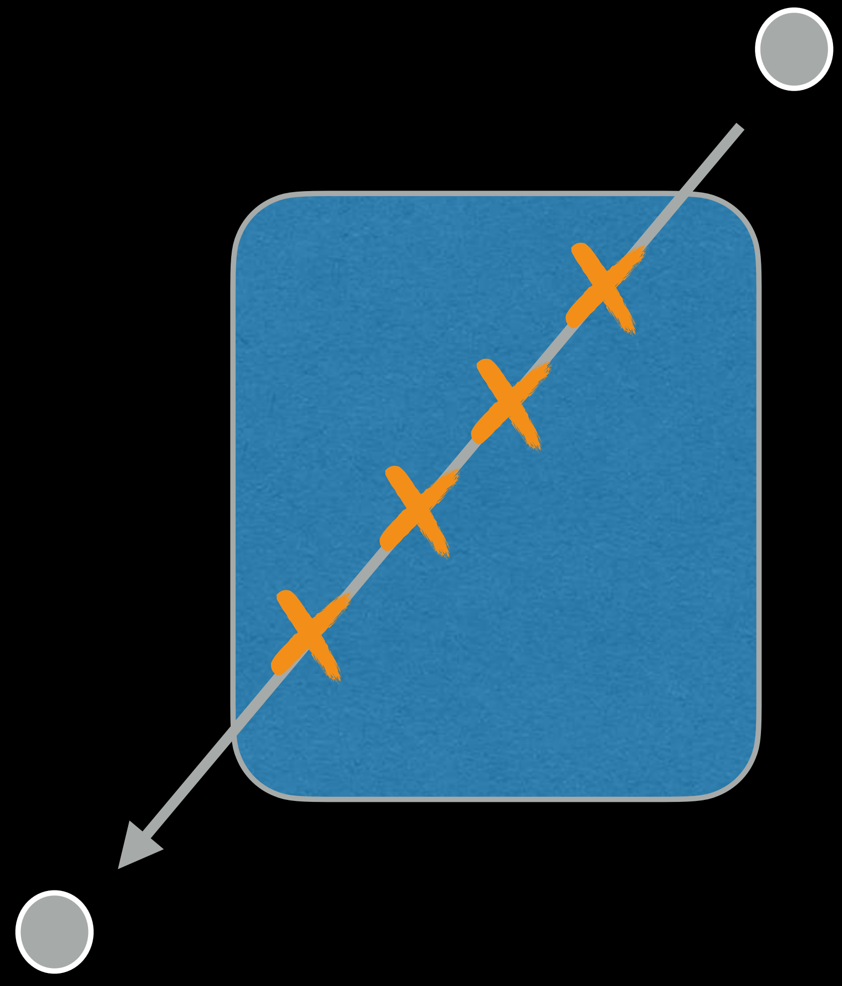

Heavy dark matter

Two models for DM interaction with nuclei:

- Spin-independent scattering:

  Loosely-bound composite DM

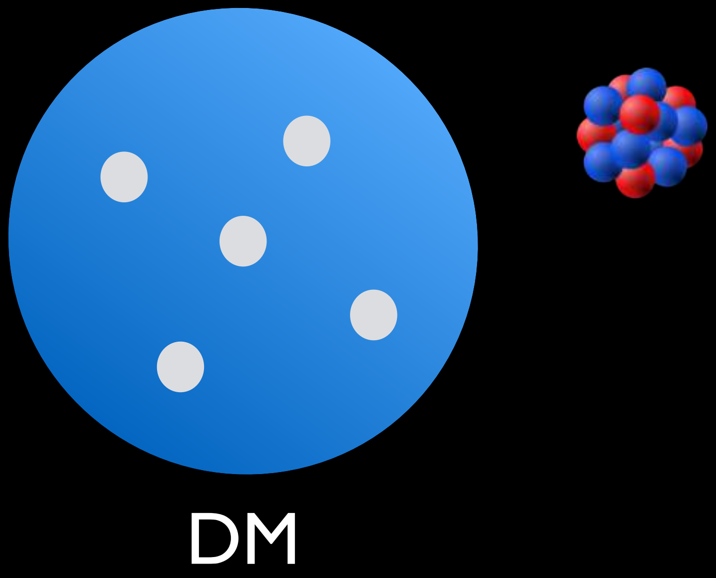

Heavy dark matter

Two models for DM interaction with nuclei:

- Spin-independent scattering:

Loosely-bound composite DM
→ Coherent interaction with all nucleons

$$\sigma_{\chi N} = A^2 \left(\frac{\mu_{\chi N}}{\mu_{\chi n}} \right)^2 \sigma_{\chi n}$$

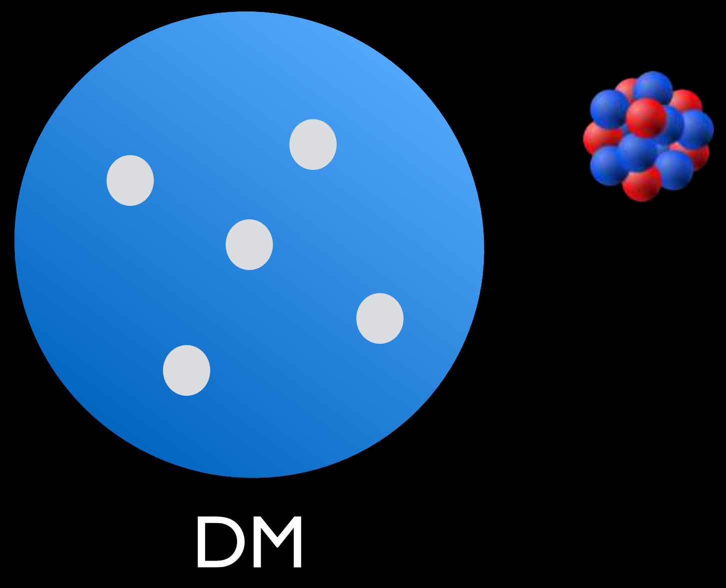

Heavy dark matter

Two models for DM interaction with nuclei:

- **Spin-independent scattering:**

  Loosely-bound composite DM
  → Coherent interaction
  with all nucleons

$$\sigma_{\chi N} = A^2 \left(\frac{\mu_{\chi N}}{\mu_{\chi n}} \right)^2 \sigma_{\chi n}$$

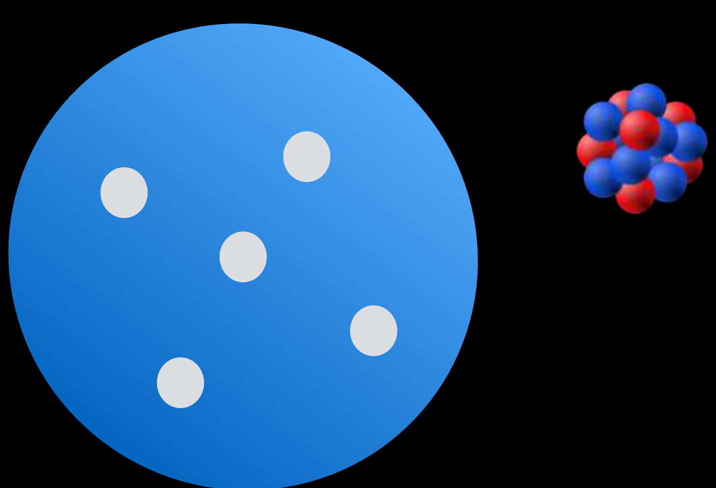

DM

- **Contact interaction:**

  Single large DM particle or
  tightly-bound composite DM

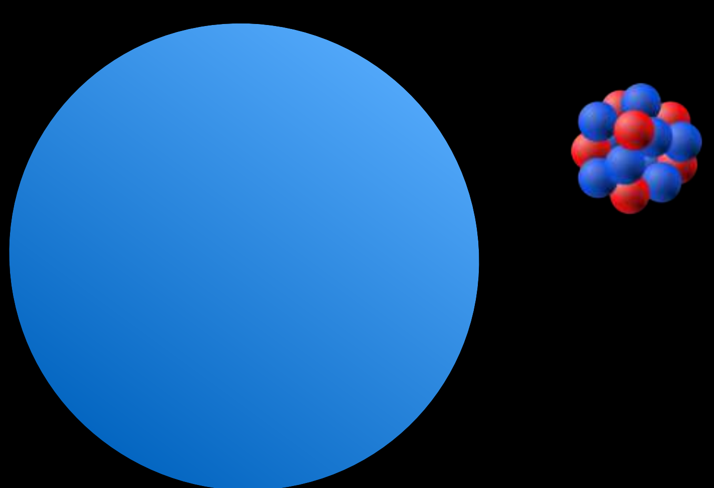

DM

Heavy dark matter

Two models for DM interaction with nuclei:

- **Spin-independent scattering:**

  Loosely-bound composite DM
  → Coherent interaction with all nucleons

  $$\sigma_{\chi N} = A^2 \left(\frac{\mu_{\chi N}}{\mu_{\chi n}} \right)^2 \sigma_{\chi n}$$

  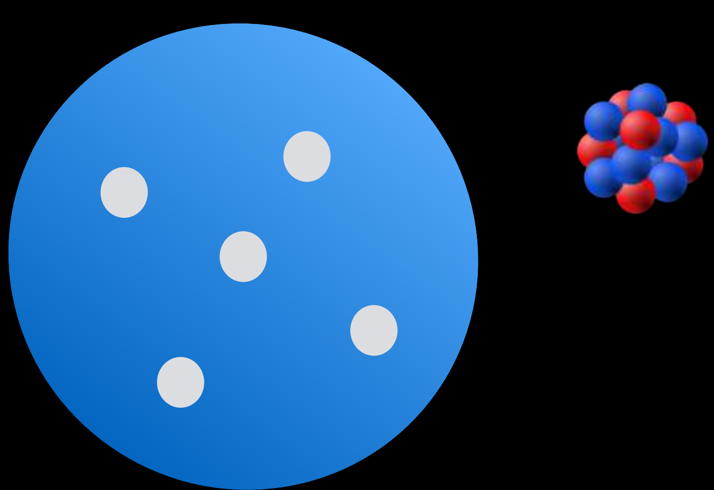

  DM

- **Contact interaction:**

  Single large DM particle or tightly-bound composite DM
  → Cross section independent of nucleus

  $$\sigma_{\chi N} = \sigma_C$$

  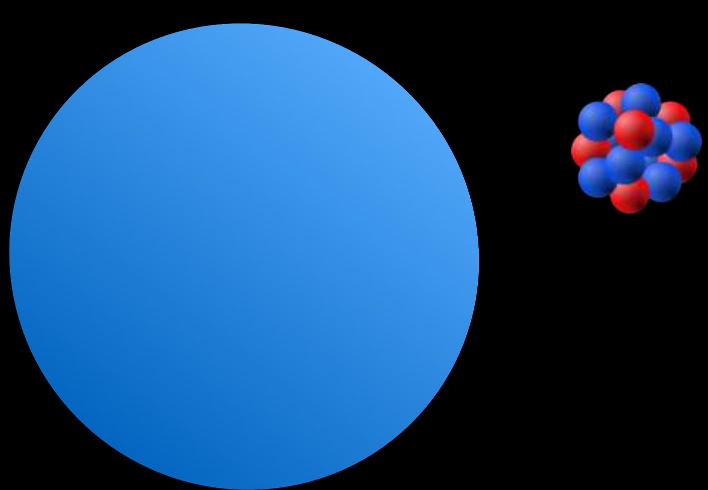

  DM

Plastic etch experiments

Searches for cosmogenic particles in etched plastic track detectors:

Skylab

Skylab space station cosmic ray search (1978)

Ohya Quarry

Underground search for monopoles and exotic particles in Japan (1990)

Plastic etch experiments

Searches for cosmogenic particles in etched plastic track detectors:

Skylab

Skylab space station cosmic ray search (1978)

Ohya Quarry

Underground search for monopoles and exotic particles in Japan (1990)

Particle passing through the plastic damages molecular bonds.

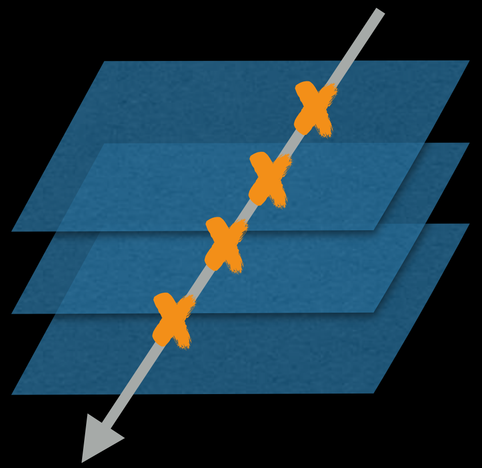

Plastic etch searches for dark matter

Skylab, Spin-independent interaction

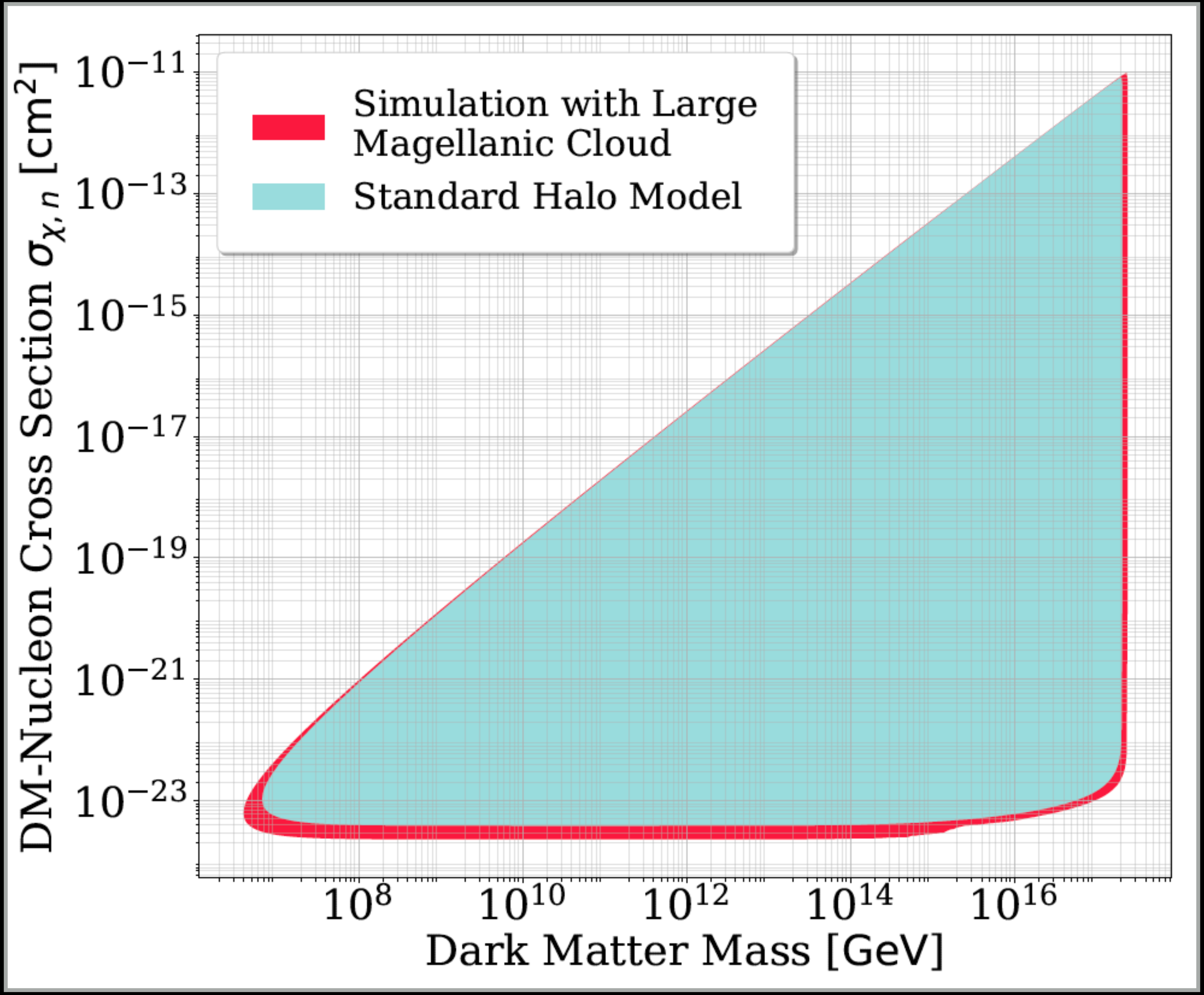

NB, Bramante, Buchanan, JCAP 04, 065 (2026)

Plastic etch searches for dark matter

Skylab, Spin-independent interaction

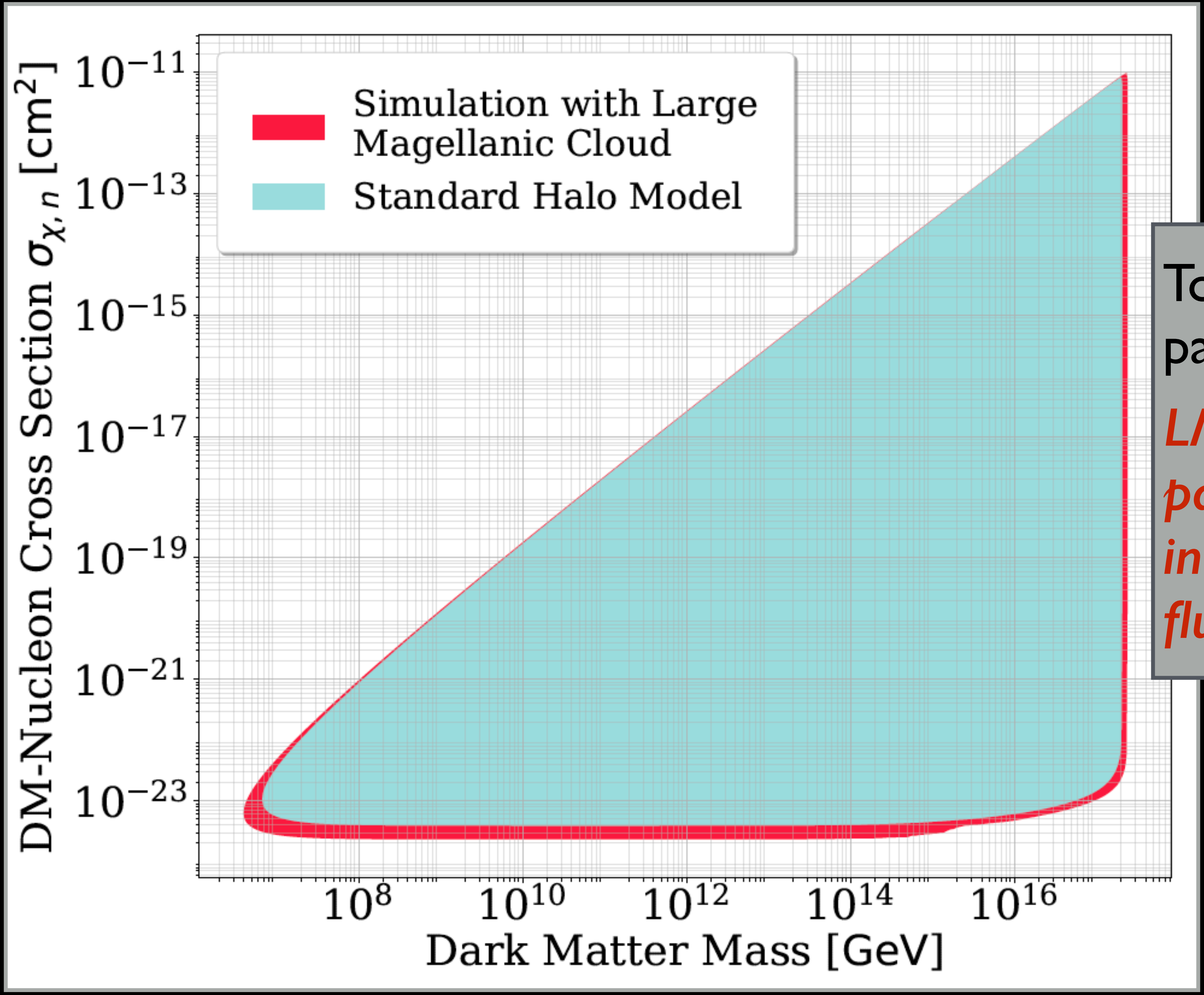

Too few particles pass the detector

LMC boosts particle speeds, increasing the flux

NB, Bramante, Buchanan, JCAP 04, 065 (2026)

Plastic etch searches for dark matter

Skylab, Spin-independent interaction

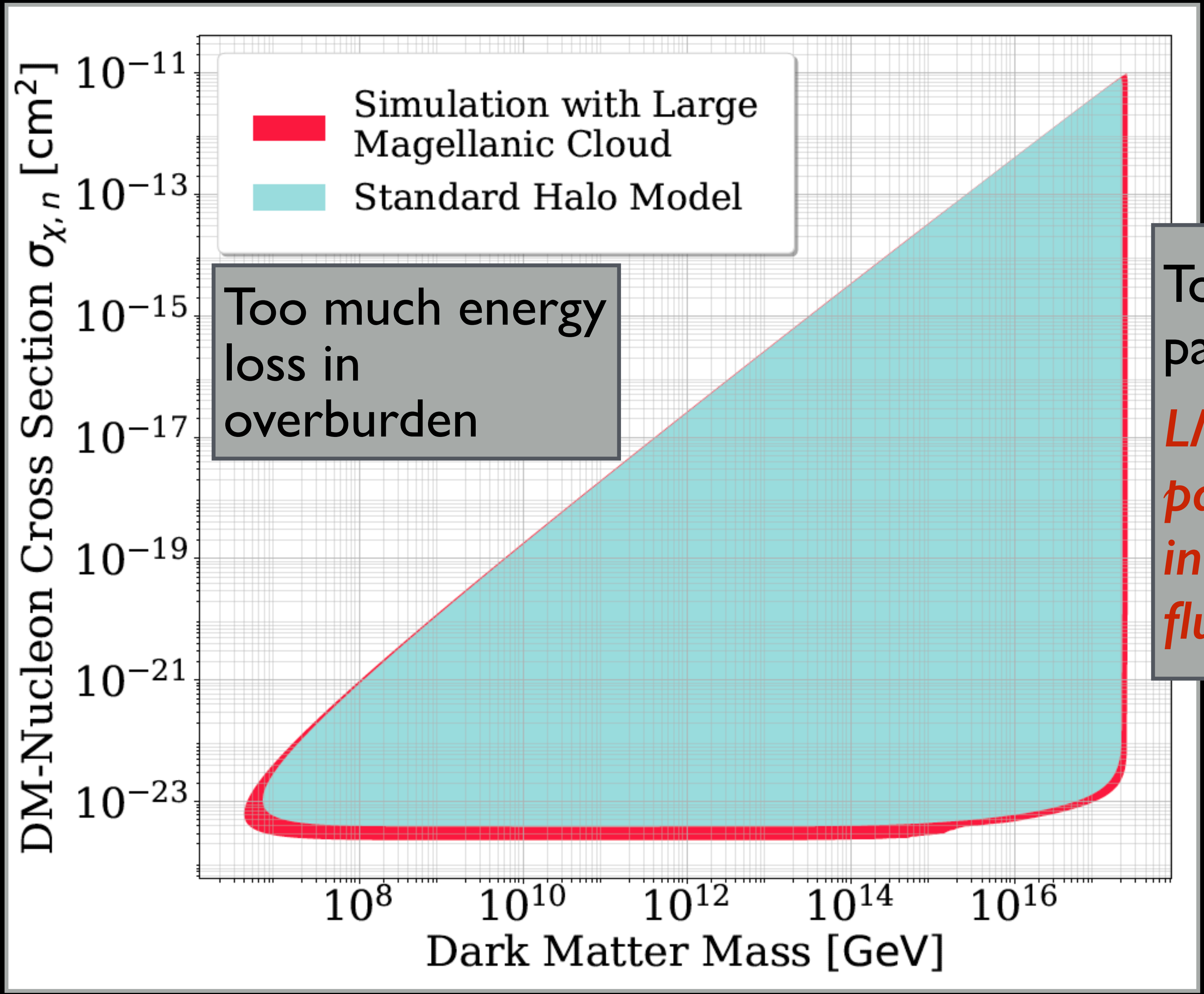

Too few particles pass the detector

LMC boosts particle speeds, increasing the flux

NB, Bramante, Buchanan, JCAP 04, 065 (2026)

Plastic etch searches for dark matter

Skylab, Spin-independent interaction

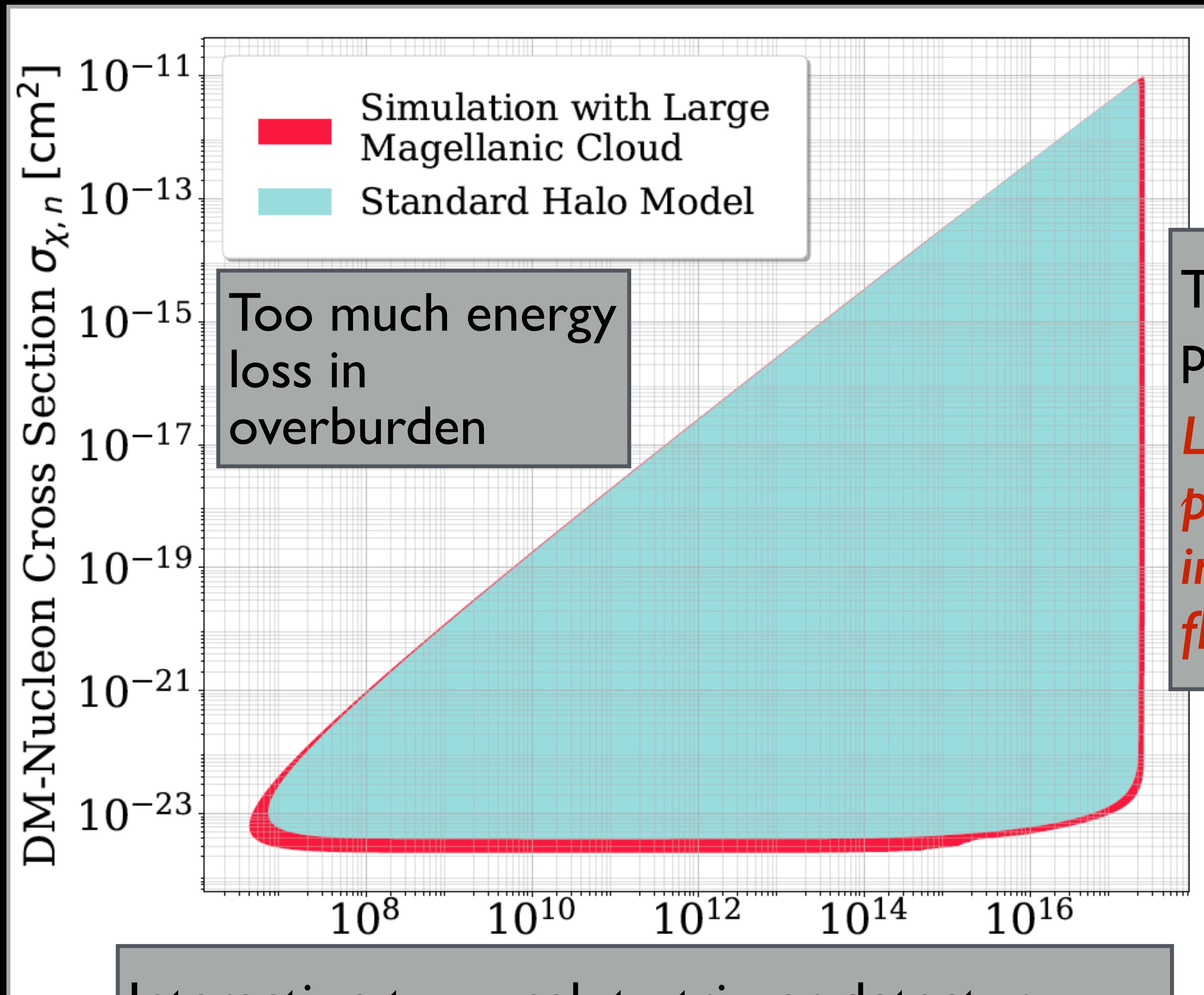

Too much energy loss in overburden

Too few particles pass the detector

LMC boosts particle speeds, increasing the flux

Interaction too weak to trigger detector

Effect of LMC most significant at low masses

Plastic etch searches for dark matter

Spin-independent

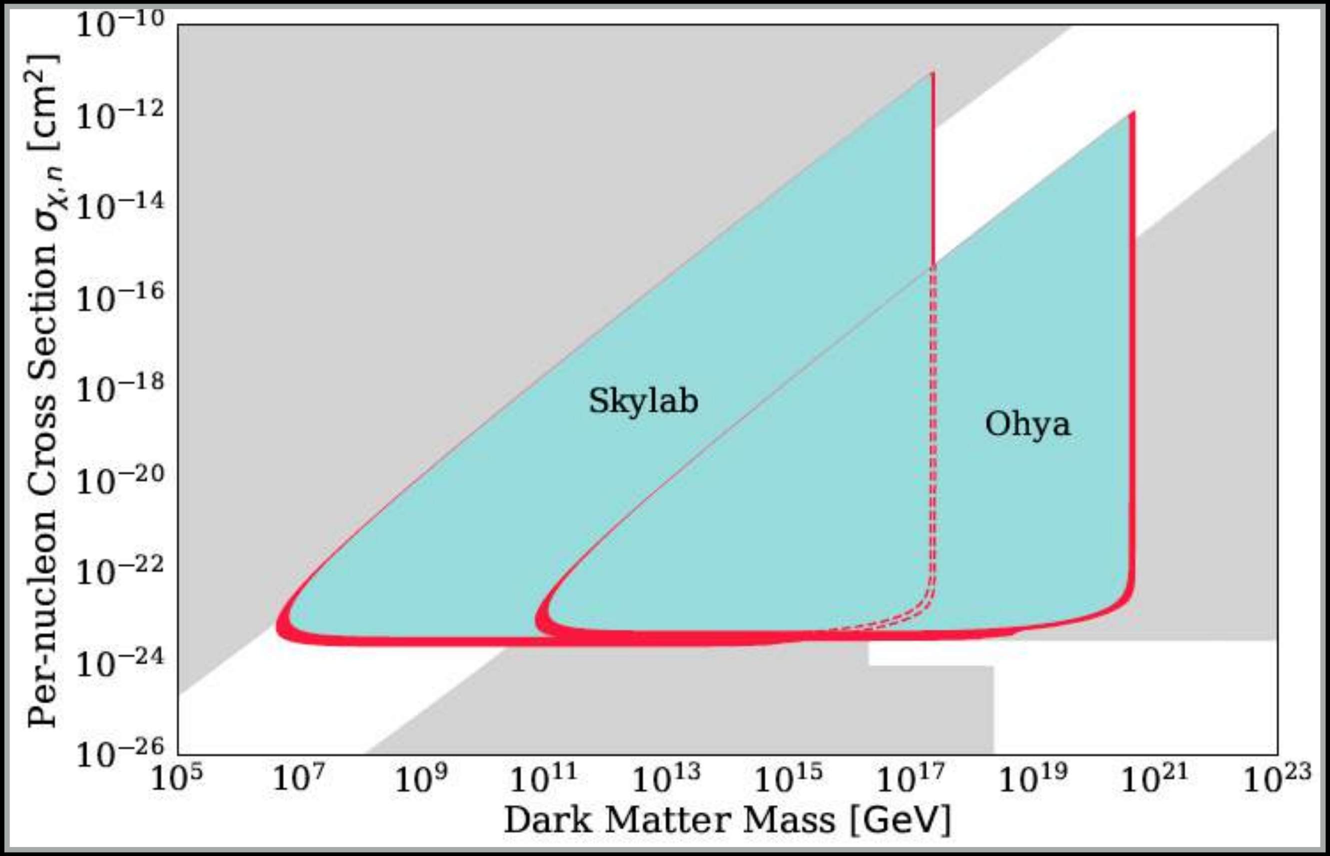

Contact

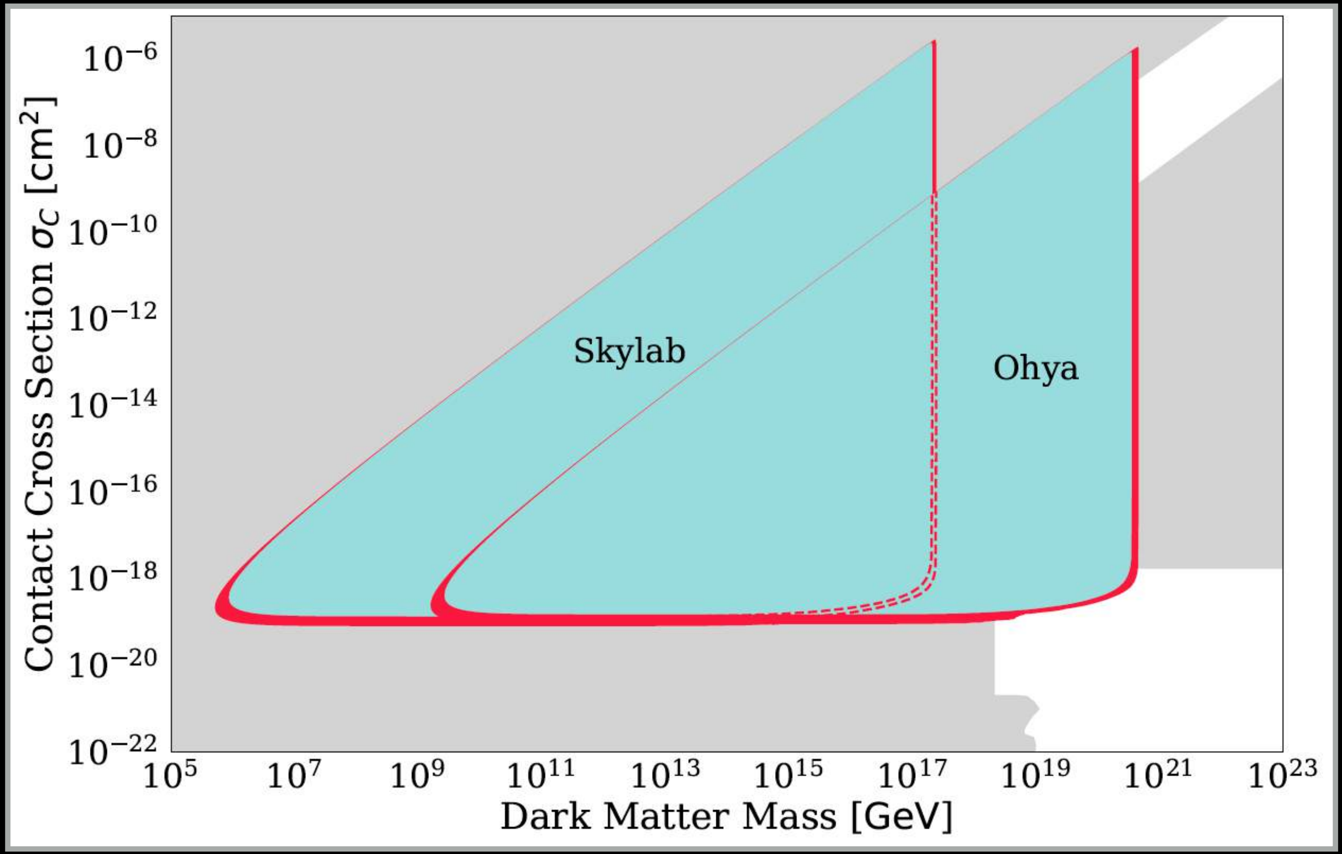

NB, Bramante, Buchanan, JCAP 04, 065 (2026)

- LMC extends the parameter space that can be probed by the heavy DM searches.

Directional signatures

Directional differential recoil rate in Galactic coordinates:

SHM

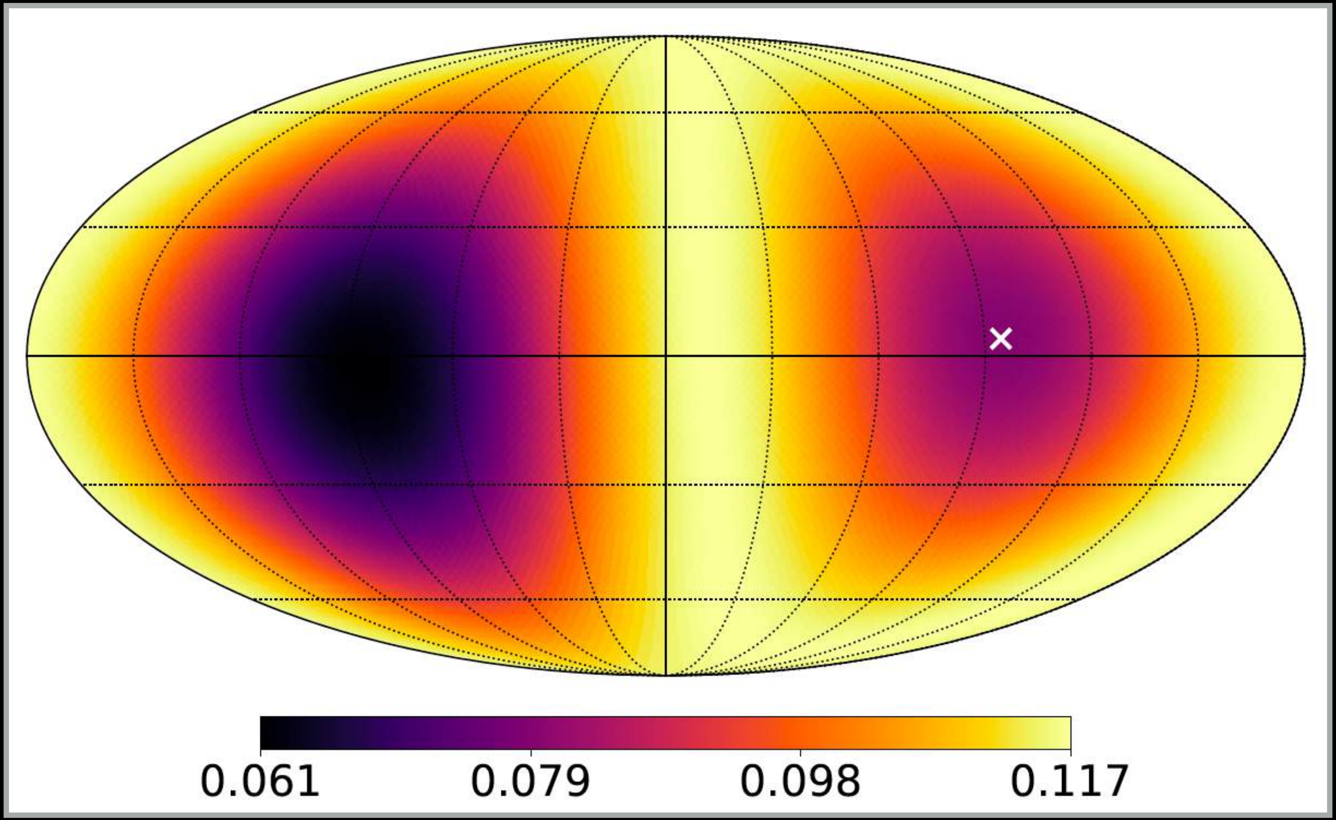

MW+LMC

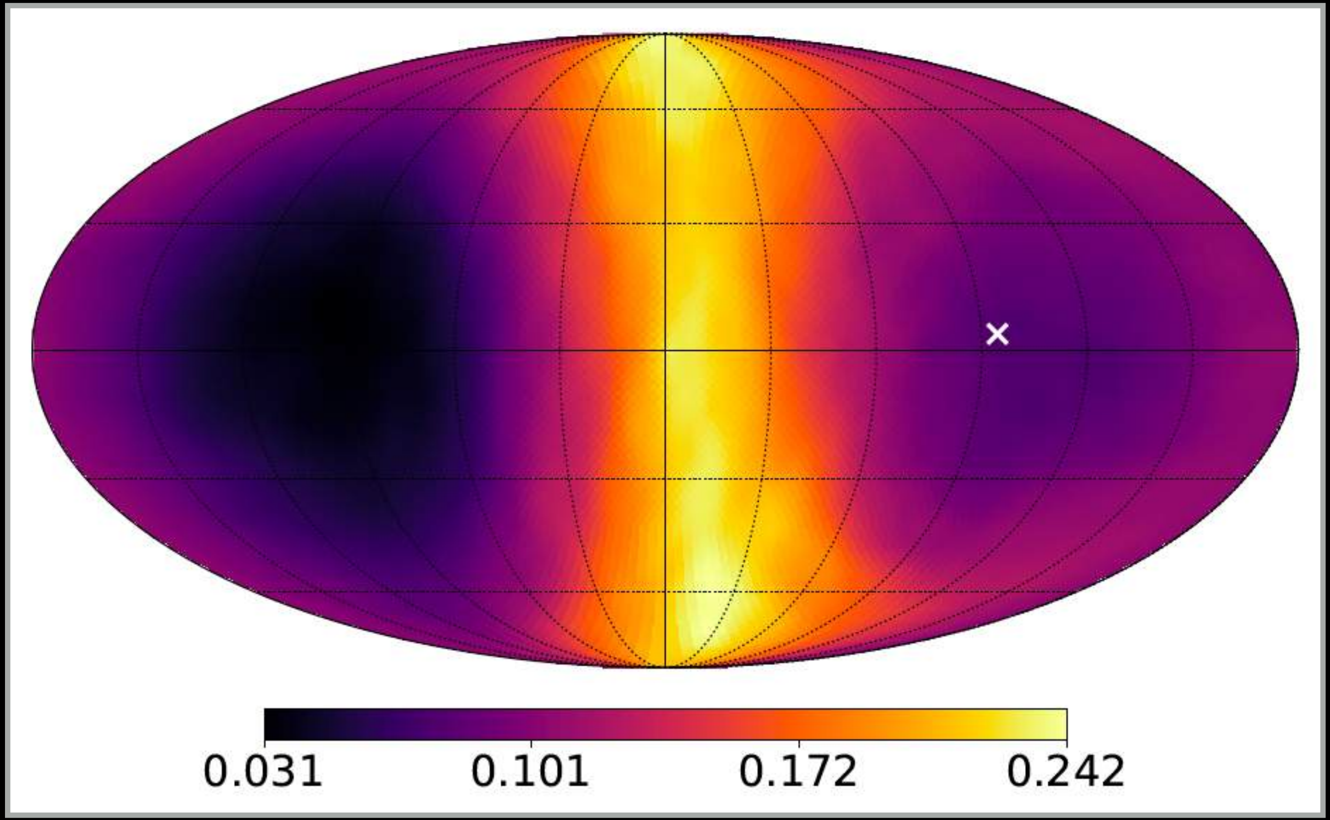

Reynoso, **NB**, Piro, 2606.12535

CYGNUS-like Experiment
He:F$_4$ (60-40) at Gran Sasso
$m_\chi = 100$ GeV, $E_R = 0.25$ keV

- LMC significantly modifies directional DM signatures.

Rejecting isotropy

Number of events required to reject isotropy at 3σ:

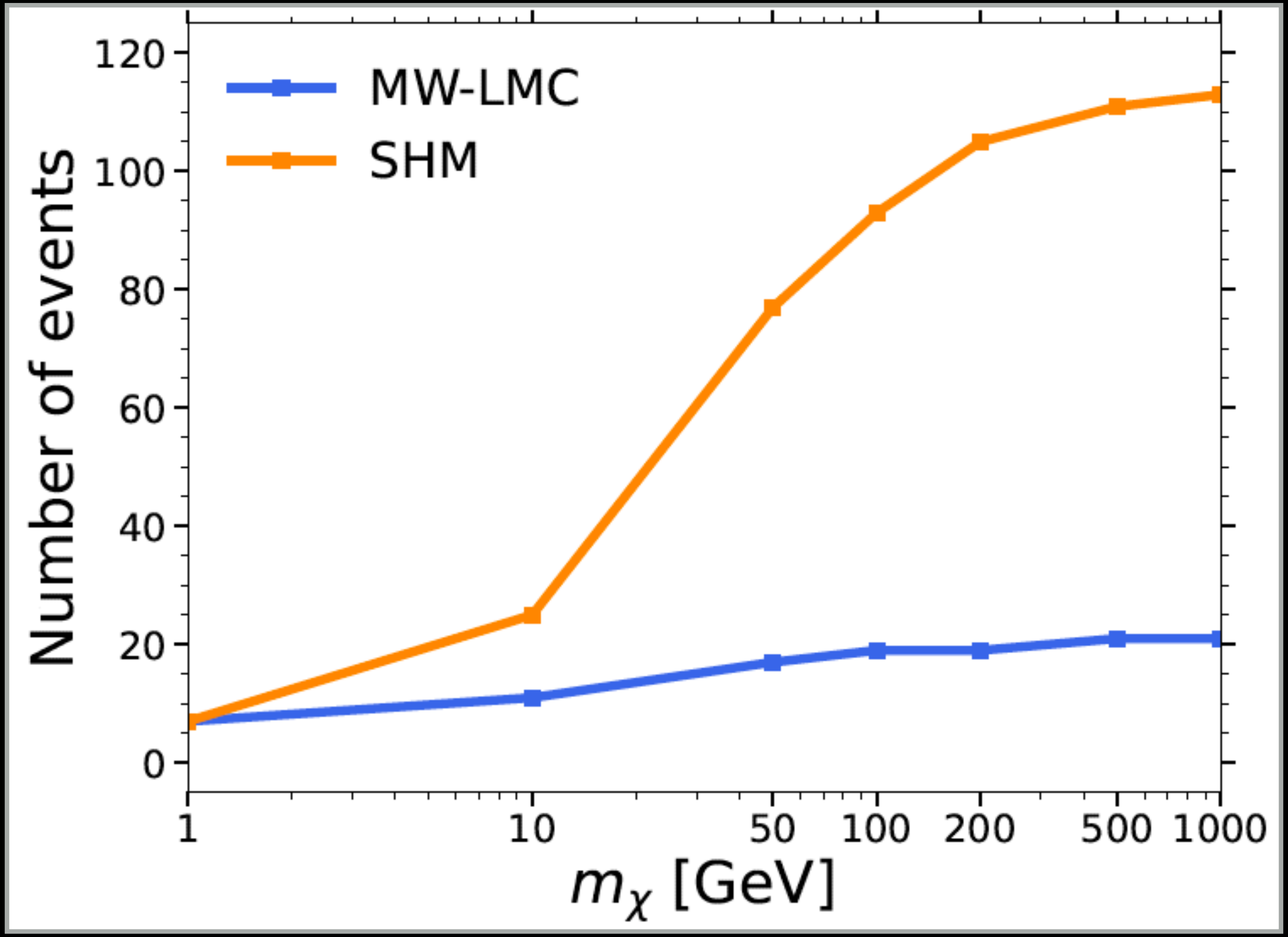

Reynoso, **NB**, Piro, 2606.12535

- LMC can significantly enhance prospects for directional detection.

Summary

- The LMC boosts the high speed tail of the local DM velocity distribution.

Summary

- The LMC boosts the high speed tail of the local DM velocity distribution.
- **This leads to substantial modifications of DM direct detection signals:**
  - Stronger direct detection limits.

Summary

- The LMC boosts the high speed tail of the local DM velocity distribution.
- **This leads to substantial modifications of DM direct detection signals:**
  - Stronger direct detection limits.
  - An even greater impact for *velocity-dependent* interactions and *inelastic DM*.

Summary

- The LMC boosts the high speed tail of the local DM velocity distribution.
- **This leads to substantial modifications of DM direct detection signals:**
  - Stronger direct detection limits.
  - An even greater impact for *velocity-dependent* interactions and *inelastic DM*.
  - Improved sensitivity to *heavy DM*.

Summary

- The LMC boosts the high speed tail of the local DM velocity distribution.
- **This leads to substantial modifications of DM direct detection signals:**
  - Stronger direct detection limits.
  - An even greater impact for ***velocity-dependent*** interactions and ***inelastic DM***.
  - Improved sensitivity to ***heavy DM***.
  - Enhanced prospects for ***directional detection***.

Summary

- The LMC boosts the high speed tail of the local DM velocity distribution.
- **This leads to substantial modifications of DM direct detection signals:**
  - Stronger direct detection limits.
  - An even greater impact for *velocity-dependent* interactions and *inelastic DM*.
  - Improved sensitivity to *heavy DM*.
  - Enhanced prospects for *directional detection*.
- ***These significant effects should not be overlooked in the analysis of future direct detection data.***

Backup Slides

Identifying LMC analogues

- Select simulated LMC analogues that have properties similar to the observed LMC:
  - Present day stellar mass of the LMC: $\sim 2.7 \times 10^9\ \mathrm{M}_\odot$
  - LMC's first pericenter distance: $\sim 48\ \mathrm{kpc}$
- Difficult to find an exact LMC analogue in cosmological simulations. → Follow the history of the simulated halos within the last 8 Gyrs to find LMC analogues.
- Identify 15 LMC analogues based on two criteria:
  - LMC's stellar mass is $> 5 \times 10^8\ \mathrm{M}_\odot$.
  - Distance from host at first pericenter is in the range of $[40,60]\ \mathrm{kpc}$.

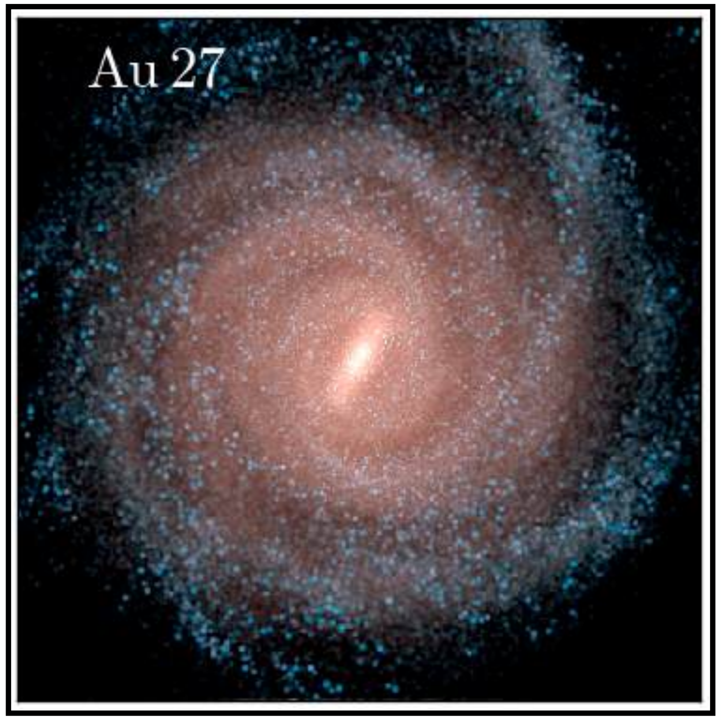

Matching the Sun-LMC geometry

Steps in matching the Sun-LMC geometry to observations:

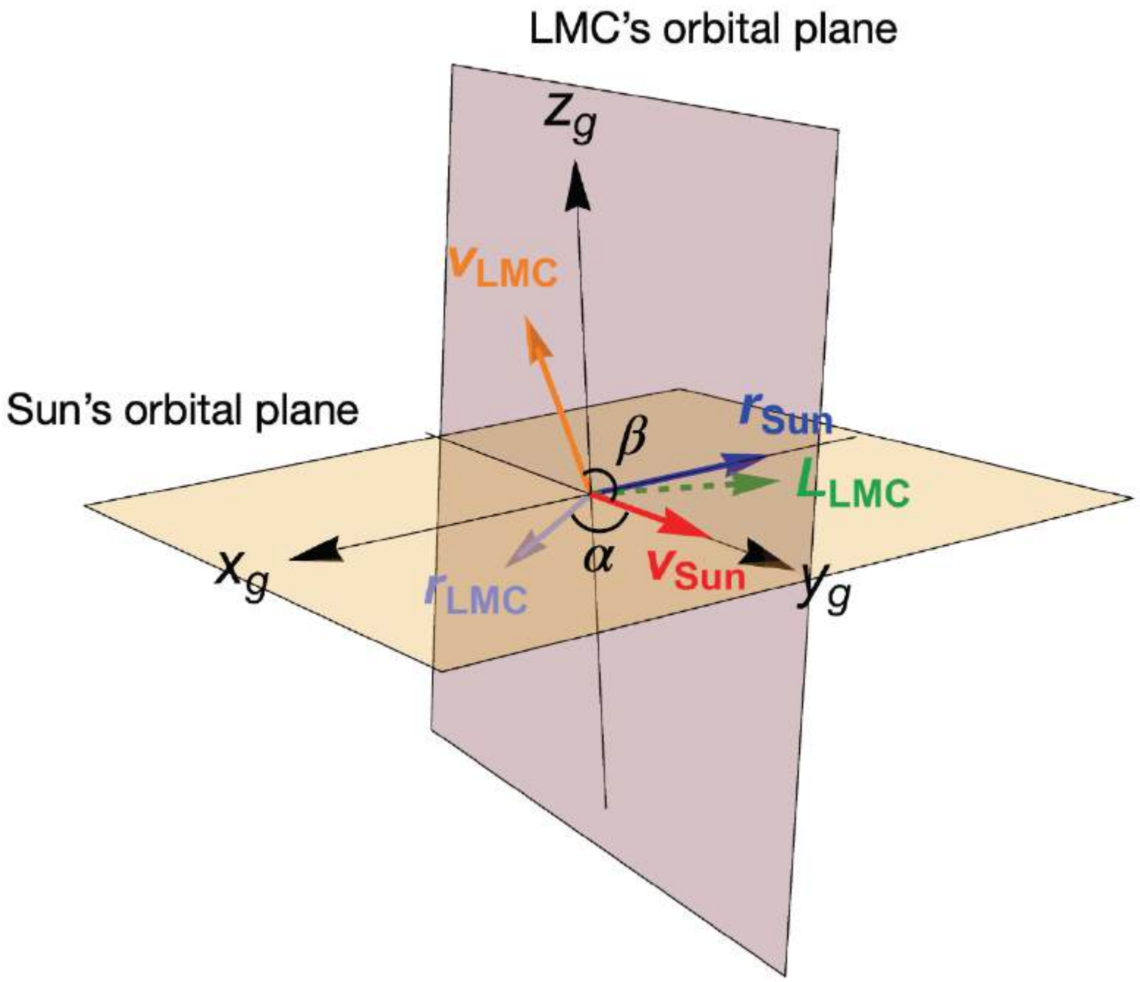

$$\cos\alpha \equiv \hat{\mathbf{v}}^{\rm sim}_{\rm Sun} \cdot \hat{\mathbf{r}}^{\rm sim}_{\rm LMC} = -0.835$$

$$\cos\beta \equiv \hat{\mathbf{v}}^{\rm sim}_{\rm Sun} \cdot \hat{\mathbf{v}}^{\rm sim}_{\rm LMC} = -0.709$$

1. Find the stellar disk orientations that make the same angle with the orbital plane of the LMC analogues as in observations.

2. Find the position of the Sun for each allowed disk by matching the angles between the angular momentum of the LMC and the Sun's position and velocity in the simulations to their observed values.

3. The best fit Sun's position is the one that leads to the closest match of the angles between the Sun's velocity and the LMC's position and velocity with observations.

Defining the Solar region

Solar region: overlap of a **spherical shell** with radius between $6 - 10$ kpc and a **cone** with opening angle $\pi/4$ with its axis aligned with the position of the Sun.

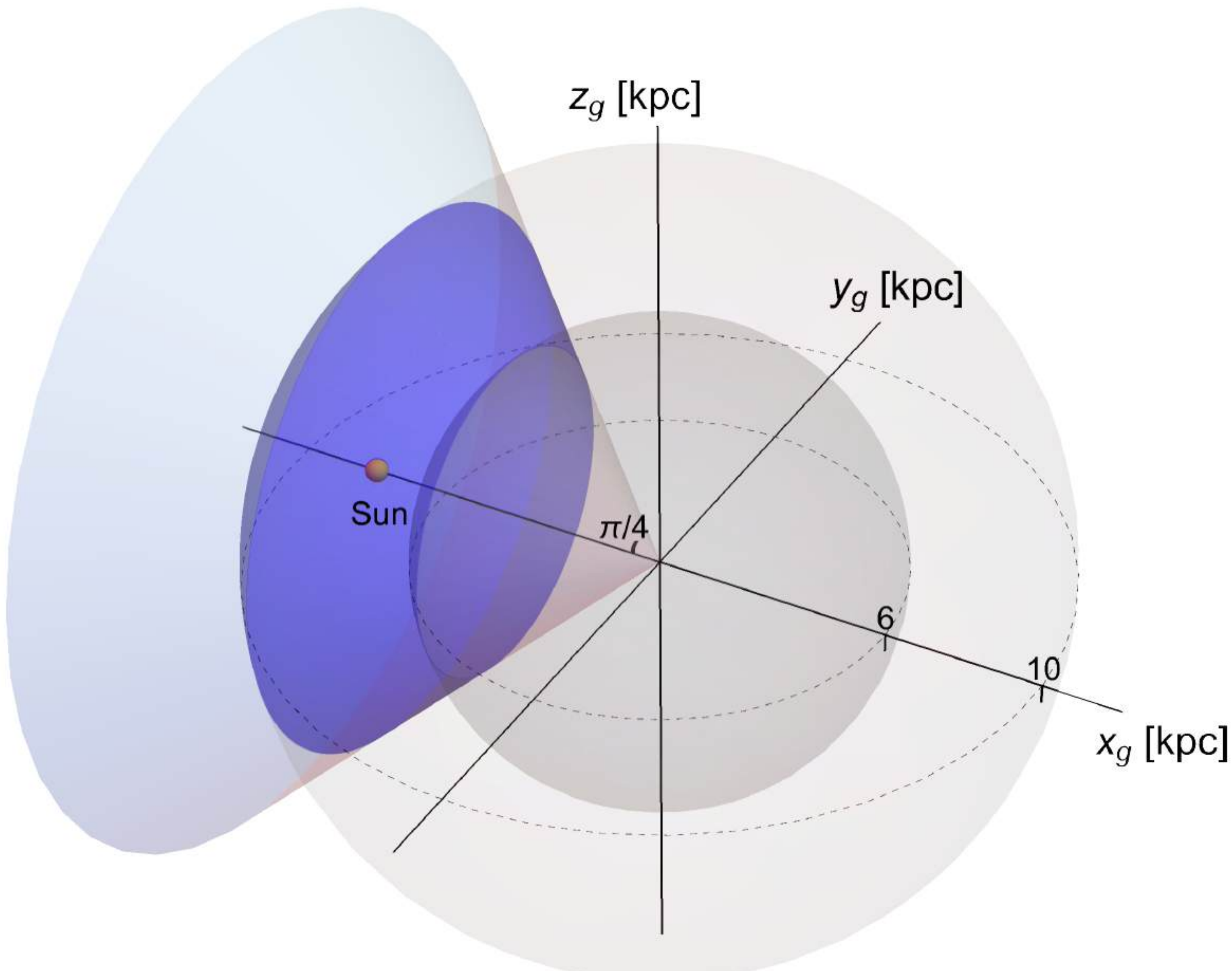

Local dark matter density

Halo ID	$M_{\rm Infall}^{\rm LMC}$ [10^{11} M$_\odot$]	ρ_χ [GeV/cm^3]	$\kappa_{\rm LMC}$ [%]
1	0.31	0.21	0.14
2	0.31	0.23	0.64
3	0.34	0.35	0.026
4	0.82	0.34	0.096
5	1.84	0.24	1.5
6	1.10	0.38	0.038
7	0.32	0.53	0.032
8	0.36	0.38	0.0077
9	0.73	0.36	0.10
10	3.28	0.39	2.8
11	1.45	0.43	0.028
12	1.43	0.53	0.17
13	3.18	0.34	2.3
14	0.84	0.60	0.26
15	1.15	0.32	1.2

Percentage of DM particles in the Solar region originating from the LMC

- The percentage of DM particles in the Solar neighborhood originating from the LMC is small.

Direct detection event rate

- The differential event rate (per unit detector mass):

astrophysics

$$\frac{dR}{dE_R} = \frac{\rho_\chi}{m_\chi m_N} \int_{v>v_{\min}} d^3v \, \frac{d\sigma_{\chi N}}{dE_R} \, v \, f_{\rm det}(\mathbf{v}, t)$$

- For standard spin-independent and spin-dependent interactions:

astrophysics

$$\frac{dR}{dE_R} = \frac{\sigma_0 \, F^2(E_R)}{2 m_\chi \mu_{\chi N}^2} \rho_\chi \, \eta(v_{\min}, t)$$

where

$$\eta(v_{\min}, t) \equiv \int_{v>v_{\min}} d^3v \, \frac{f_{\rm det}(\mathbf{v}, t)}{v}$$

Halo integral

Halo integrals

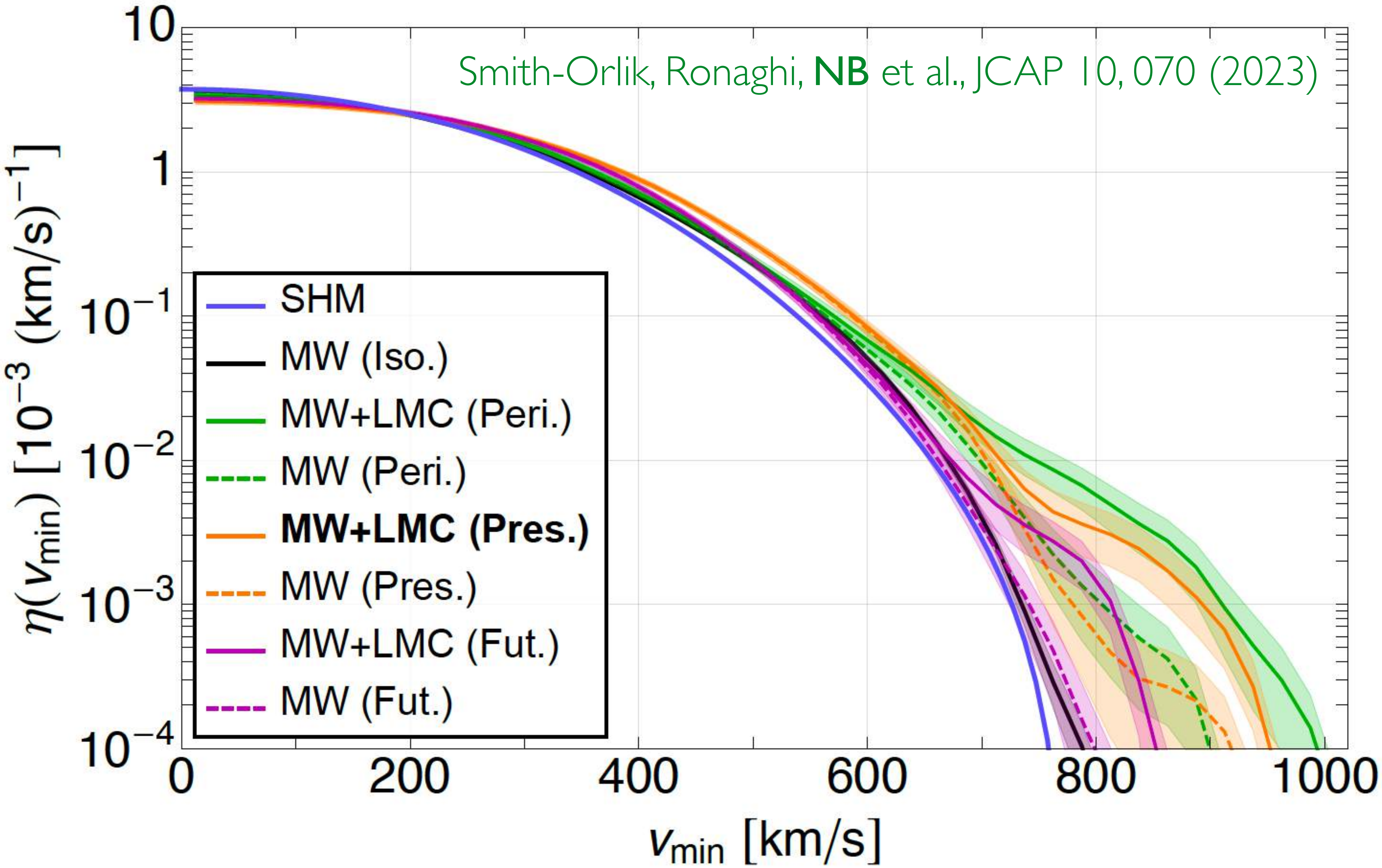

- **Two effects:** High speed LMC particles in the Solar region + Milky Way's response to the LMC.

  → ***Shift of*** $> 150\ \mathrm{km/s}$ ***in the high speed tail of the halo integrals at the present day.***

Direct detection exclusion limits

- Simulate the signals in 3 idealized near future direct detection experiments that would search for nuclear or electron recoils.

Nuclear recoils

Xenon based

$[2 - 50]$ keV
5.6×10^6 kg days
Based on LZ

Germanium based

- $[40 - 300]$ eV, 1.6×10^4 kg days
- $[3 - 30]$ keV, 2.04×10^4 kg days

Based on SuperCDMS

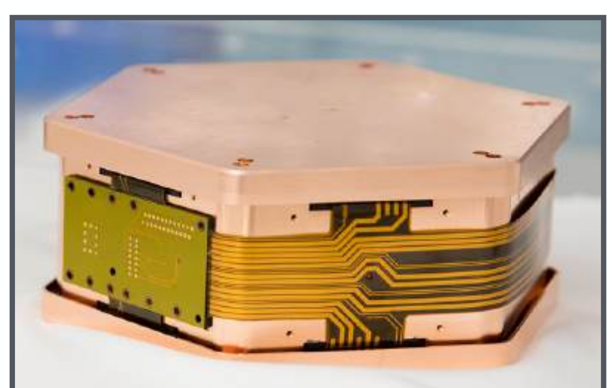

Electron recoils

Silicon CCD

1 electron threshold
1 kg yr
Based on DAMIC

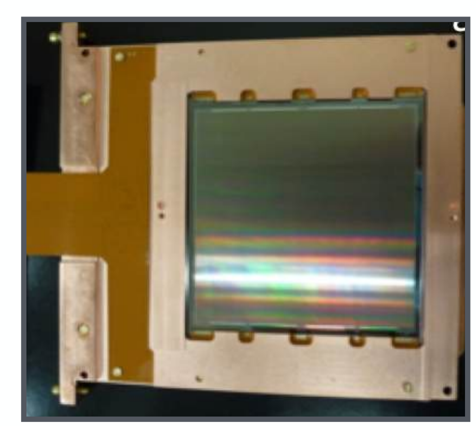

Direct detection: nuclear recoils

Germanium based detector:

Fix $\rho_\chi = 0.3\ \mathrm{GeV/cm^3}$

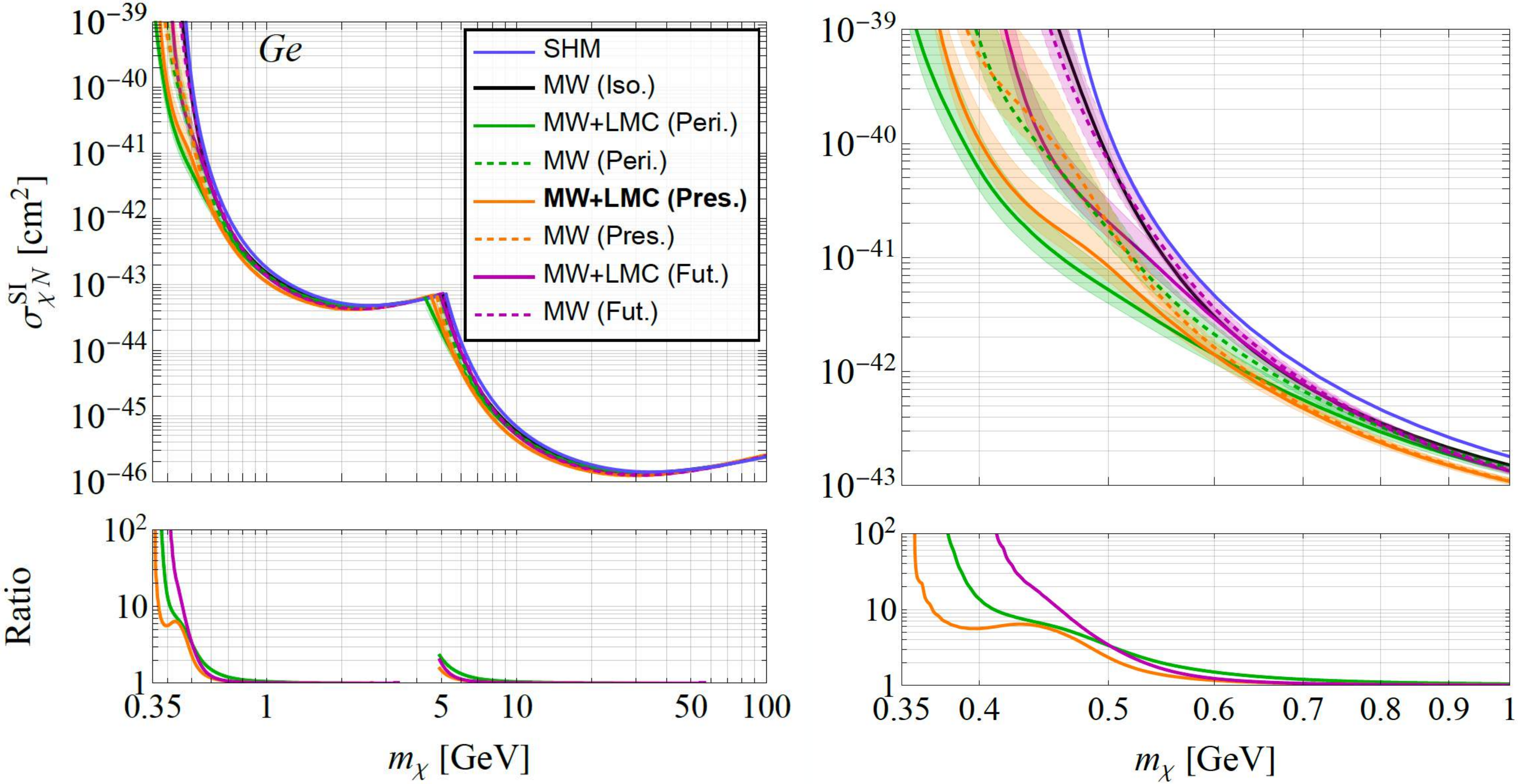

Smith-Orlik, Ronaghi, **NB** et al., JCAP 10, 070 (2023)

Direct detection: electron recoils

Silicon CCD detector:

Fix $\rho_\chi = 0.3\ \mathrm{GeV/cm^3}$

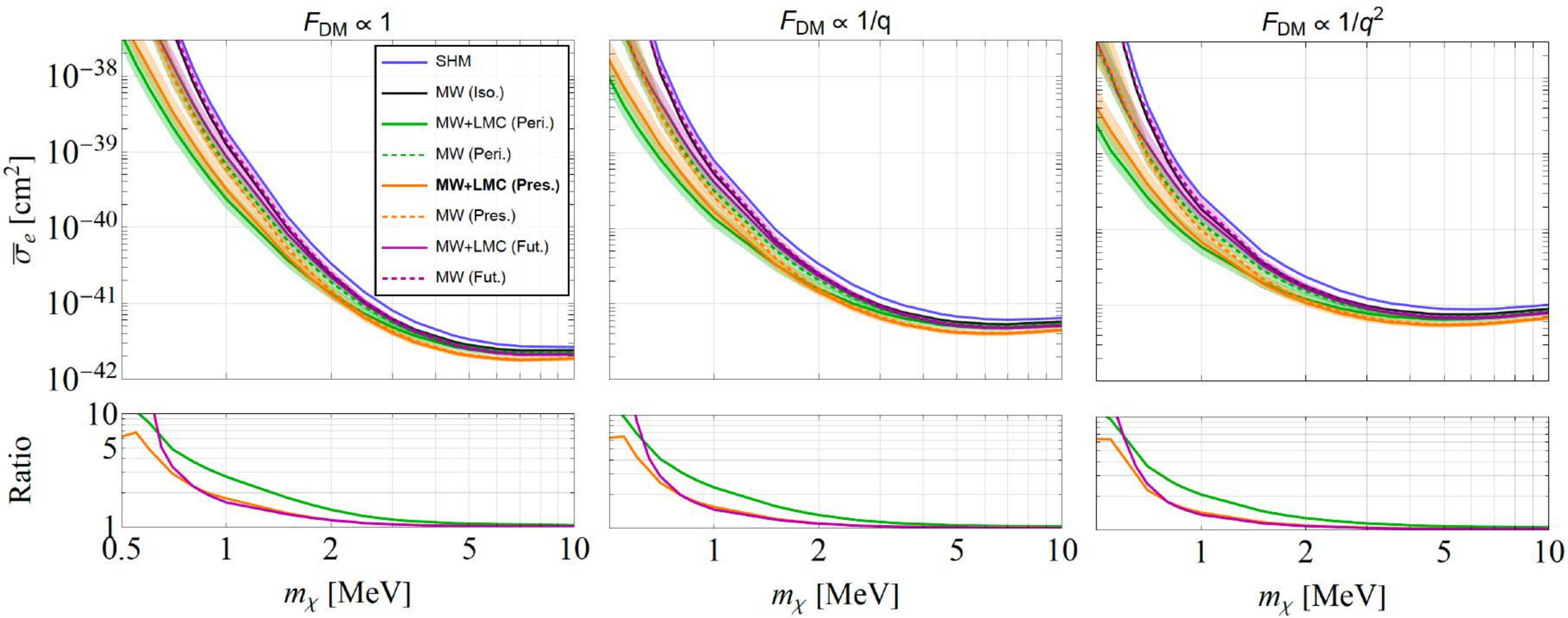

Smith-Orlik, Ronaghi, **NB** et al., JCAP 10, 070 (2023)

Direct detection exclusion limits

- Simulate the signals in 6 near-future direct detection experiments, which use different detector technology and target nuclei:

Experiment	Target Nucleus	Exposure [kg.day]	Energy range [keVnr]
DarkSide-20k	^{40}Ar	3.65×10^7	[30 - 200]
SBC	^{40}Ar	3.65×10^3	[0.1 - 10]
DARWIN/XLZD	Xe	7.3×10^7	[5 - 21]
SuperCDMS	Ge	1.6×10^4	[0.04 - 0.3]
NEWS-G	^{20}Ne	18	[0.03 - 1]
DarkSPHERE	^{4}He	7.4×10^3	[0.03 - 1]

DarkSide-20k

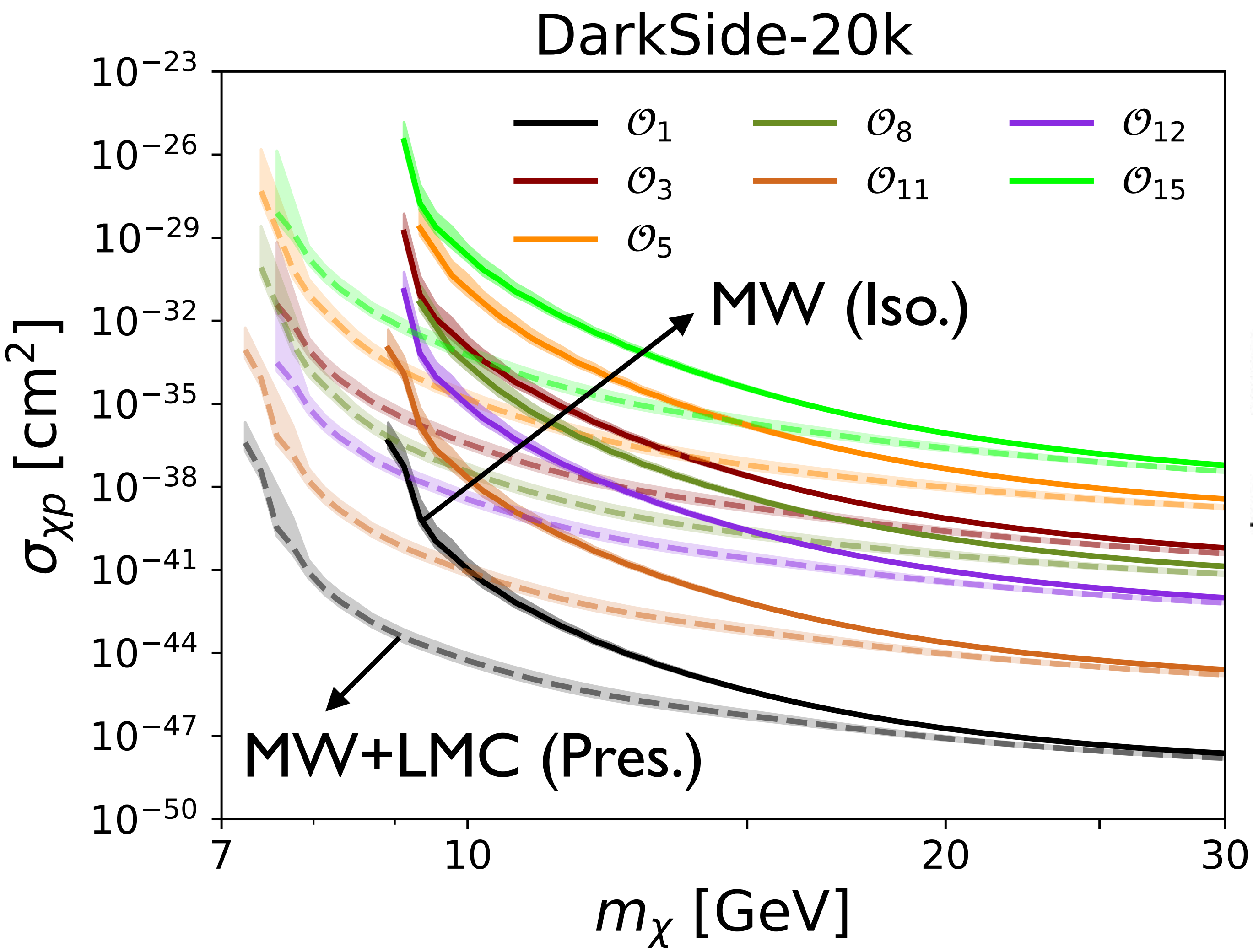

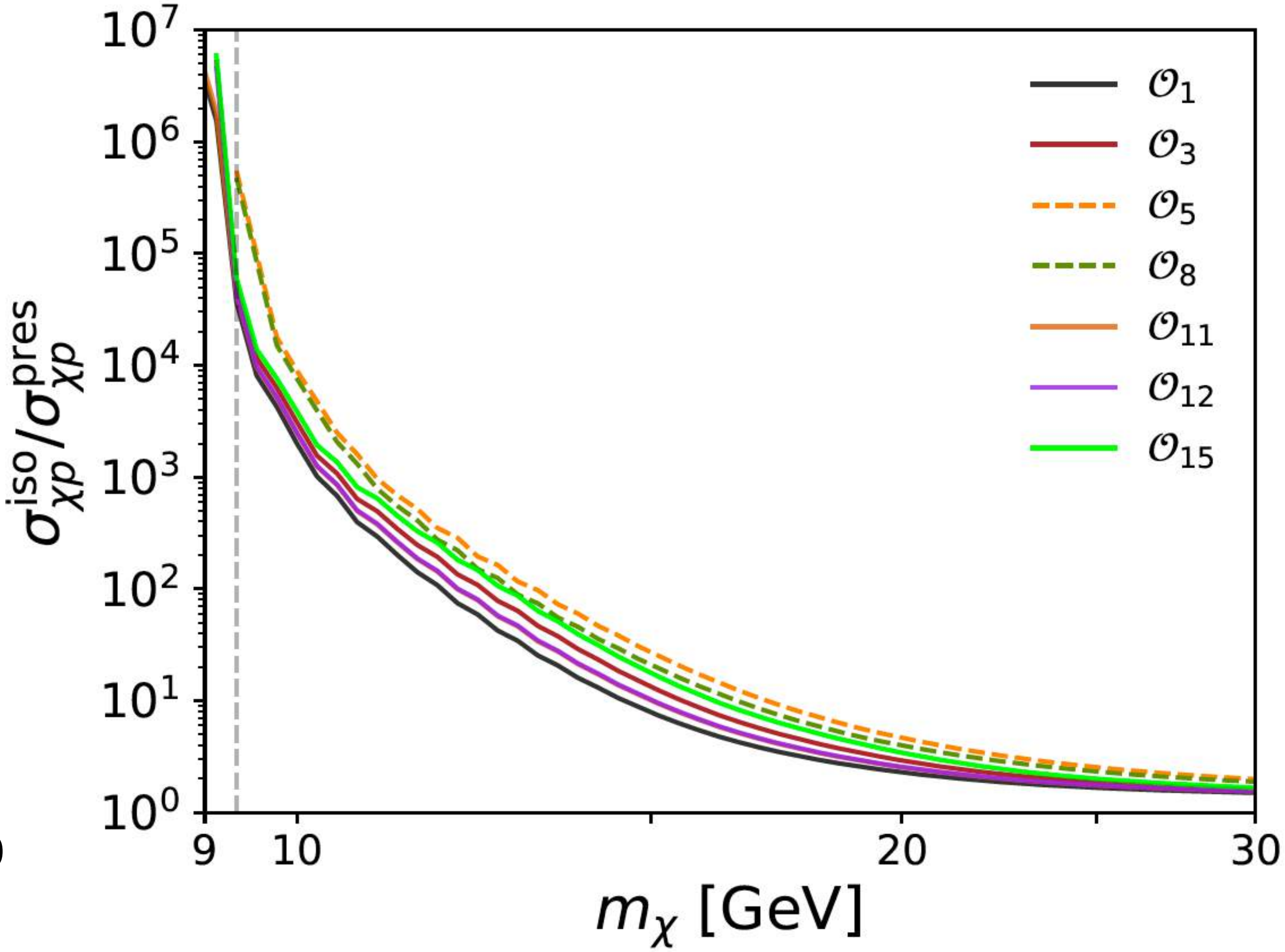

Reynoso, **NB**, Piro, JCAP 12, 037 (2024)

SBC

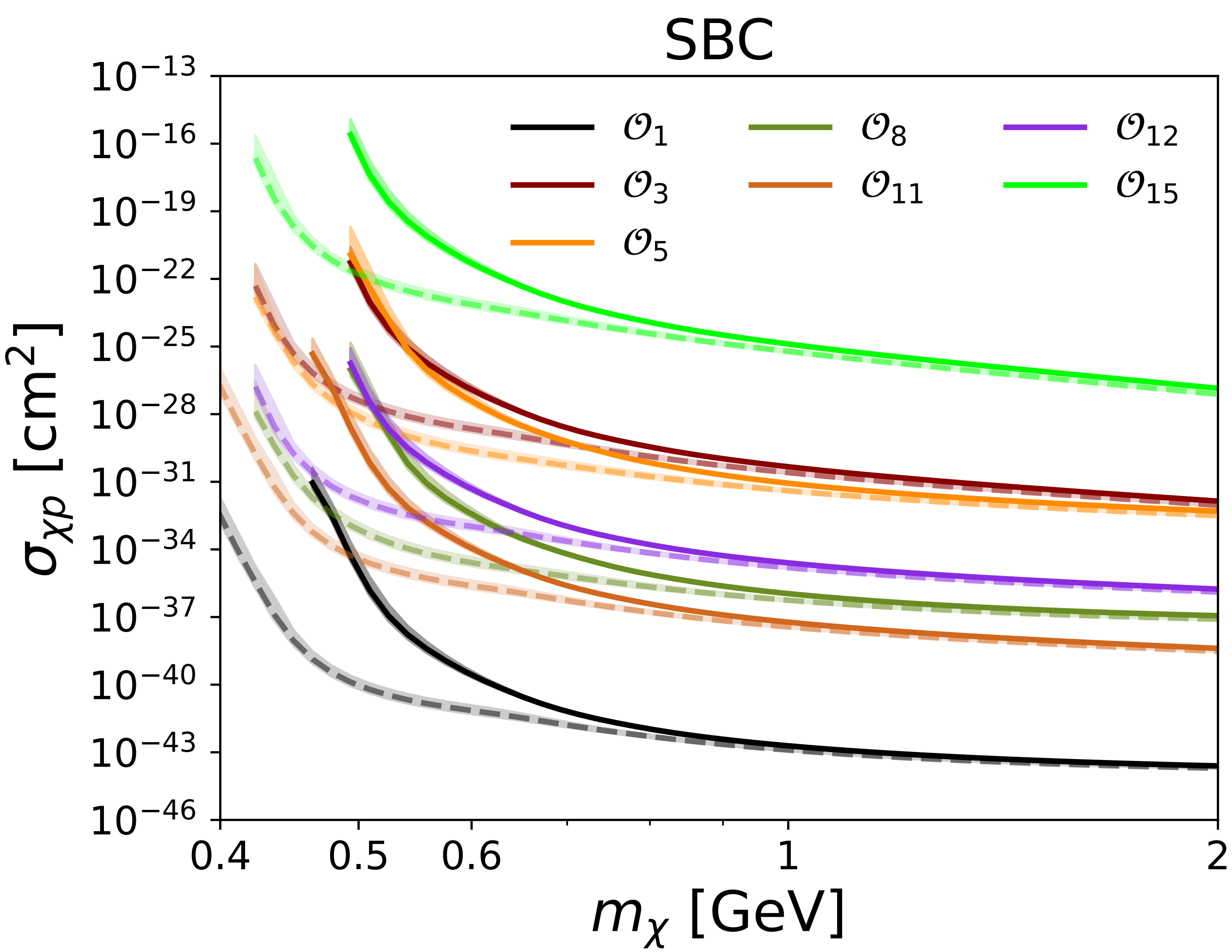

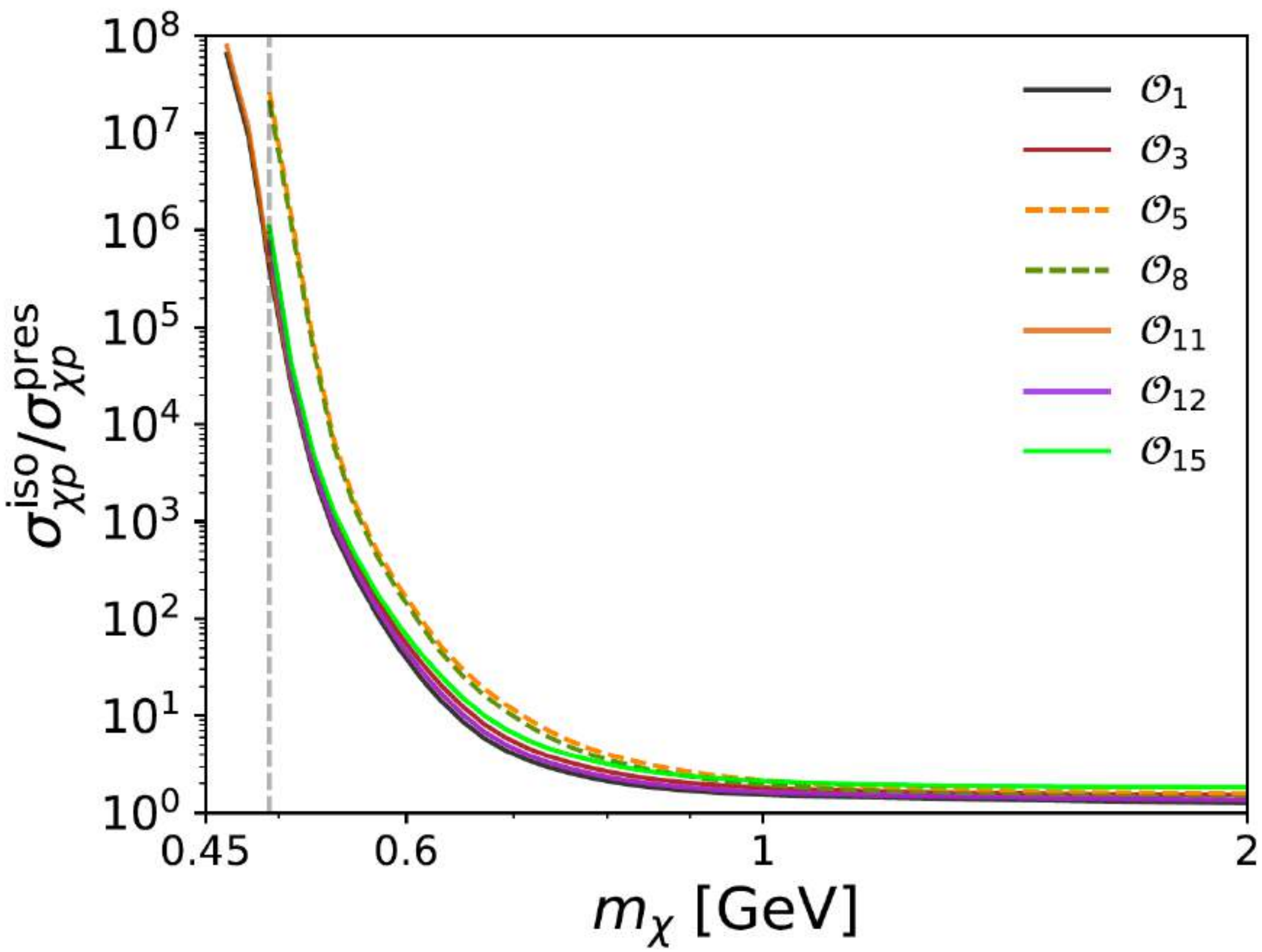

Reynoso, **NB**, Piro, JCAP 12, 037 (2024)

SuperCDMS

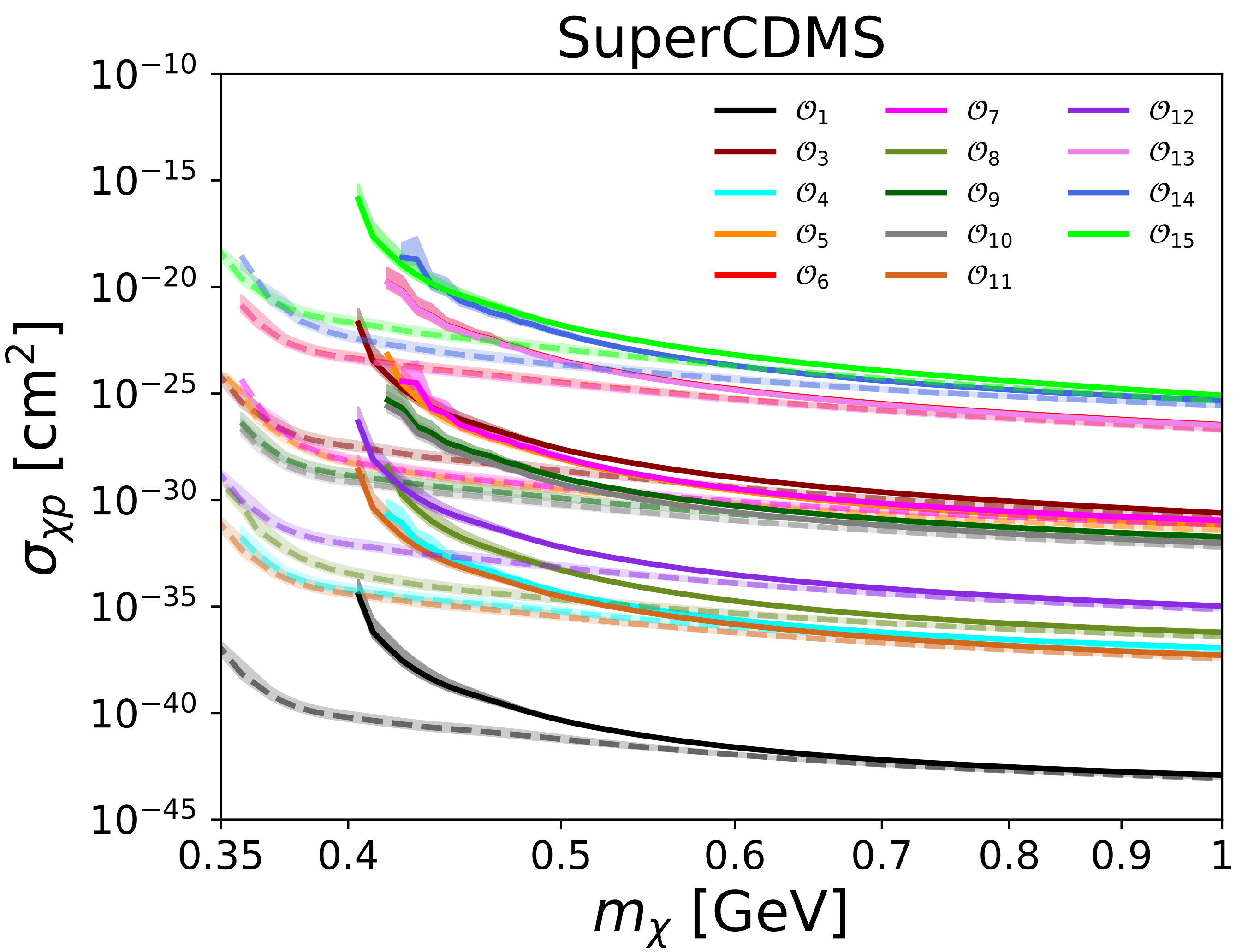

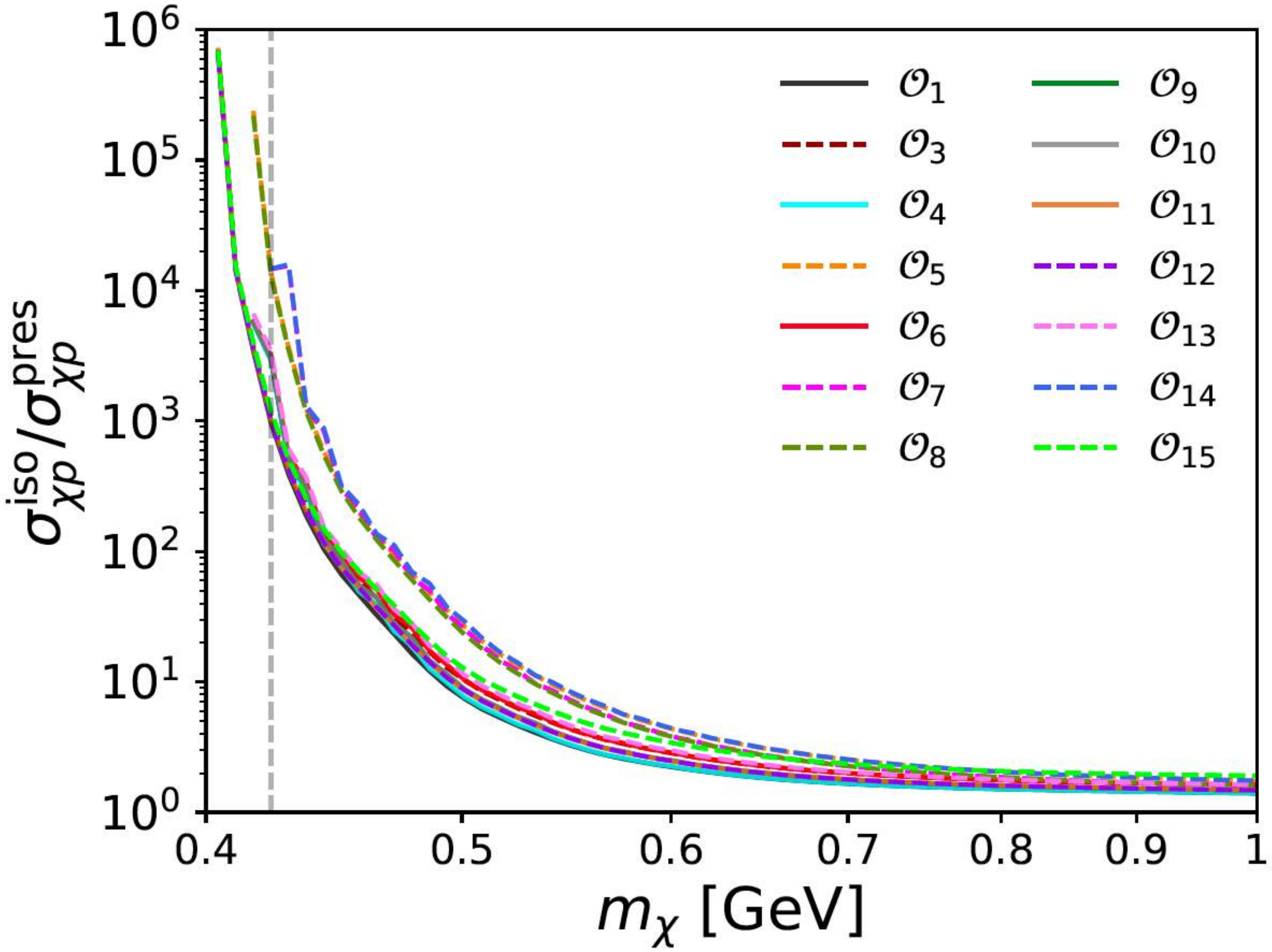

Reynoso, **NB**, Piro, JCAP 12, 037 (2024)

NEWS-G

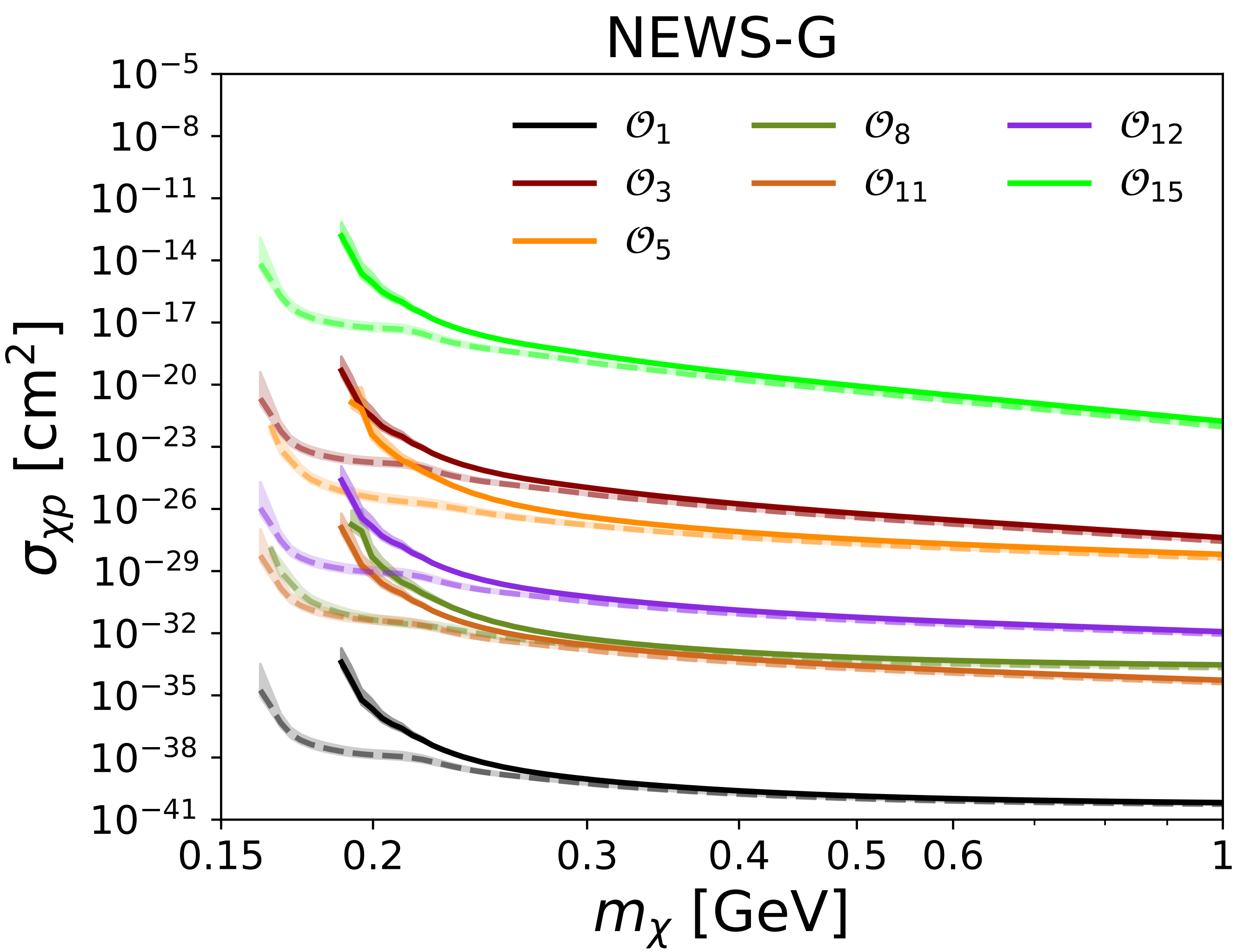

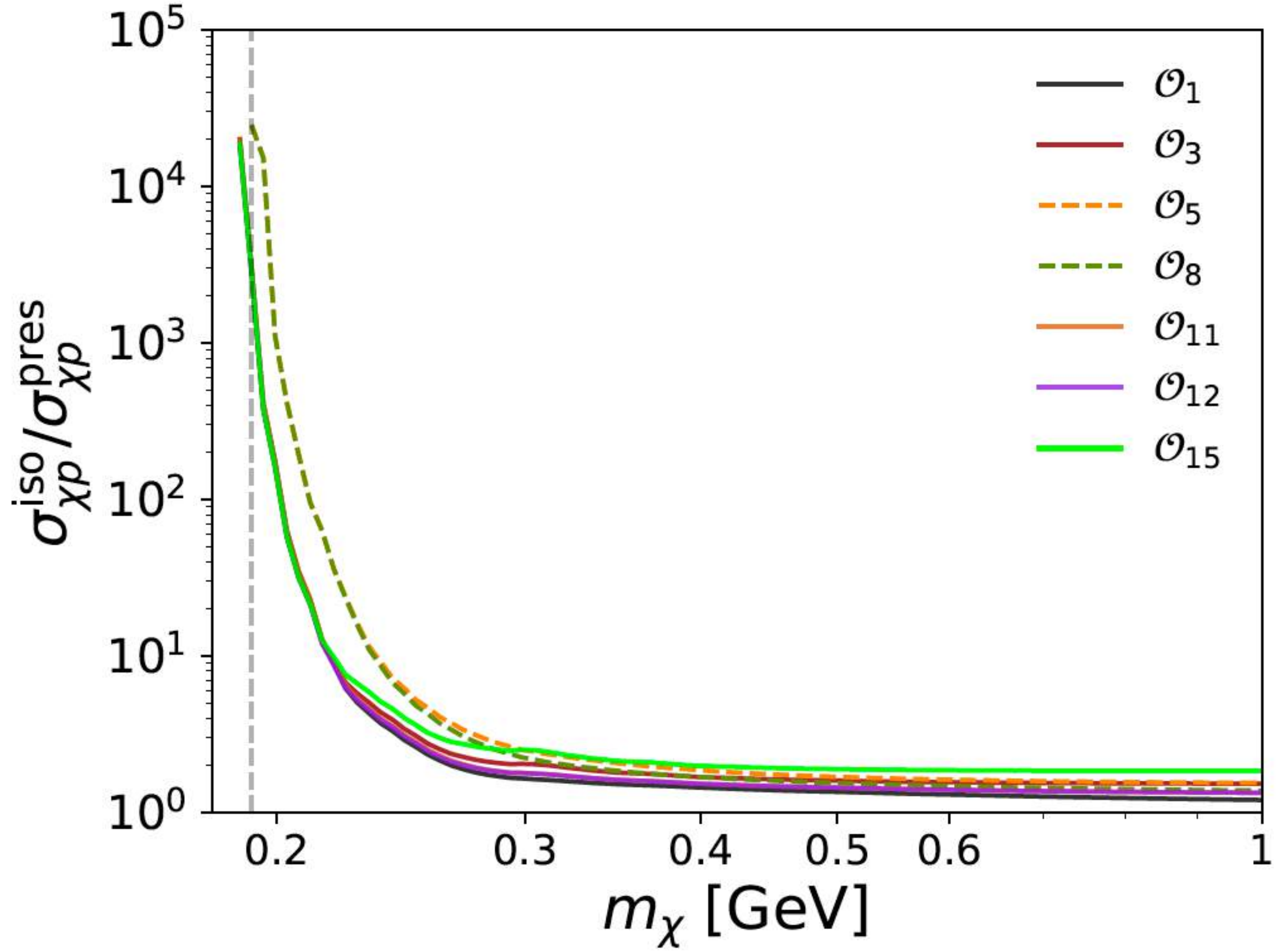

Reynoso, **NB**, Piro, JCAP 12, 037 (2024)

DarkSPHERE

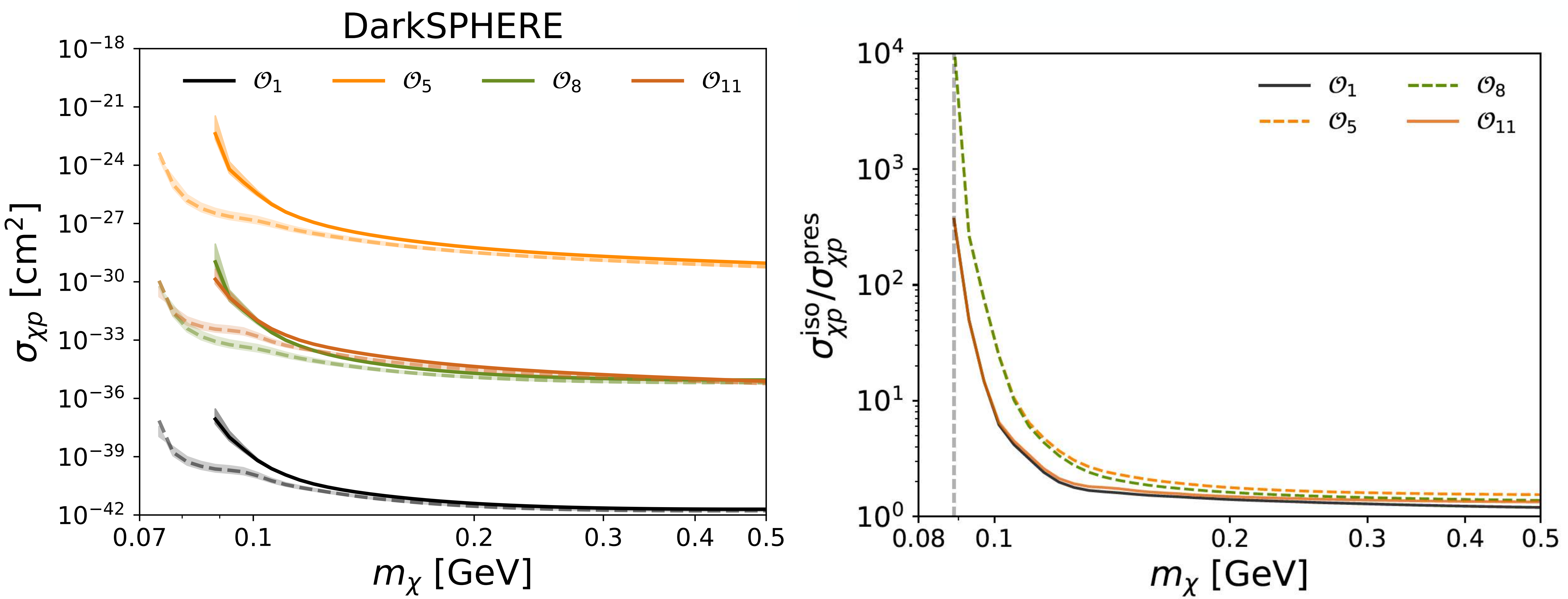

Reynoso, **NB**, Piro, JCAP 12, 037 (2024)

Skylab and Ohya Experiments

	Ohya	**Skylab**
Area A	$2442\,\mathrm{m}^2$	$1.17\,\mathrm{m}^2$
Duration T	$2.1\,\mathrm{yr}$	$0.70\,\mathrm{yr}$
Tolerance Angle θ_{tol}	$18.4°$	$60°$
Overburden Material	Atmosphere + $2.7\,\frac{\mathrm{g}}{\mathrm{cm}^3}$ Crust	$2.7\,\frac{\mathrm{g}}{\mathrm{cm}^3}$ Aluminum
Solid Overburden Length at θ_{tol}	$39\,\mathrm{m}$	$0.74\,\mathrm{cm}$
Column Density of Atmospheric Overburden at θ_{tol}	$960\,\frac{\mathrm{g}}{\mathrm{cm}^2}$	$0\,\frac{\mathrm{g}}{\mathrm{cm}^2}$
Detector Material	$1.2\,\frac{\mathrm{g}}{\mathrm{cm}^3}$ Lexan ($C_{16}H_{14}O_3$)	$1.34\,\frac{\mathrm{g}}{\mathrm{cm}^3}$ CR-39 ($C_{12}H_{18}O_7$)
Detector Length at θ_{tol}	$0.66\,\mathrm{cm}$	$1.6\,\mathrm{cm}$
Detection Threshold E'_{th}	$0.3\,\frac{\mathrm{GeV}}{\mathrm{cm}}$	$0.5\,\frac{\mathrm{GeV}}{\mathrm{cm}}$

Dark matter velocity distribution

Earth's reference frame:

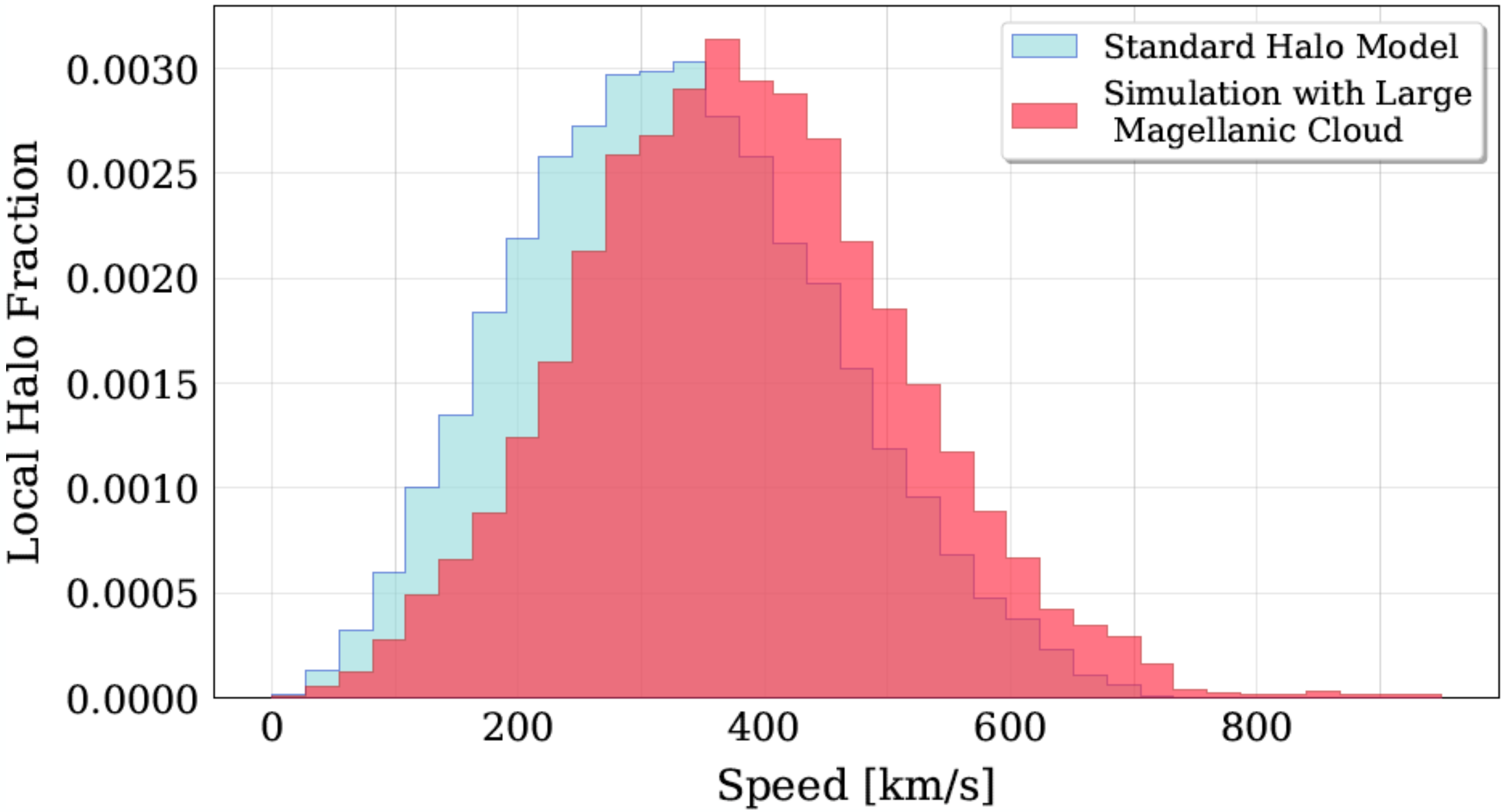

NB, Bramante, Buchanan, JCAP 04, 065 (2026)

Dark matter velocity distribution

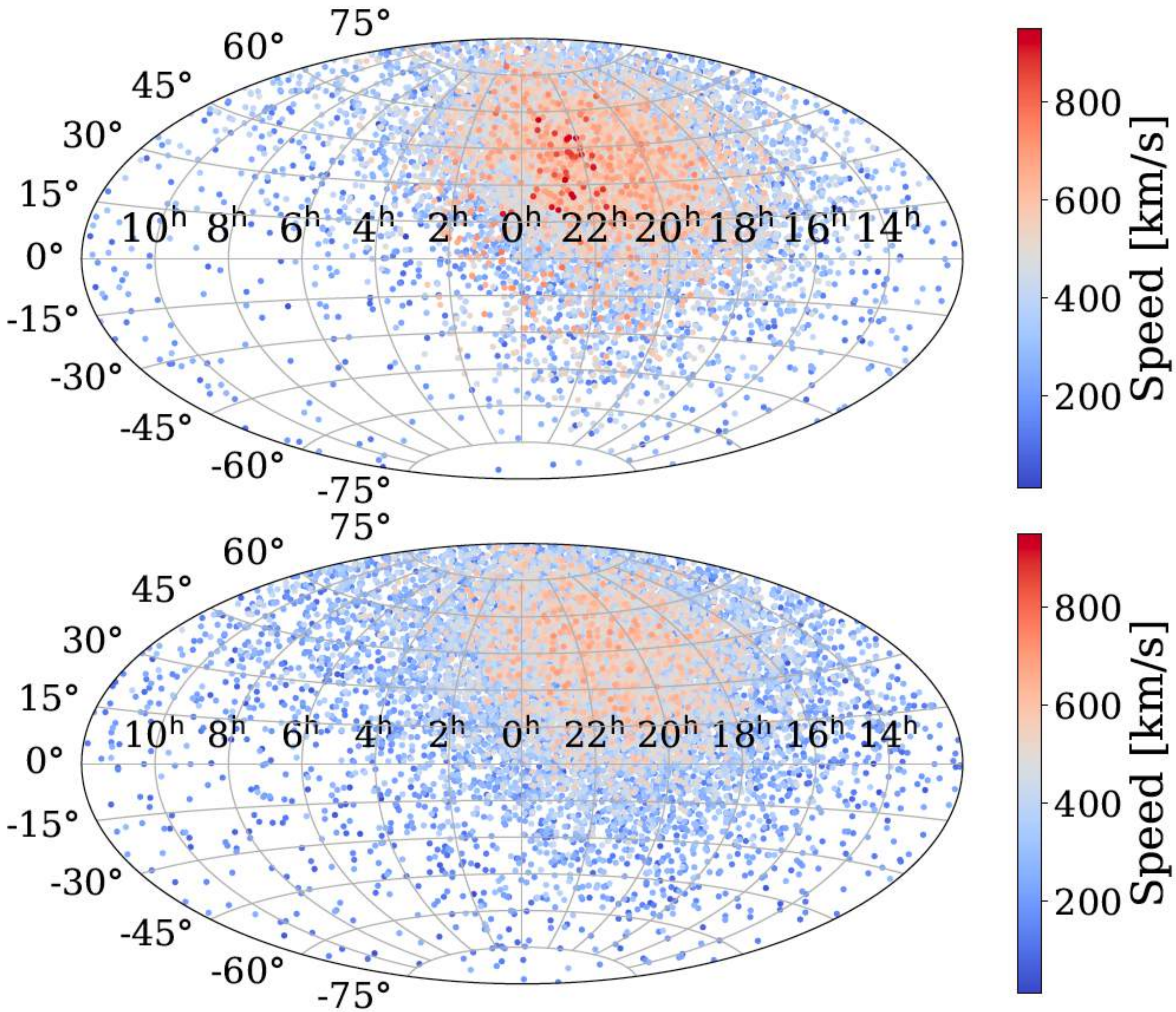

NB, Bramante, Buchanan, JCAP 04, 065 (2026)

Dark matter energy loss

Number of DM particles above a given speed v_0, which pass through the detector:

$$N_{\geq v_0}(m_\chi) = \frac{A_d T \rho_\chi}{m_\chi} \int_{v>v_0} d^3v \, f_{\text{det}}(\mathbf{v}) \, I(\mathbf{v})$$

detector quantities

As a DM particle crosses through a medium, it will lose energy to background nuclei at a rate of

$$\frac{dE}{dx} = -\frac{2E}{m_\chi} \sum_{A \in M} \frac{\mu_{\chi A}^2}{m_A} n_A \sigma_{\chi A}$$

where the sum is over all nuclei in the material, with number density n_A.

Integrated dark matter mass flux

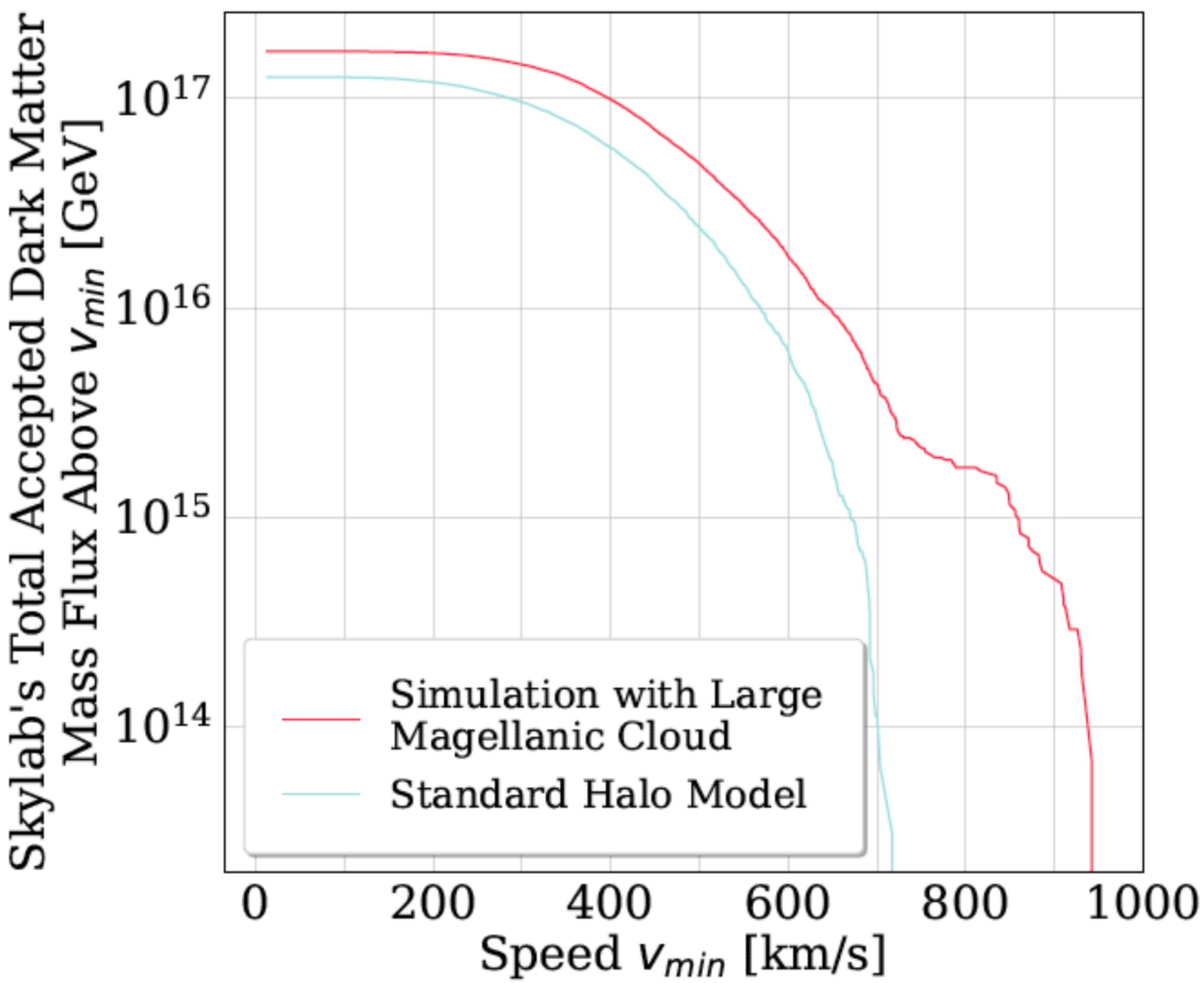

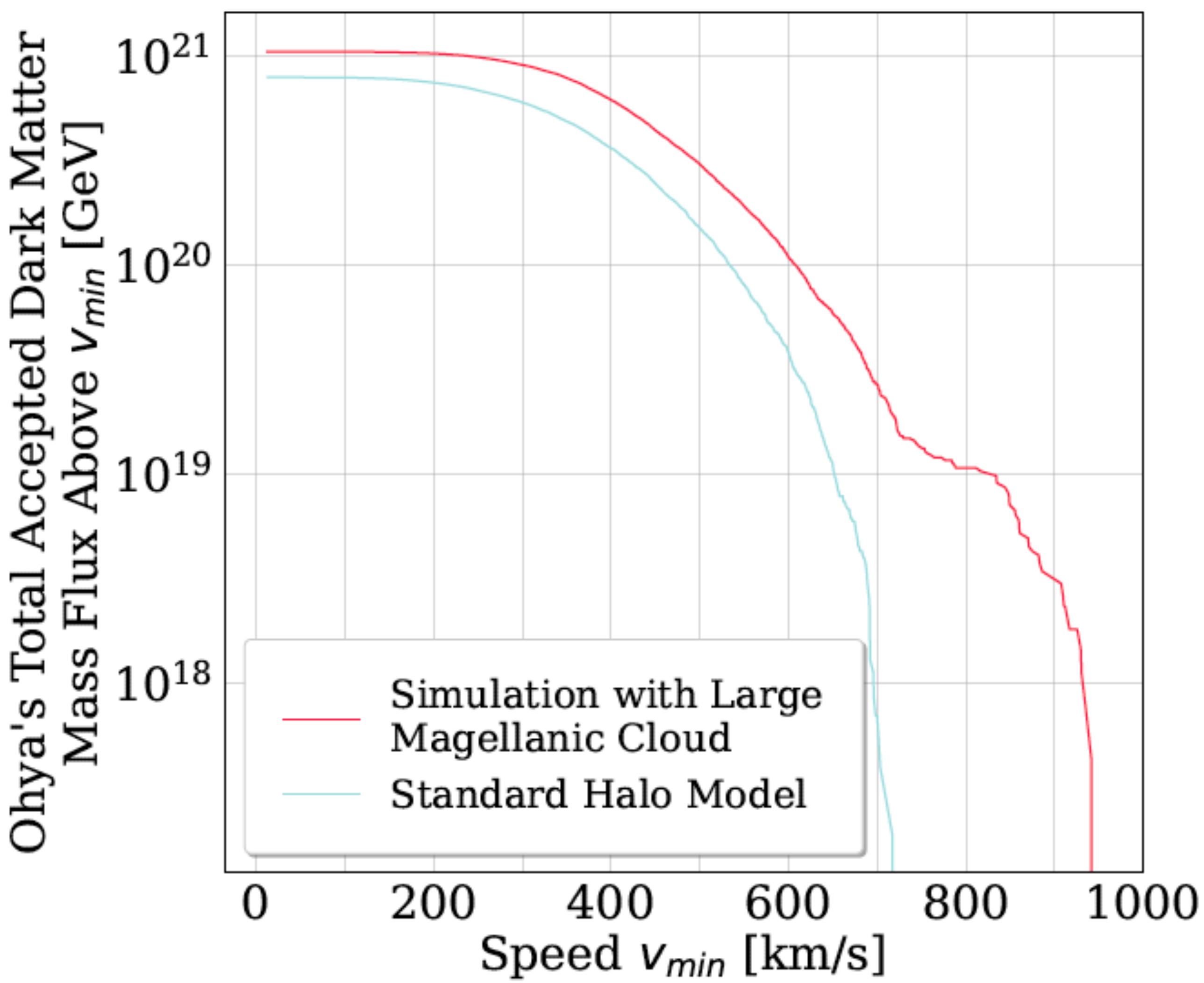

NB, Bramante, Buchanan, JCAP 04, 065 (2026)

Heavy dark matter bounds

Contact

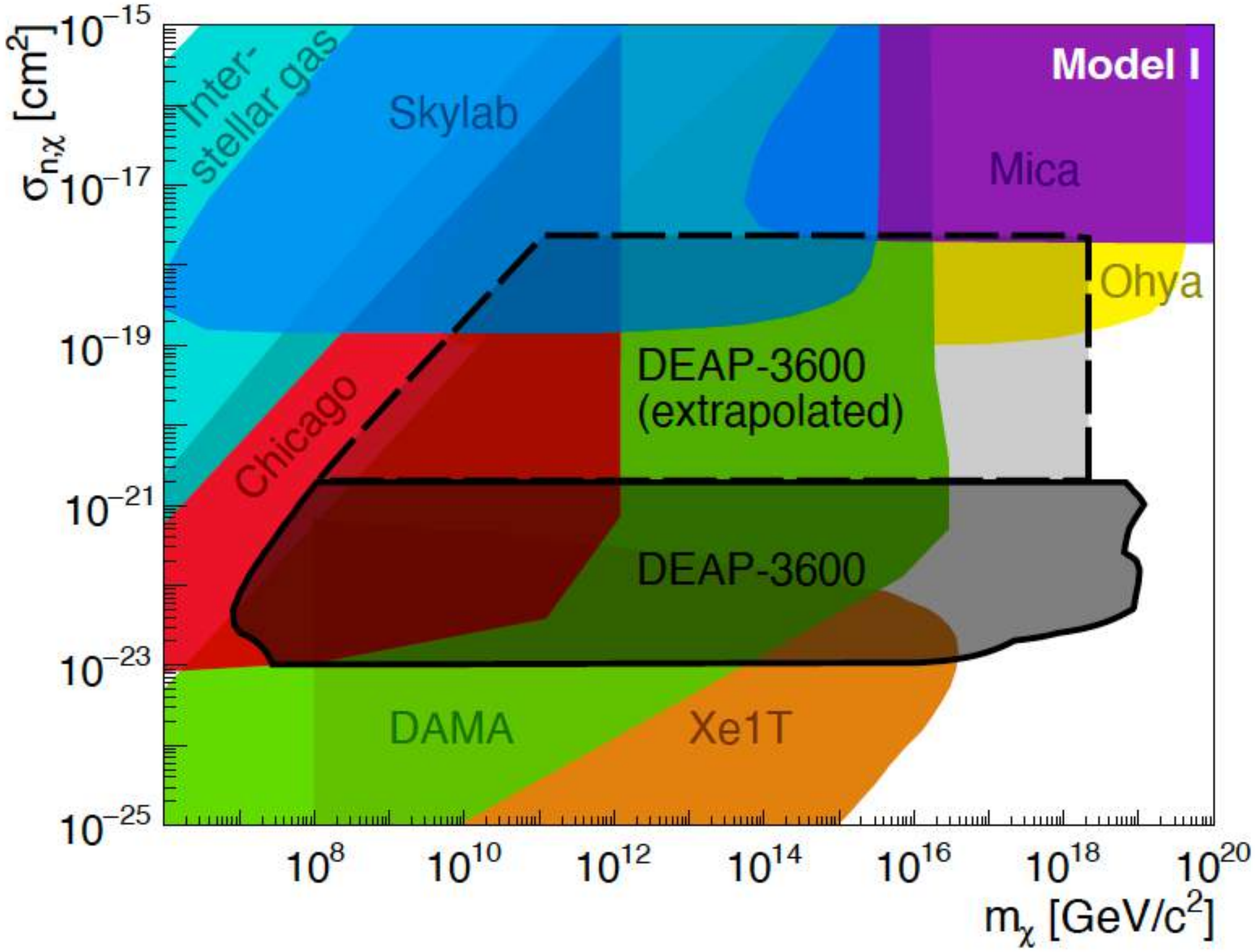

Spin-independent

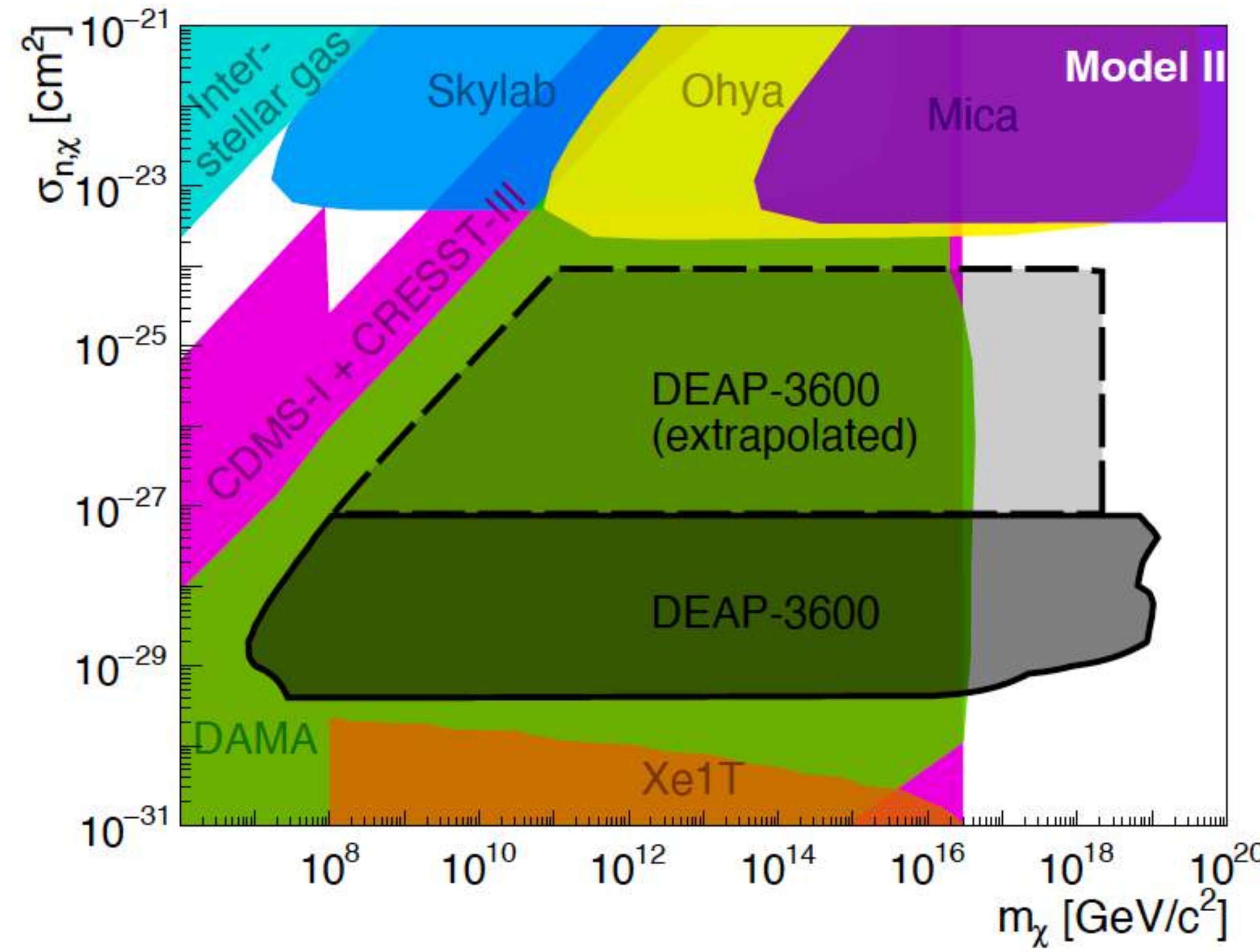

DEAP, 2108.09405

Velocity distribution components

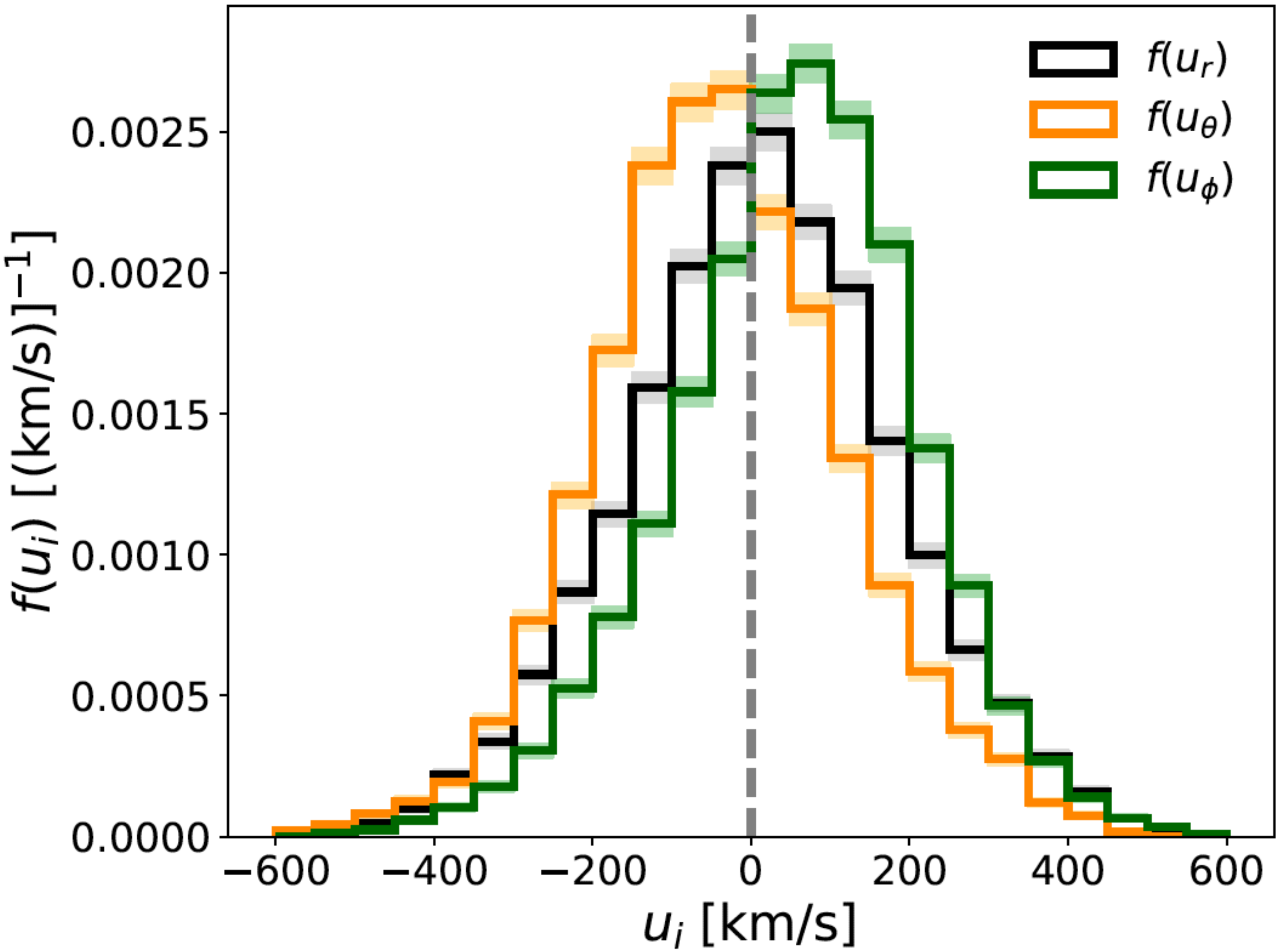

Reynoso, **NB**, Piro, 2606.12535

Directional signatures

Directional differential recoil rate in Galactic coordinates:

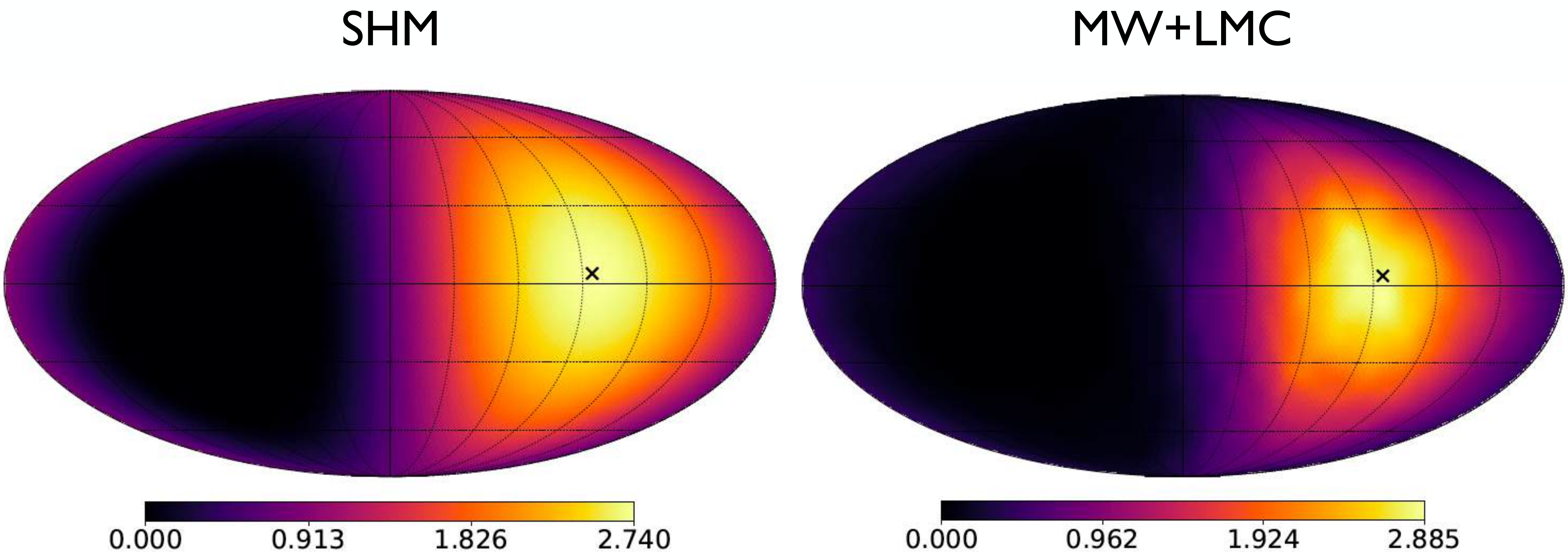

Reynoso, **NB**, Piro, 2606.12535

CYGNUS-like Experiment
He:F4 (60-40) at Gran Sasso
$m_\chi = 5$ GeV, $E_R = 3$ keV